Feasibility and Economics of Existing PWR Transition to a Higher Power Core Using Annular Fuel

by

Julien Beccherle

Submitted to the Department of Nuclear Science and Engineering
in partial fulfillment of the requirements for the degree of

Master of Science in Nuclear Science and Engineering

at the

MASSACHUSETTS INSTITUTE OF TECHNOLOGY

September 2007

Author .....
Department of Nuclear Science and Engineering
August 27, 2007

Certified by .....
Mujid S. Kazimi
Professor of Nuclear and Mechanical Engineering
Thesis Supervisor

Read by .....
Pavel Hejzlar
Principal Research Scientist, Department of Nuclear Science and Engineering
Thesis Reader

Accepted by .
Professor Jeff Coderre
Chairman, Department Committee on Graduate Students

Feasibility and Economics of Existing PWR Transition to a Higher Power Core Using Annular Fuel

by

Julien Beccherle

Submitted to the Department of Nuclear Science and Engineering
on August 27, 2007, in partial fulfillment of the
requirements for the degree of
Master of Science in Nuclear Science and Engineering

Abstract

The internally and externally cooled annular fuel is a new type of fuel for PWRs that enables an increase in core power density by 50% within the same or better safety margins as the traditional solid fuel. Each annular fuel assembly of the same side dimensions as the solid fuel has 160 annular fuel rods arranged in a 13x13 array. Even at the much higher power density, the fuel exhibits substantially lower temperatures and a MDNBR margin comparable to that of the traditional solid fuel at nominal (100%) power. The major motivation for such an up-rate is reduction of electricity generation cost. Indeed, the capital cost per kWh(e) of the construction is smaller than the standard construction of a new reactor with solid fuel.

Elaborating on previous work, we study the economic payoff of such an up-rate of an existing PWR given the expected cost of equipment and also cost of money using different assumptions. Especially, the fate of the already bought solid fuel is investigated. It is demonstrated that the highest return on investment is obtained by gradually loading annular fuel in the reactor core such that right before shutting the reactor down for the up-rate construction, two batches in the core are of annular fuel.

This option implies running a core with a mixture of both annular fuel and solid fuel assemblies. In order to prove the technical feasibility of such an option, the thermal-hydraulics of this mixed core is investigated and the Minimum Departure From Nucleate Boiling is found to be either unaffected or even improved by using a mixed core. Consequently, a neutronic model is developped to verify and validate the neutronic feasibility of the transition from solid fuel to annular fuel.

The overall conclusion of this work is that annular fuel is a very promising option for existing reactors to increase by 50% their power, because it enables such an up-rate at very attractive return on investement. We show that, by a smart management of the transition, a return on investment of about 22 to 27 % can be achieved.

Thesis Supervisor: Mujid S. Kazimi
Title: Professor of Nuclear and Mechanical Engineering

Acknowledgments

I would like to express my warmest thanks to Professor Mujid S. Kazimi, my reasearch supervisor. Professor Kazimi is a very knowledgeable, competent and helpful advisor. He had a great influence on my education and has been a great model to follow. His availabality and kind-heartness were very much appreciated.

I also thank Pavel Hejzlar, my research co-supervisor and the reader of this thesis. Pavel is a very sharp person with whom I really appreciated discussing issues I was facing and who was always available to comment and advice me on my progress.

Doctor Ed Pillat, and Professor Richard de Neufville offered me valuable advice throughout my research. Doctor Ed Pillat extensive experience in the Nuclear Industry and his patience were key inputs into my research, especially as far as neutronic modeling is concerned. Professor de Neufville helped me sharpen my Economic skills, and his advices were very useful to develop the Economic assesment.

My colleagues and friends from my research group also diserve many thanks for their advices and their friendship: Lara Pierrepoint, Bo Feng, Nicephore Bonnet, Rodney Busquin, Taylor Moulton, Tyler Ellis.

My eternal gratitute belongs to my family for their love and support. Finally I thank from the bottom of my heart my beloved girlfriend Mathilde who was always here to support me, and with whom I share everything.

Contents

List of Figures

List of Tables

Chapter 1

Introduction

Nuclear energy is on the edge of a so-called renaissance due to a combination of economic and environmental factors. In a CO_2 constrained world, nuclear energy is likely to play an important, if not central, role in providing economic, reliable, carbon-free and safe energy.

They are two major challenges to this renaissance. The first one is economic competitiveness with other technologies. In order to expand, nuclear power needs to be less expensive than other alternatives. The other challenge is disposal of the waste. Even though technical solutions exist to the issue of waste, because of political concerns and economic unatractiveness of these solutions, a fuel that produces as little waste as possible using the existing LWR technology is very much desirable.

The general idea of the annular fuel, developed at the Center for Advanced Nuclear Energy Systems (CANES) at MIT, is to try to mitigate these two issues with a new type of fuel that enables a higher power density in the core and produces less waste per unit of generated energy.

Through a U.S. DOE funded Nuclear Energy Research Initiative (NERI) program, a comprehensive study [9] of the annular fuel was performed. The major results, summarized in the next sections showed that by using annular fuel, a PWR power density could be increased by 50 % within the same safety margins, and that the burn-up of the fuel can be increased substantially.

Taking this analysis one step further the objective of this work is to evaluate the

attractiveness of using a high power density fuel in an existing reactor and establish the feasibility of a transition from solid to annular core. We demonstrated that by gradually transitioning from solid to annular core, substantial rate of returns on the up-rate project can be reached. We also proved that such a transition core is technically feasible, both on a thermal-hydraulic and on a neutronic basis.

1.1 Annular fuel description and performance

1.1.1 Fuel description

The annular fuel is a new type of fuel that is both internally and externally cooled (see Figure 1-1). It is composed of UO_2 so existing data can be used readily. Because of its geometry, the annular fuel shows significant performance improvement compared to the solid fuel. It has a reduced thermal conduction path thickness that improves the margin from peak fuel temperature to melting, and it has an increased heat transfer surface area which improves the margin for Departure from Nucleate Boiling Ratio (DNBR).

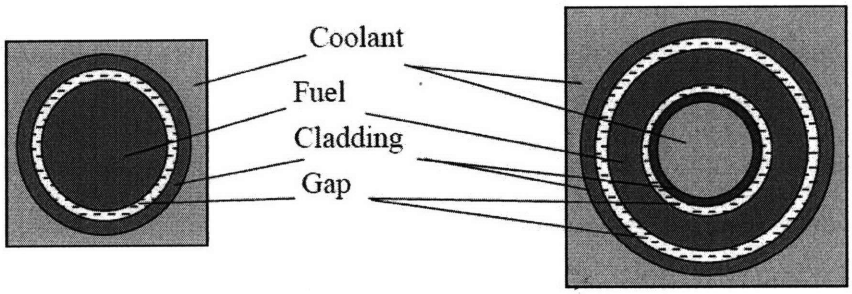

Figure 1-1: Schematic of solid and internally and externally cooled annular fuel (not to scale)

While staying within the same safety margins as the solid fuel, annular fuel enables the core to run at an estimated 150 % power for the same cycle length if the flow rate is increased proportionnaly.

To reach this target the design that was defined in Ref. [9] is a 13x13 assembly with a mean enrichment of 8.5 %. The actual size of the assembly remains the same.

The dimensions of the fuel are given in Table 1.1.

Table 1.1: Dimensions (in cm) of annular fuel and reference solid fuel (from Ref. [9])

Array	D_{cii}	D_{cio}	D_{fi}	D_{fo}	D_{coi}	D_{coo}	Pitch
13x13	0.863	0.978	0.990	1.410	1.422	1.537	1.651
17x17-ref.	Solid pin	-	-	0.826	0.838	0.952	1.263

Note: D=Diameter ; f,c=fuel,cladding ; i,o=inner,outter ; i,o=inside,outside

1.1.2 Fuel performance

The 6 major objectives of the previous investigation were the following:

- Identify the best fuel assembly arrangement for PWRs to achieve maximum uprating, while still using UO_2 fuel, by assessing the thermal-hydraulic limiting parameters like DNBR.

- Perform a safety analyses for several types of accidents to assure that the fuel at higher power can meet the required safety limits.

- Evaluate the neutronic fuel design to achieve high reactivity-limited burn-up and a refueling cycle comparable to existing PWR.

- Select and assess the fabrication processes to produce annular fuel elements within the required product characteristics.

- Evaluate the materials and mechanical performance of the proposed fuel under irradiation.

- Estimate the economic costs and benefits of using annular fuel in a PWR.

The findings to date can be summarized as follows:

1. Thermal-hydraulic assessment An optimum search in square lattice design of the annular fuel was performed using a VIPRE-01 whole core model. Based on DNBR considerations, the most promising designs were found to be either a 12x12 lattice or a 13x13 lattice. In particular the 13x13 design allows for a 50% uprate in power if the flow rate is also increased by 50%.

Key features of the design are that *(i)* even at 150% power the maximum temperature of the fuel is about 1300 ° C lower than that of solid fuel as illustrated in Figure 1-2; *(ii)* the pressure drop of annular fuel assembly at 100% power and flow rate is very close (within a few percents) to the pressure drop of the solid fuel assembly at 100% flow rate.

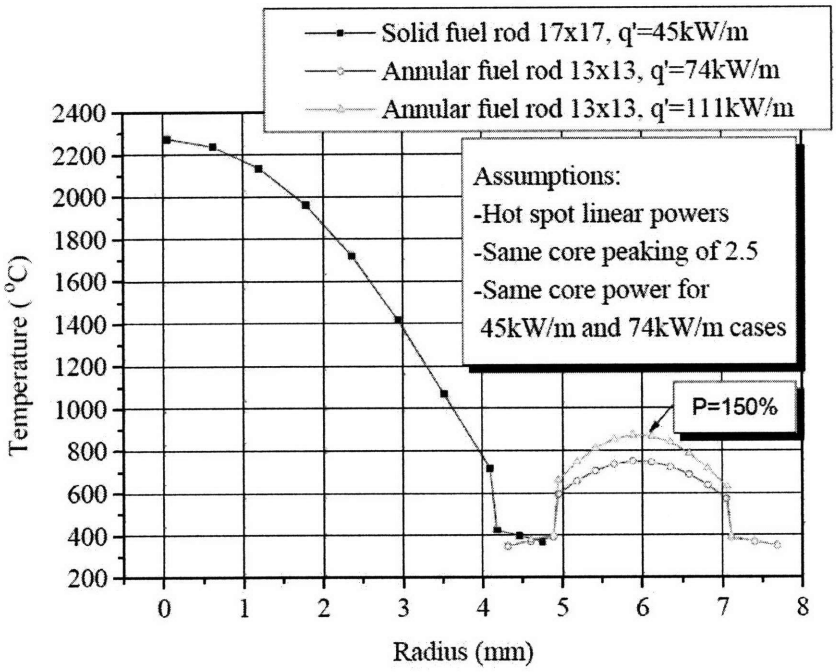

Figure 1-2: Comparison of hot-spot radial temperatures profiles for solid and annular fuel (from Ref. [9])

2. Safety analysis Four accidents of annular fueled PWRs were evaluated and compared to the reference solid fueled PWR: Loss-Of-Coolant Accident (LOCA), Loss Of Flow Accident (LOFA), Main Steam Line Break (MSLB) and Rod Ejection

Accident(REA) [9].

The accidents were evaluated using RELAP3D/ATHENA and VIPRE-01 and showed satisfactory performance of the annular fuel at 150% nominal power.

3. Neutronic analysis Starting from the design that was selected by the thermal-hydraulic optimization, the major challenge of the neutronic analysis was to design the core, and develop a fuel management scheme able to achieve an 18 months cycle at 50% over power. The target criteria were sustaining an 18 months cycle with 90% capacity factor, keeping the boric acid concentration below 1750 ppm, keeping radial pin power peaking below 1.65, and keeping a hot spot factor of 2.5 or less.

The core was desigend using the CASMO/TABLES/SIMULATE package. The 150% power annular fuel was designed for 3 batches. Each batches are composed of 72 reload assemblies: 24 assemblies have an enrichment of 8.1 wt% and 48 assemblies have an enrichment of 9.0 wt%. In order to stay below 1750 ppm of boric acid, the Gd poisoning needed to be increased substantially.

The general layout of the core is summarized in Figure 1-3. The assembly is labeled as follow: the first digit (0,1 or 2) stands for fresh, once-burned, twice-burned ; H or L means High enrichment or Low enrichment ; the next two digits indicate the total number of poisonned rods ; the last two digits indicate the Gd content of the poisonned rods. For instance 2L2410 is a twice-burned, low enrichment assembly with 24 poisonned rods at 10 wt% Gd content.

4. Fuel fabrication A key issue for a new fuel was the assessment of the feasibility and cost of its industrial fabrication. Therefore, a lot of attention was devoted to the demonstration of the feasibility of a fabrication process. Among several existing manufacturing technologies, two most promising processes were selected for further investigation: the sintered ring pellet and the VIPAC technology.

Near prototypical annular fuel rods were fabricated using these two processes. It appeared that the VIPAC technology could not reach satisfactory density, whereas the sintered ring pellet method proved to reach sufficiently high density and high tolerance

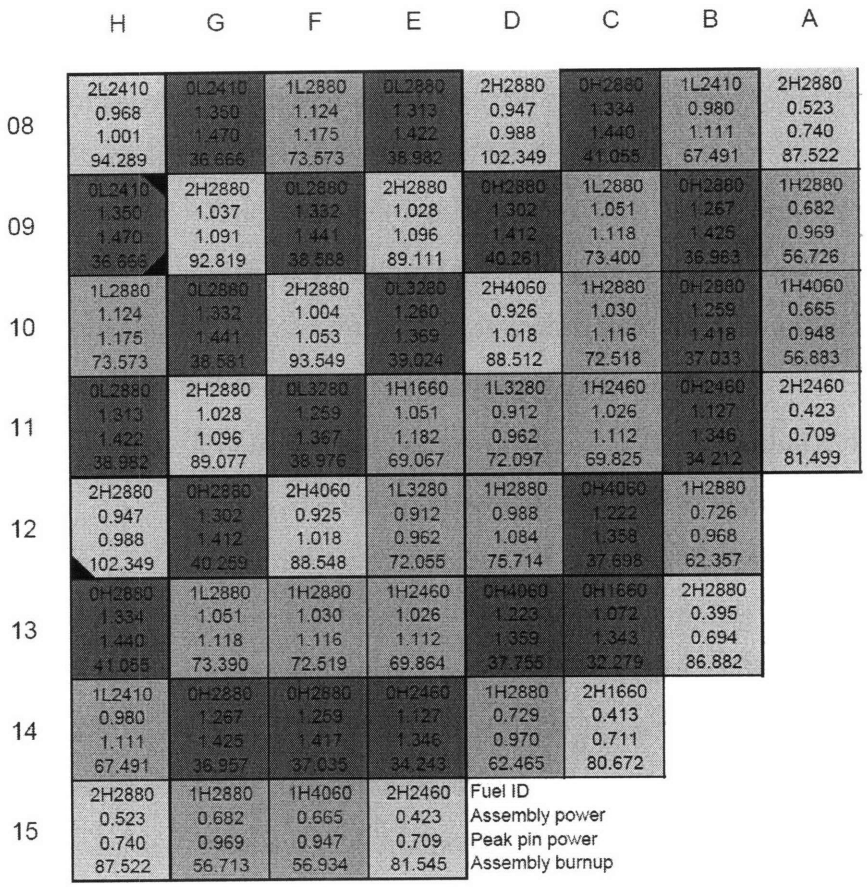

Figure 1-3: Assembly power distribution at EOC for the annular fuel, 150% power core (from Ref [9]).

requirements in pellets pressed at the Westinghouse Columbia plant. The latter process was therefore pursued and another set of annular fuel rods was manufactured (see Figure 1-4) this time at an Argentian facility.

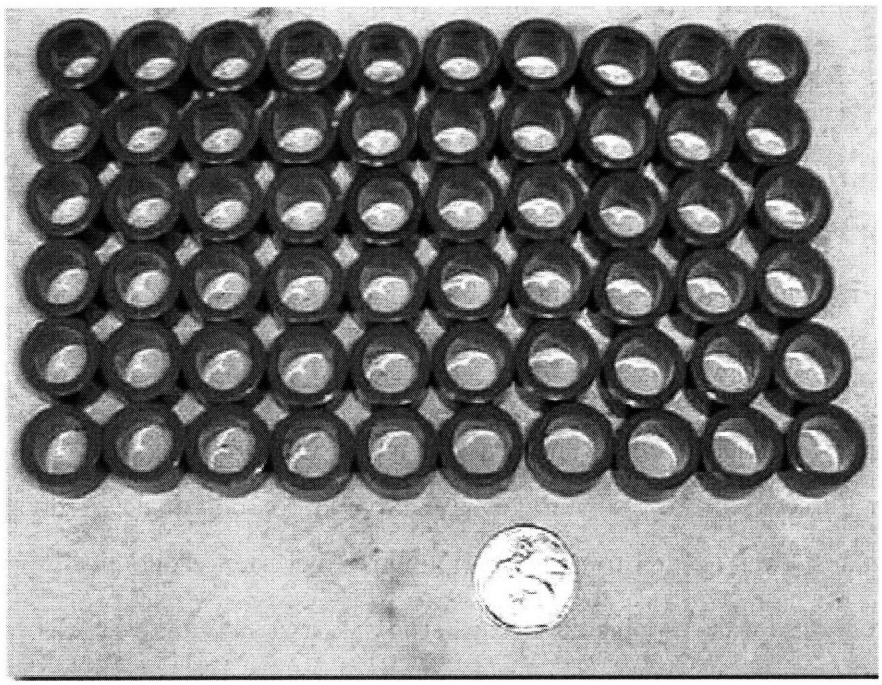

Figure 1-4: Sintered pellets manufactured at Westinghouse (from Ref [9]).

The conclusion of the fabrication tests is that annular fuel elements can be manufactured by existing commercial processes to reach required specifications using the sintered ring pellet technique. Furthermore, this technique yields a reasonable cost of fabrication cost (see Ref. [9]).

5. Materials and mechanical performance First of all the thermo-mechanical performance of the sintered pellets fuel was assesed using a modified version of FRAPCON-3 (FRAPCON-ANNULAR). The total fission gas release was calculated to be relatively low (less than 6%) for both sintered and VIPAC condition. Even though both the inner and outer cladding experience larger strains than solid fuel cladding because of the larger initial diameter, the strains remain within the regulatory margins of 1%.

In order to assess the behavior of the annular fuel under new conditions (low temperature, different geometry) two sample VIbrationally PACked (VIPAC) annular fuel were irradiated in the MITR.

The major concern for VIPAC fuel is the fission gas release. A post irradiation examination (PIE) of the VIPAC fuel samples was conducted in August 2005, and showed lower than expected fission gas release at the burnup level of 7MWd/kg. Unfortunately, funding did not permit longer irradiation. The fission gas release was found to be of the order of 0.5%, and even though this number is subject to uncertainties, the overall FGR must lie within a few percents.

6. Economic assessment The use of annular fuel will be considered only if it proves to be economically advantageous compared to solid fuel. A detailed cost-benefit analysis was needed to examine if annular fuel is an economically viable fuel.

Westinghouse was responsible for this study. A two step analysis was performed. First, the manufacturing costs of annular fuel were evaluated. Since the manufacturing process of the annular fuel is very similar to the one used for solid fuel, and since the total volume of UO2 required is almost the same, the total cost of manufacturing annular fuel is expected to be only sligthly higher than that of solid fuel. The only additional costs are due to: capital costs of adding furnaces (the overall density of the fuel is smaller so more furnaces are required), capital costs for additional welding stations, marginal costs due to increased zirconium usage. Overall, the cost of manufacturing annular fuel was estimated to be \$5.02/MWh(e) *versus* \$5.00/MWh(e) for solid fuel.

The second step was to evaluate the effect of using annular fuel in an uprated PWR. Several options were considered for the type of plant and the Return On Equity (ROE) of these options are summarized in Table 1.2.

The case of up-rating an existing nuclear reactor will be discussed in greater details in the next chapter, and the effects of conservative assumptions involved in the early analysis will be examined.

Table 1.2: Summary of evaluated options and corresponding ROE (from Ref. [9]).

Plant type	Fuel type	ROE
1,717 MW(e) Generation III PWR	Annular	11.3%
1,717 MW(e) Generation III PWR	Solid	10.8%
1,117 MW(e) Generation III PWR	Annular	7.3%
1,117 MW(e) Generation III PWR	Solid	6.9%
600 MW(e) uprate to a Generation II PWR	Annular	6.3%

1.2 Motivation and Methodology

As of May 2007, 436 reactors operate worldwide. In the U.S. only, 103 nuclear reactors are in operation, providing 20 % of the electricity. Most of the cost of a nuclear power plant is capital cost: indeed building a reactor is an important investment but has a very low operating cost (including fuel cost).

Starting from these facts, a very intersting question arises: Is it both economically worthwhile and technically feasible to up-rate an existing reactor to use annular fuel? Indeed, annular fuel allows with relatively small capital investment, an increase by 50% of the power of an existing reactor. But the reactor will need to be shut down for a period of time to add new equipment.

In Ref. [4] a detailed cost analysis was performed to obtain a good evaluation of the cost involved. A simple transition to annular fuel was also investigated. The objective of the present work is to elaborate on this question, and look into more sophisticated ways of transitioning from solid to annular fuel through a mixed core composed of annular and solid assemblies to yield an economically more attractive solution. The question of whether this mixed core is technically feasible is then adressed and the demonstration of the feasibility of transitioning from an all solid core to an annular core at the nominal refueling rate is established.

Following this scope the present report is organised around three main tasks. First (Chapter 2), different cases of up rate transition are defined and evaluated from an economic point of view, and the most promising case is identified. Then (Chapter 3) the transition core with mixed solid and annular assemblies is evaluated in terms

of thermal-hydraulic performance. Finally (Chapter 4), the feasibility of the fuel management scheme within given constraints is established using a neutronic solver.

Chapter 2

Economic Assessment

Before getting into the technical challenge of using a mixed core, it is important to assess the economics of such an upgrade in an existing plant. Three main options will be studied, these options represent the three different ways of up-rating a Generation II PWR operating at 1200 MW(e) to 1800 MW(e).

2.1 The different options

The Base Case is the up-grade that was assessed in Ref. [9]. At year 0 the reactor is shutdown a one year construction period starts and money is invested. The construction is assumed to be undertaken co-incident with a scheduled 3 months steam generator replacement. The investment cost obviously takes into account the fact that the steam generator was to be replaced, and that the plant would have had to shut down for 3 months. Right after the construction, the 'old' solid core is removed, and a fresh core of annular fuel is charged in the reactor vessel.

Option 1 follows the same process (investment at year 0) except that the 'old' solid core is gradually replaced by an annular core. This means that at year 1 after all the components necessary to accomodate the uprate are replaced, the reactor will operate with 1/3 of annular fuel and 2/3 of solid fuel; at year 2.5 it will operate with 2/3 of annular fuel and 1/3 of solid fuel; and from year 4 on it will operate with annular fuel only. Essentially here no fuel is thrown away, but the fuel is rather

gradually replaced. This means that the up-rate in power is also gradual at 16.7% first, than 33.3% and eventually 50%.

Option 2 proceeds the other way around, but with the objective being still to avoid early replacement of the unburnt fuel. From year 0 to year 3, at every refueling of the reactor a batch of solid assemblies is discharged and a batch of annular assemblies is charged. This means that just at the end of year 3, the only remaining batch of solid assemblies is to be discharged. During this transition period, no up-rate is possible (plant runs at 100% power). At year 3 the investment is made, and the construction runs until year 4 when the plant is loaded with an annular core and can run at 150% power.

A summary of the three options is given in Table 2.1

Table 2.1: Schedule of the different options

<table>
<tr><th>Time (months)</th><th>Base-case</th><th>Case 1</th><th>Case 2</th></tr>
<tr><td>0</td><td rowspan="2">Construction period, core disposed</td><td rowspan="2">Construction period, remaining core kept</td><td rowspan="3">1/3 annular, 2/3 solid at 100% power</td></tr>
<tr><td>6</td></tr>
<tr><td>12</td><td rowspan="3">3/3 annular, at 150% power</td><td rowspan="3">1/3 annular, 2/3 solid at 117% power</td></tr>
<tr><td>18</td><td rowspan="3">2/3 annular, 1/3 solid at 100% power</td></tr>
<tr><td>24</td></tr>
<tr><td>30</td><td rowspan="3">3/3 annular, at 150% power</td><td rowspan="3">2/3 annular, 1/3 solid at 133% power</td></tr>
<tr><td>36</td><td rowspan="2">Construction period, remaining core kept</td></tr>
<tr><td>42</td></tr>
<tr><td>48</td><td rowspan="3">3/3 annular, at 150% power</td><td rowspan="3">3/3 annular, at 150% power</td><td rowspan="3">3/3 annular, at 150% power</td></tr>
<tr><td>54</td></tr>
<tr><td>60</td></tr>
</table>

2.2 The Internal Rate of Return Method

The method that is used here to assess the economic attractiveness of the different options is the so-called "Internal Rate of Return" or IRR [3](note that this rate is referred to as a Return On Equity in Ref. [4]).

The definition of the IRR (r) of a given financial flux F_j where j represents the

period of the flux, and N is the total number of periods during which the project operates, is the following:

$$\sum_{j=1}^{N} \frac{F_j}{(1+r)^j} = 0 \tag{2.1}$$

This rate is usually one of the tools used to assess the economic attractiveness of a given project.

For our case the most adequate time-scale is 6 months. Indeed the plant will be under construction for 12 months, and we considered an 18-month length refueling cycle, so the largest common divider is 6. Thus, in equation 2.1, $2j$ represents year j, and $2j+1$ represents year j and a half. This means that the r obtained is a rate over a six month period. As such a rate does not make lot of sense in terms of economic comparison, it is more convenient to convert it into an annual rate. To do this, simply assume that a bank will pay you an interest rate i_{6m} every 6 months. After one year, the interest received is $(1+i_{6m}) * (1+i_{6m}) = (1+i_{6m})^2$. Let us now compute the equivalent rate received over one year i_{1y}: the interest received simply amounts to $(1+i_{1y})$. Equating the two interests we obtain:

$$(1+i_{6m})^2 = (1+i_{1y}) \tag{2.2}$$

And therefore:

$$i_{1y} = (1+i_{6m})^2 - 1 \tag{2.3}$$

Note that if i_{6m} is small enough we get that $i_{1y} = 2i_{6m}$.

Consequently, an annual IRR is given by Equation 2.4

$$r_{1y} = (1+r_{6m})^2 - 1 \tag{2.4}$$

Difference between Internal Rate of Return and Return On Equity In Ref. [4], the Return On Equity (ROE) of the project is computed and used to assess the project. This value differs from the IRR in the sense that it accounts for the

discount rate. Essentially, the financial fluxes at each periods are discounted using the assumed discount rate, and the ROE is the rate at which the discounted cash flows should be discounted to obtain 0. Let us call r^* the ROE, and d the discount rate (needs to be specified). If the cash flow at period j is F_j then, over N periods, the ROE satisfies equation 2.5, where $\frac{F_j}{(1+d)^j}$ is the discounted cash flow over period j.

$$\sum_{j=1}^{N} \frac{\frac{F_j}{(1+d)^j}}{(1+r^*)^j} = 0 \tag{2.5}$$

For a given set of cash flows F_j with $j = \{1, 2, ..., N\}$, we therefore see that $(1+d)(1+ROE) = (1+IRR)$. If IRR, ROE and d are small enough compared to 1, then we have that:

$$IRR \approx ROE + d \tag{2.6}$$

What equation 2.6 tells us is that the ROE is what one can expect to earn on top of the discount rate. Therefore, a ROE of 0% would mean that the investment will earn a rate of return equals to the discount rate.

2.3 Evaluation of Options

2.3.1 Assumed Costs and Economic Conditions

The economic parameter used and their values are listed in Table 2.2

Although most of the costs come from Ref. [4] and Ref. [9], some important figures appear to need some discussion.

Cost of the lost fuel: To compute this cost, one can consider a 3 batchs core with a refueling period of 18 months. The first figure to obtain is the cost of a fresh batch. At steady-state, a nuclear reactor consumes one batch of fuel every 18 months. Knowing the electricity production during 18 months, and the price of fuel, one can easily compute the net price of a batch of fresh fuel per unit energy. The cost of the solid fuel per kWhr(e) indicated in Table 2.2 is 0.005 \$/kWhr(e). The energy,

Table 2.2: Parameters used in the calculations (from Ref. [4] and [9])

Description	Value
Total initial power	1200 MW(e)
Increase in power	600 MW(e)
Discount rate	11% /yr
Inflation rate for electricity price	1% /yr
Inflation rate for Fuel and O&M Costs	2% /yr
Capacity factor	95%
Former total capital cost	$1,090,200,000
Cost of Marginal Power Increase	$1,817 /kW(e)
Lost Power Supply during classic 3 months maintenance	$124,830,000
Replacement Cost of standard Steam Generators	$150,000,000
Total Capital Cost (w. steam generator cost, w/o 3 months lost power supply)	$940,200,000
Total Capital Cost (w/o steam generator cost, w/o 3 months lost power supply)	$815,370,000
Cost of solid fuel batch	$74,898,000
Construction time for power upgrade	1 year
Economic life-time (for capital cost recovery)	20 years
Retail Price for Produced Power	$0.050 /kWhr(e)
O&M Costs (BOP only)	$0.005 /kWhr(e)
Annular Fuel Cost	$0.00502 /kWhr(e)
Solid Fuel Cost	$0.005 /kWhr(e)

in kWhr(e), generated per batch is approximatly equal to $\frac{1200\ MW(e)}{3} \times 4.5 year \times 365\ days \times 24\ hr \times 95\% \approx 15,000\ GWhr(e)$. Therefore the product of these two figure is a good estimation of the price of a fresh batch of solid fuel, and one get for one fresh batch approximetly $0.005\$/kWhr(e) \times 15,000 GWhr(e) \approx \$75,000,000$.

The remaining estimation is to determine what is the value of the remaining core after a full cycle, or what is the money lost if the remaining core would be disposed of during a refuelling.

A good estimation is provided by Equation 2.7 [5], where n is the number of batches in the cycle, and P the price of a fresh batch.

$$\frac{n-1}{2}P \tag{2.7}$$

For a three batch core, equation 2.7 yields simply P.

Therefore, the price of the lost fuel, in case the remaining core is disposed of, is approximetly 75 M$.

Cost of Lost Power Supply during classic 3 months reconstruction: This is simply the price of electricity times the energy that would have been produced during 3 months.

Replacement Cost of standard Steam Generators: This figure is an estimation of the cost of a routine steam generator replacement (not including the lost production).

2.3.2 Results

An Excel Spreadsheet model was developped to compute the IRR of the project under the three different cases. Appendix A displays the details of the model, and shows the details of the calculations. The time step used is 6 months, in order to define accurately the schedule of the different cases. Two different options were considered. The first one is to assume that the construction of the up-rate equipment is done during a steam generator replacement (therefore the cost of the replacement of the

Steam Generator shall not incur financial costs for the project). This option is referred to as *w/o SG*: without the SG cost. The second option is simply that we do not deduce the cost of the SG replacement from the capital cost of the project. This is referred to as *w SG*.

Table 2.3 is a summary of the results for the three different cases of the IRR of the project.

Table 2.3: Internal Rate of Return for different options

Option	IRR w/o SG	IRR w SG
Base case	24.6%	20.7%
Case 1	20.8%	17.6%
Case 2	**27.4%**	**22.5%**

As explained earlier, the IRR differs from the ROE in that the IRR does not take the discount rate into account. The ROE of the project are given in Table 2.4 below.

2.3.3 Comments

It is interesting to note that Case 2 can boost the IRR by around 3 points simply by delaying the investment and "preparing" the core gradually for use of annular fuel. By managing the uprating of an existing plant, it is therefore possible to reach an IRR higher than 20%, which might make it an economically viable investment for utilities. This encouraging result is a strong incentive to pursue the technical assessment of such an option.

Table 2.4: Return On Equity for different options

Option	ROE w/o SG	ROE w SG
Base Case	12.3%	8.7%
Case 1	8.8%	5.9%
Case 2	**14.8%**	**10.4%**

On the other hand, it is clear that investigating Option 1 is probably not worthwhile. The cost of the wasted fuel is far too small compared to the loss of potential production.

One can also note that the inputs to the model are relatively conservative. Given the recent increase in the price of uranium, the price of fuel used in this assessment (around \$5/MWh(e)) might underestimate the actual cost of the fuel.

To illustrate this last point, a sensitivity analysis on the price of the fuel was performed. The result is presented in Figure 2-1.

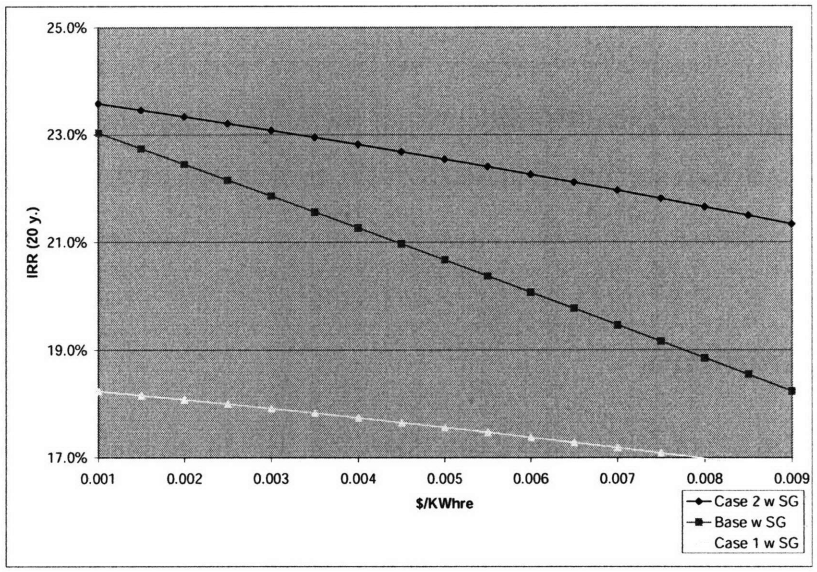

Figure 2-1: Evolution of IRR for Base Case, Case 1 and Case 2 with the fuel cost

For a broad range of fuel prices (ranging from \$0.001/kWh(e) to \$0.01/kWh(e)), Case 2 is still the most competitive option. In addition, given the fact that Option 1 and Option 2 "save" some fuel, the IRRs of these options are less sensitive to an increase in the fuel price. Therefore, we have strong reasons to believe that even if Uranium price increases Option 2 will remain the most competitive option.

2.4 Results in a Stochastic Environment

Even though the assessment above clearly identified a best option compared to the others, one could argue that one key assumption of the previous work, namely that inputs are known with certainty, is questionnable. To answer this legitimate question an analysis in uncertain environment was performed.

2.4.1 Methodology

The same model as for the deterministic analysis was used (namely an IRR calculation) in an Excel spread-sheet. Different input parameters (the "drving factors") were allowed to have normal distribution, thus taking random values at each calculation step. This distribution was created using the function *RAND()* in Excel. This function returns a real number between 0 and 1 with a uniform distribution [1]. The target value V was allowed to vary between a lower bound value V_{min} and an upper bound value V_{max} (see equation 2.8).

$$V = V_{min} + (V_{max} - V_{min}) * RAND() \tag{2.8}$$

From this on, a Monte-Carlo method is used to assess the response of the model to the stochastic input. Using the function *TABLE* of Excel, the model is run 2000 times, and the outputs are stored in a separate Spreadsheet. The outputs are easy to handle, and the most efficient way to analyse them is to sort them from minimum value to maximum value and order them in 20 different bins ranging between this two extreme values.

With the results, it is very easy to plot both the empirical probability distribution of the IRR and the probability density function as well. These curves will give information on both the mean IRR in stochastic environment and also the standard deviation of IRR.

The methodology is adapted from Ref. [11].

[1] Because of the Central Limit Theorem, the distribution type does not affect the results, so any kind of a distribution could be picked.

2.4.2 Uncertain Driving factors

The uncertainty about three main driving factors was investigated: the inflation of the cost of fuel, the inflation of the price of electricity sold and the capital cost. The assumptions on the variations of these parameters are summarized in Table 2.5. The choice of the three particular factors may seem over restrictive, but they can by themselves already cover a lot of the uncertainties carried by the project. For instance, even if then total duration of the construction period was not considered it can be argued that an increase in the construction period can be more or less reflected in an increase in the capital cost. Similarly, the Operation and Maintenance costs are assumed to behave as planned but in fact their fluctuation can be embeded in the variation of the fuel cost.

Table 2.5: Mean and range of studied driving factors

Driving factor	Mean value	Normally distributed btw.
Fuel cost inflation	2%	1-3%
Price of electricity inflation	1%	0-2%
Capital cost	$ 815,370,000	(-10%)-(+30%)

2.4.3 Results and discussion

The resulting effects of introducing uncertainties in the model will be that the mean value will be changed, and also that the possible outcomes will be spread around the mean.

The following Tables represent the results of the different assessments. Tables 2.6, 2.7 through 2.11 give an idea of the mean of the IRR, but also of the spread around this mean.

The first thing to be noted is that even when allowing for uncertainties, case 2 remains the most promising one. The second observation is that the impact of uncertainties is small compared to the perturbation applied.

In order to have a more visual representation of the results, the variation in IRR

Table 2.6: Stochastics results for Base Case with Steam Generator cost

	Probability that IRR is smaller than cell value				
	P=95%	P=75%	P=50%	P=25%	P=5%
Fuel price inflation (50%)	20.76%	20.72%	20.68%	20.64%	20.59%
Elec price inflation (50%)	20.82%	20.73%	20.67%	20.61%	20.53%
Capital cost (10%)	22.92%	20.75%	18.63%	16.71%	15.29%

Table 2.7: Stochastics results for Case 1 with Steam Generator cost

	Probability that IRR is smaller than cell value				
	P=95%	P=75%	P=50%	P=25%	P=5%
Fuel price inflation (50%)	17.64%	17.59%	17.56%	17.53%	17.49%
Elec price inflation (50%)	17.70%	17.62%	17.56%	17.51%	17.42%
Capital cost (10%)	19.30%	17.47%	15.65%	14.18%	13.00%

Table 2.8: Stochastics results for Case 2 with Steam Generator cost

	Probability that IRR is smaller than cell value				
	P=95%	P=75%	P=50%	P=25%	P=5%
Fuel price inflation (50%)	22.79%	22.69%	22.54%	22.41%	22.29%
Elec price inflation (50%)	23.10%	22.86%	22.56%	22.22%	21.94%
Capital cost (10%)	25.17%	22.76%	19.78%	17.47%	16.02%

Table 2.9: Stochastics results for Base Case without Steam Generator cost

	Probability that IRR is smaller than cell value				
	P=95%	P=75%	P=50%	P=25%	P=5%
Fuel price inflation (50%)	24.79%	24.74%	24.70%	24.66%	24.61%
Elec price inflation (50%)	26.68%	26.46%	26.29%	26.10%	25.84%
Capital cost (10%)	27.67%	24.70%	21.82%	19.29%	17.65%

Table 2.10: Stochastics results for Case 1 without Steam Generator cost

	Probability that IRR is smaller than cell value				
	P=95%	P=75%	P=50%	P=25%	P=5%
Fuel price inflation (50%)	20.90%	20.85%	20.82%	20.79%	20.74%
Elec price inflation (50%)	20.95%	20.84%	20.76%	20.69%	20.58%
Capital cost (10%)	23.11%	20.82%	18.41%	16.31%	15.01%

Table 2.11: Stochastics results for Case 2 without Steam Generator cost

	Probability that IRR is smaller than cell value				
	P=95%	P=75%	P=50%	P=25%	P=5%
Fuel price inflation (50%)	27.56%	27.52%	27.49%	27.46%	27.42%
Elec price inflation (50%)	31.55%	30.95%	30.24%	29.52%	28.87%
Capital cost (10%)	31.14%	27.38%	23.62%	20.81%	18.86%

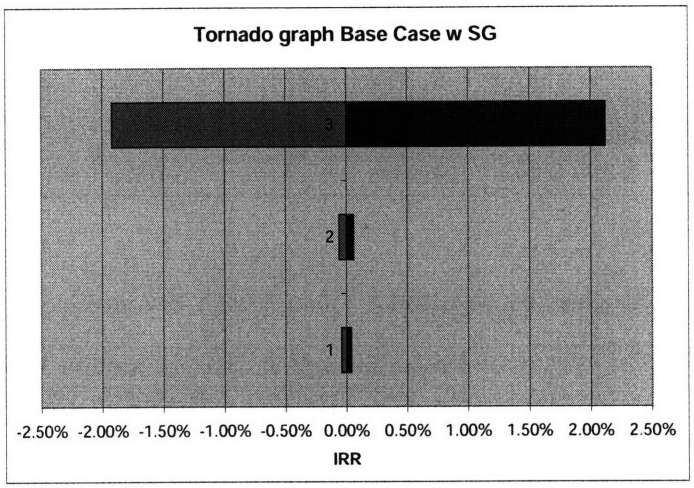

Figure 2-2: Effect of uncertainties for Base Case w. Steam Generator cost (1=Fuel price inflation, 2=Electricity price inflation, 3=Capital Cost)

are plotted on a *tornado* graph. This graph compares the effect of the different driving factors studied on the IRR.

In Figures 2-2 through 2-7 each histogram is centered at zero. The left side represents the maximum negative deviation of IRR with probability 75%. The right side represents the maximum positive deviation of IRR with probability 25%. In a sense, the tornado graph represent the risk of the project to specific factors.

In addition, (1) represents fuel inflation factor, (2) represents Electricity price inflation factor, (3) represents the capital cost factor.

From these graphs we conclude that the uncertainties effect of the fuel cost and

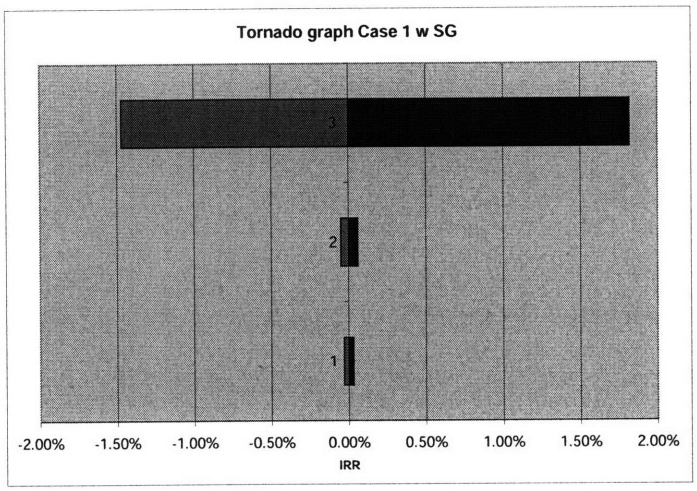

Figure 2-3: Effect of uncertainties for Case 1 w. Steam Generator cost (1=Fuel price inflation, 2=Electricity price inflation, 3=Capital Cost)

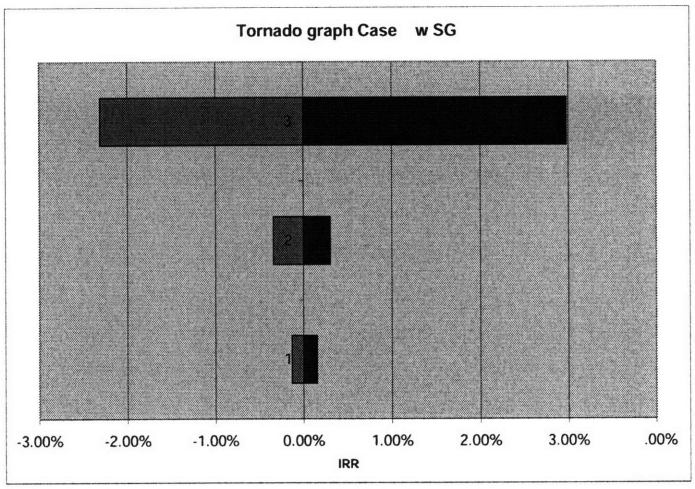

Figure 2-4: Effect of uncertainties for Case 2 w. Steam Generator cost (1=Fuel price inflation, 2=Electricity price inflation, 3=Capital Cost)

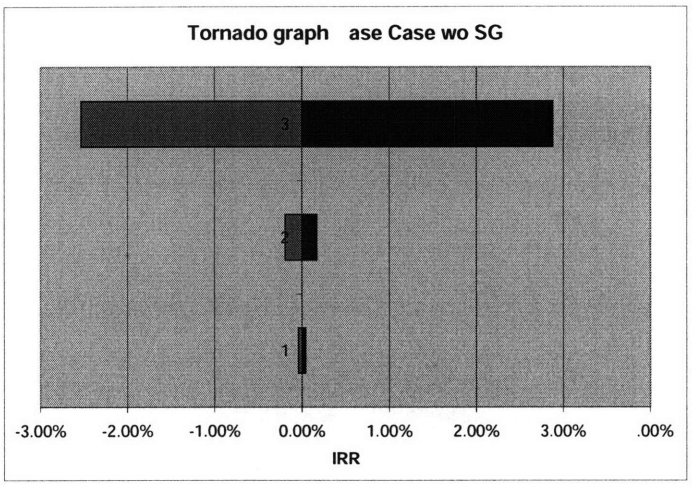

Figure 2-5: Effect of uncertainties for Base Case w/o Steam Generator cost (1=Fuel price inflation, 2=Electricity price inflation, 3=Capital Cost)

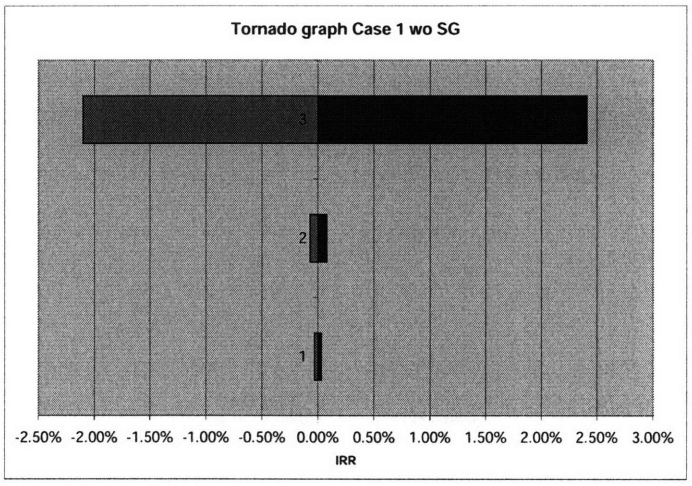

Figure 2-6: Effect of uncertainties for Case 1 w/o Steam Generator cost (1=Fuel price inflation, 2=Electricity price inflation, 3=Capital Cost)

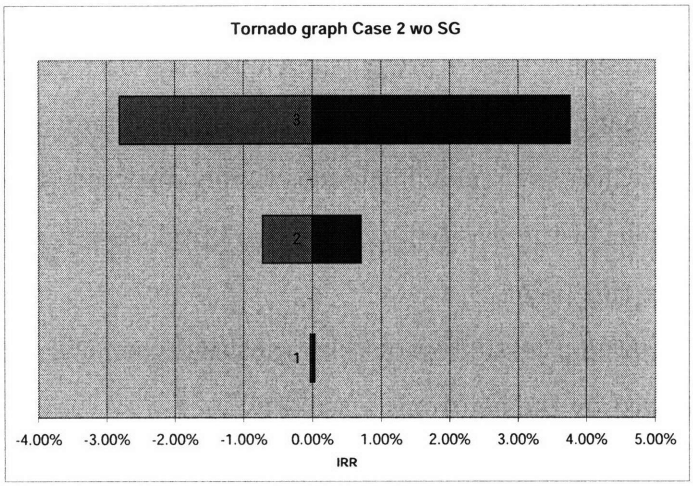

Figure 2-7: Effect of uncertainties for Case 2 w/o Steam Generator cost (1=Fuel price inflation, 2=Electricity price inflation, 3=Capital Cost)

the price of electricity do not have a very large impact on the economic attractiveness of the project. The capital cost has the largest impact. In addition, the effects of uncertainties are more pronounced for Case 2.

2.5 Conclusion

The economic assessment was performed as a two step process. First a deterministic analysis was done. We concluded that Case 2, the case in which the investement is postponed until the core is ready to be uprated, is with comfortable margins the most attractive with a mean IRR of 27.4% if the cost of the Steam Generator can be deduced or 22.5% if not.

Following this outcome, uncertainties were introduced. We showed that the effects of uncertainties are moderate. Uncertainties in the capital cost have the largest influence on the IRR of the project. Nevertheless the main conclusion is that even when introducing uncertainties, with a large probability (over 95%) Case 2 is still the

most attractive one.

As a general conclusion in the following chapters, we will focus primarily on Case 2 for further investigations. Case 2 presents obviously the best economic asset. Let's also keep in mind that Case 2 is a more subtle, and therefore complicated, option than the Base Case where the remaining core is simply disposed of. This implies that a technical assessment of the feasibility of such an option is not trivial and remains an open-question at this point.

The thermal-hydraulic feasibility of this transition core will be assessed in the next chapter, followed by the neutronic feasibility.

Chapter 3

Thermal-hydraulic Assessment

In order to assess the technical feasability of using a core composed partly of annular fuel and partly of solid fuel assemblies in a PWR, it is necessary to assess the thermal-hydraulic behavior of such a core. The particular features we need to investigate are whether the flow distribution through the core will still provide acceptable MDNBR value and the total pressure drop.

The thermal-hydraulic simulations were performed using VIPRE-01 code (Ref. [12]).

The analysis is made in two steps: *(1)*first create a simple model composed of two eigths of a solid assembly and an annular assembly, respectively. This simple model is used to acquire insight into the behavior of the two fuel types put next to one another. *(2)* secondly, the whole core is modeled to account for mixing effects and the core-wide flow distribution. The insights obtained from the simple model guided the development of the whole-core model.

The first simple model is referred to as *"Mixed assembly model"*, whereas the full core model is referred to as *"Mixed core model"*.

3.1 Descritpion of VIPRE code, and input data

3.1.1 VIPRE-01 code application to annular fuel

The assessment was done using VIPRE-01 (Versatile Internals and Component Program for Reactors; EPRI) code [12]. This thermal-hydraulic code has been used in a previous study to model a whole annular core [9] and is widely used by nuclear reactor utilities. The code has also been certified by the NRC.

Initially the code was developed for solid fuel, but wisely enough the code included a large margin for user inferred geometry and inputs. When dealing with solid fuel, an option allows the user to define the fuel rod as a "rod". But it is also possible to model a "hollow cylinder" composed of different materials. Therefore it is actually very simple to model an annular rod by first creating the annular rod material (composed of 5 layers: inside cladding, inside gap, fuel, outside gap and outside cladding), and then creating a hollow rod. This rod is internally cooled by an inside channel, and externally cooled by four adjacent external channels. This pattern is summarized in Figure 3-1.

It is also important to note that VIPRE-01 inputs have to be specified in British units.

3.1.2 Parameters and correlations used

Geometry of the fuels

The two kinds of fuel assemblies we are intersted in are the typical solid fuel rod of the Westinghouse 17x17 design and an annular fuel rod in a 13x13 assembly [9].

Table 3.1 summarizes the geometrical parameters of both the 13x13 annular fuel assembly, and the solid 17x17 fuel assembly.

Parameters of the reactor

For our modelling the parameters of a typical Westinghouse 4-loop PWR were used based on [6]. We recall the different parameters in Table 3.2

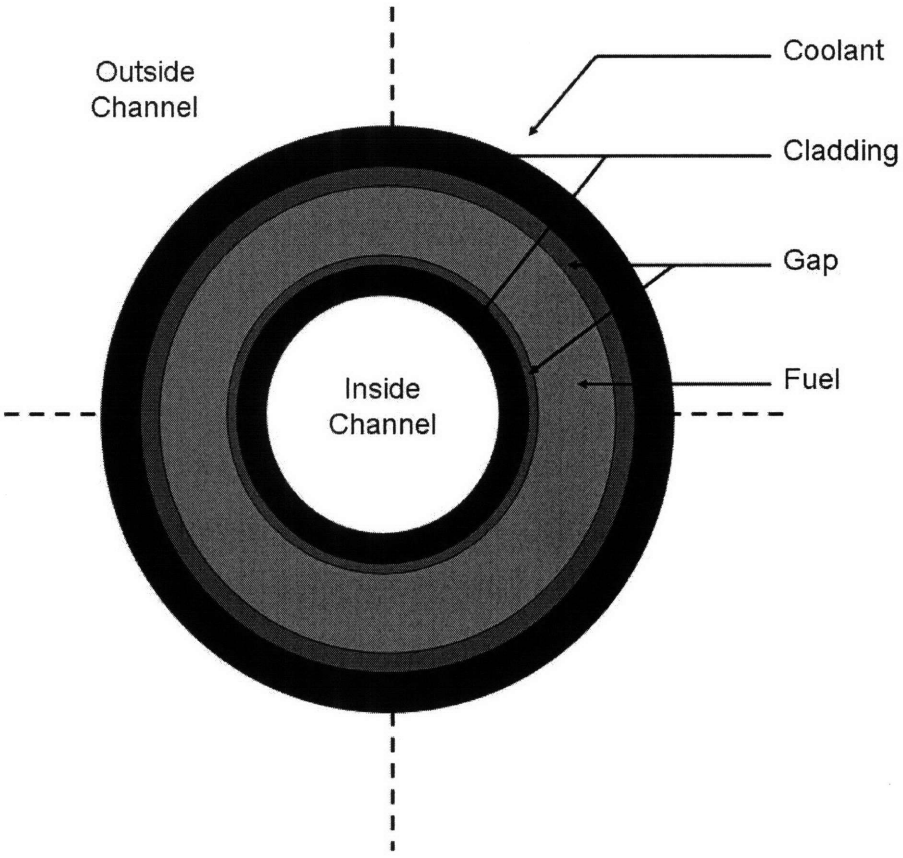

Figure 3-1: Cross-section of an annular fuel pin with hydraulic channels

Table 3.1: Geomerty of the annular fuel assembly and the solid fuel assembly

Annular fuel assembly	Array size	13x13	
	Assembly pitch	8.465 in	21.5 cm
	Pin pitch	0.650 in	1.651 cm
	Rod inner dia.	0.340 in	0.864 cm
	Inner clad outer dia.	0.385 in	0.978 cm
	Fuel inner dia.	0.390 in	0.991 cm
	Fuel outer dia.	0.555 in	1.410 cm
	Outer clad inner dia.	0.560 in	1.422 cm
	Rod outer dia.	0.605 in	1.537 cm
	Guide tube dia.	0.605 in	1.537 cm
	Outer channel area	0.135 in^2	0.871 cm^2
	Inner channel area	0.091 in^2	0.587 cm^2
	Heated perim. out.	1.901 in	4.829 cm
	Heated perim. in.	1.068 in	2.713 cm
	Equivalent dia. out.	0.284 in	0.721 cm
	Equivalent dia. in.	0.340 in	0.864 cm
Solid fuel assembly	Array size	17x17	
	Assembly pitch	8.465 in	21.5 cm
	Pin Pitch	0.497 in	1.262 cm
	Fuel outer dia.	0.325 in	0.826 cm
	Clad inner dia.	0.330 in	0.838 cm
	Clad outer dia.	0.375 in	0.953 cm
	Guide outer dia.	0.482 in	1.224 cm
	Coolant channel area	0.137 in^2	0.884 cm^2
	Heated perim.	1.178 in	2.992 cm
	Equivalent dia.	0.465 in	1.181 cm

Table 3.2: Major parameters for a typical 4-loop PWR using solid fuel (from [6])

Parameters for a 4-loop PWR	
1. Plant	
Number of primary loops	4
Reactor thermal power ($MWth$)	3411
Total plant thermal efficiency (%)	34
Plant electrical output (MWe)	1150
Power generated directly in coolant (%)	2.6
Power generated in fuel (%)	97.4
2. Core	
Core barrel inside diameter / outside diameter (m)	3.76/3.87
Rated power density (kW/L)	104.5
Core voume (m^3)	32.6
Effective core flow area (m^2)	4.747
Active heat transfer surface area (m^2)	5546.3
Average heat flux (kW/m^2)	598.8
Design axial enthalpy rise peaking factor ($F_{\delta h}$)	1.65
Allowable core total peaking factor (F_Q)	2.5
3. Primary coolant	
System pressure (MPa)	15.5
Core inlet temperature ($\circ C$)	292.7
Average temperature rise in reactor ($\circ C$)	33.4
Total core flow rate (Mg/s)	18.63
Effective core flow rate for heat removal (Mg/s)	17.7
Average core inlet mass flux (kg/m^2s)	3,729
4. Fuel rods	
Total number	50,952
Fuel density (% *of theoretical*)	94
Cladding material	Zircaloy-4
Active fuel height (m)	3.66
5. Fuel assemblies	
Number of assemblies	193
Number of heated rods per assembly	264
Number of grids per assembly	7
Fuel assembly effective flow area (m^2)	0.02458
Location of first spacer grid above beginning of heated length (m)	0.3048
Grid spacing (m)	0.508
Grid-type	L-type
Number of control rod thimbles per assembly	24
Number of instrument tubes	1
6. Rod cluster control assemblies	
Neutron absorbing material	Ag-In-Cd
Cladding material	Type 304 SS
Cladding thickness (mm)	0.46
Number of cluster Full/Part length	53/8
Number of absorber rods per cluster	24

Based on Table 3.2, the parameters used for the models are given in Table 3.4.

Table 3.4: Inputs used for the mixed assembly and the full core models

Operating pressure	2248.1 psi
Inlet temperature	562.4 $°F^*$
Flow rate (1/8 whole core)	4877.31 lb/s^{**}
Flow rate (1/4 assembly)	50.42 lb/s^{**}
Assembly peaking factor	1.587
Over-power margin (transient)	18 %

*: Table 3.2 value increased by 2 °C

**: Table 3.2 value decreased by 5 % to account for bypass

Correlations employed

Before giving an exhaustive list of correlations used in the VIPRE-01 models, two main features have to be discussed more in details: the turbulent mixing coefficient β, and the resistance to lateral flow. These two parameters have an appreciable effect on the thermal-hydraulic behavior of the system.

First, let us discuss the turbulent model adopted. The way of defining the cross flow w' (in $lb/sec - ft$) resulting of an axial flow $\bar{G}$ (in $lb/sec - ft^2$) over a gap of length s (in ft) is given by Equation 3.1.

$$w' = \beta s G \tag{3.1}$$

The effect of turbulent mixing is a better mixing of the enthalpy, which leads to a reduction in magnitude of enthalpy differences among channels and thus increased MDNBR. Larger turbulent mixing coefficient *i.e.* larger β will lead to a larger MDNBR. According to [13], a mixing coefficient of 0.076 for a rod bundle with small mixing vanes has been observed. Nevertheless, given the fact that annular channels have smaller gap width, it has been assumed that $\beta = 0.0$. This means that no mixing is allowed and this assumption will yield a conservative MDNBR. NRC also states that a zero mixing should be assumed unless experiments could demonstrate a stricly positive value.

Secondly, the resistance to lateral flow is the key parameter determining the pressure drop across channels Δp_{cross} which drives cross flow. Δp_{cross} is defined in 3.2.

$$\Delta p_{cross} = K_G \frac{|w|wv'}{2s^2} \tag{3.2}$$

K_G is the lateral resistance coefficient, w is the cross flow, v' the specific volume for momentum, and s is the gap width. A good value for K_G is 0.5, but as stated later K_G was taken to be a maximum of a laminar term and a turbulent term. The turbulent term was taken as the more conservative between the annular and the solid fuel using correlations from [1]. In addition, it was showed by a sensitivity analysis that this parameter had no impact at all on the MDNBR.

Axial power distribution: The axial power distribution was assumed to be a chopped cosine with peak to average of 1.55.

Water properties function: the water properties function used is the EPRI water properties function, which is applied to compute all fluid properties. No tables are needed for this correlation.

Void correlation: The EPRI correlation was used for the subcooled void. We used the Zuber-Findlay void drift correlation with coefficients developed for the EPRI void model; finally the Columbia/EPRI correlation was used for the two-phase friction multiplier.

Heat transfer correlation: The Dittus-Boelter correlation was used for the single-phase flow, whereas the Thom correlation was used for subcooled and saturated nucleate boiling

DNB analysis for inner channel: The W-3S correlation was used which does not have any grid mixing factor.

DNB analysis for outer channel: The W3-L correlation was used with a grid mixing factor of 0.043, a grid spacing factor of 0.066 and a grid factor leading coefficient of 0.986.

Turbulent mixing model: As discussed above, we conservatively choose $\beta = 0.0$.

Turbulent momentum factor: FTM=0.0, which means that the turbulent cross flow can only mix enthalpy (and not momentum). Again this value is conservative.

Axial friction factor: The correlation is of the form

$$f_{ax} = Max(0.316Re^{-0.25}; 64.0Re^{-1.0}) \tag{3.3}$$

The first term represents the turbulent case, the second term the laminar one.

Lateral drag correlation: This correlation is also defined as the maximum of a laminar term and a turbulent term. $K_G = Max(K_{turb}; K_{lam})$, with $K_{turb} = 3.098Re^{-0.2}$ and $K_{lam} = 0.5$ (from Ref. [12]).

Form loss coefficients: The inlet form loss is assumed to be 0.4. The outlet form loss is 1.0. A form loss of 0.6 was assumed for the mixing vanes grids (this grids are only seen by outside channels).

The correlations are summarized in Table 3.5.

3.2 Mixed Assembly model

3.2.1 Overall presentation of the model

The basic idea of this first model is to simulate the thermal-hydraulic behavior of two assemblies of respectively solid and annular fuel. The overall picture of the model is given by Figure 3-2 which represents two eigths of assemblies joined together.

Table 3.5: Correlations used in the VIPRE-01 models

Parameter	Correlation or value
Axial power distribution	Chopped cosine with peak to average of 1.55
Water properties function	EPRI water properties function
Void correlation for subcooled void	EPRI correlation
Void drift correlation	Zuber-Findlay correlation, coefficients from EPRI
Two-phase friction multiplier	Columbia/EPRI correlation
Heat transfer correlation (single phase)	Dittus-Boelter correlation
Heat transfer correlation (subcooled and saturated nucleate boiling)	Thom correlation
DNB analysis for inner channel	W-3S, grid mixing factor of 0.0
DNB analysis for outer channel	W3-L, grid mixing factor of 0.043, grid spacing factor 0.066, grid factor leading coefficient 0.986
Turbulent mixing model	$\beta = 0$
Turbulent momentum factor	$FTM = 0$
Axial friction factor	$f_{ax} = Max(0.316Re^{-0.25}; 64.0Re^{-1.0})$
Lateral drag correlation	$K_G = Max(3.098Re^{-0.2}; 0.5)$
Form loss coefficients	inlet: 0.4, outlet 1.0, mixing vanes grids 0.6

In order to provide a reference "solid" case to compare our results with, a similar model of two eights of solid assemblies joined together was set up. The overall representation of the solid assemblies model is given on Figure 3-3.

3.2.2 Power Distribution and detailed model description

Parameters

At this stage of the study, the neutronic analysis had not been performed yet because it seemed more important to first evaluate the thermal-hydraulic part of the problem before assessing the neutronic of the core. Therefore, the power distribution adopted is, for the solid part the standard Westinghouse "hot assembly" distribution (see Figure 3.2.2), and for the annular part the power distribution obtained in the case of

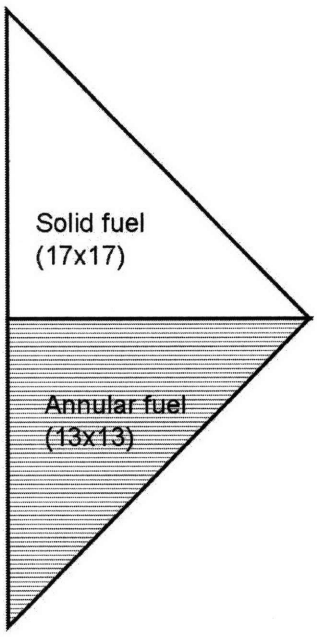

Figure 3-2: Schematic of one fourth of the mixed assembly model

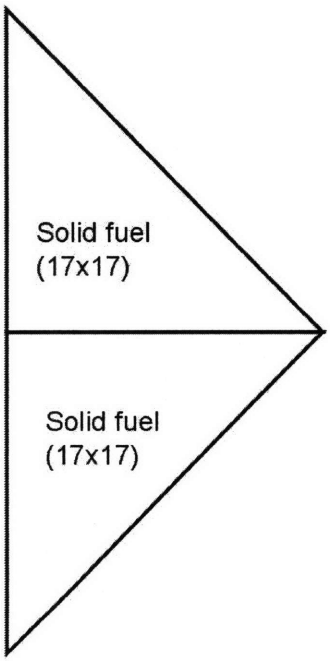

Figure 3-3: Schematic of one eigth of the solid assembly model

a full annular core [9], and reproduced on Figure 3-5.

Note that Figure 3-5 factors are not normalized to 1.000 but to the assigned peaking factor of 1.587, whereas in Figure 3.2.2 the intra-assembly factors are normalized to 1.000.

The principal parameters of the models are summarized in Table 3.6. The average assembly power per rod q_M is a weighted average of the power per rod in the annular assembly, and in the solid assembly.

$$q_M = \frac{q_A(13^2 - 9) + q_S(17^2 - 25)}{13^2 - 9 + 17^2 - 25} \tag{3.4}$$

Where q_A and q_S are the power per rod in the annular assembly and the solid assembly respectively. So we have $q_A = \frac{Q_{th}}{Total\ number\ of\ rod\ in\ annular\ core} = \frac{3411\ MW(th)}{193*(13*13-9)} \approx$ 110.5 kW/rod. Similarly, $q_S = 66.9\ kW/rod$.

Given the different number of rods in the annular assembly $(13^2 - 9)$ *versus* solid assembly $(17^2 - 25)$, it is clear that the peaking factor assigned to each rod in the input file has to reflect this difference. In order to get a good representation, each 1/8th of assembly was treated seperatly. The peaking factor were normalized to 1.000 and then the annular rods where weighted with $n_A = \frac{N_A+N_S}{2N_A} \approx 1.325$ and the solid rods with $n_S = \frac{N_A+N_S}{2N_S} \approx 0.803$, where N_A is the number of annular rods in an assembly, and N_S the number of solid rods in an assembly.

Table 3.6: Parameters in the Mix-assembly model

Model size	2*1/8th of assembly
Operating pressure	2248.1 psi (15.5 MPa)
Inlet Temp.*	558.9 F (294.7 C)
Mass flux**	50.421 lb/s (22.87 kg/s)
Average power per rod†	156.2 kW/rod
Peaking factor	1.587
Additional power margin	18%

* *2 C higher than operating Temp.*
** *5% lower than total flow to account for bypass*
† *18% overpower*

The input file for VIPRE-01 is given in Appendix B.

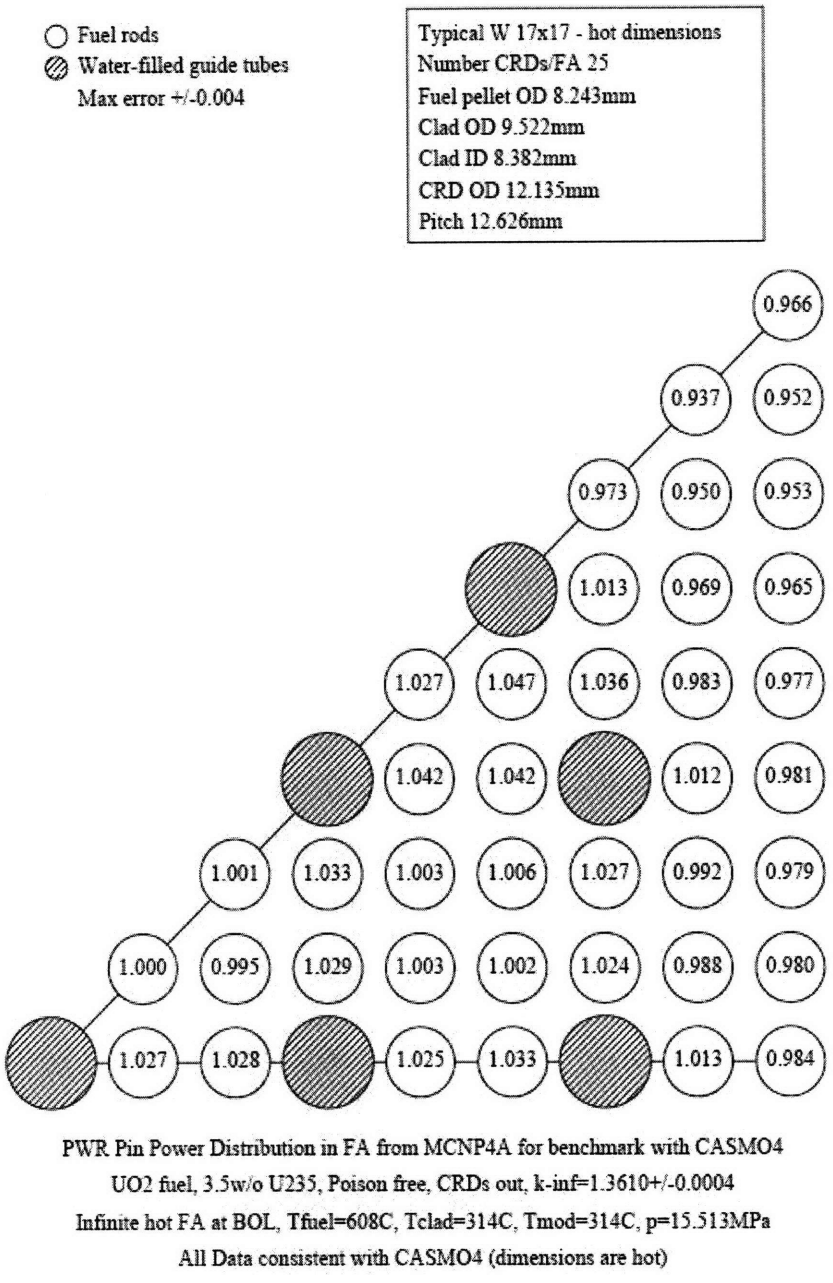

Figure 3-4: Westinghouse power distribution for hot solid assembly

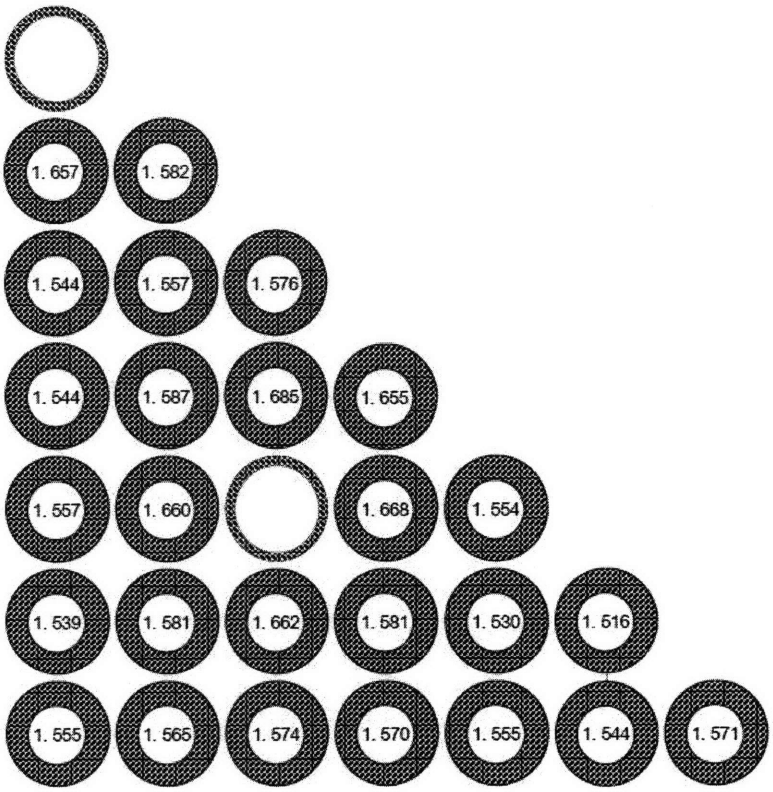

Figure 3-5: Power distribution for hot annular assembly (fron [9])

Channel numbering

Figure 3.2.2 and 3.2.2 show the numbering of the channels and the rods for the mixed assembly model, and the solid assembly model.

Methodology

The methodology employed was a two step method. The idea is to make our simple model as close to the real "hot" assembly as possible. The first step consists of a run at average core power (plus 18% overpower) and VIPRE-01 solves for the core-average pressure drop. This gives a good approximation for what the core pressure drop will be. The second step is a run at hot assembly power with the assigned pressure drop from step one calculation.

Adopting this methodology yields more conservative results than directly simulating an unconstrained pressure drop at hot power because the pressure drop at core average power is expected to be smaller than the pressure drop at hot power, and there was no opportunity for having this feedback in the two-step approach.

3.2.3 Results

Pressure drop at 100% power

For a 100% power, which correponds in the solid case to $P_{Solid} = 66.9\ kW/rod$ and in the mixed case to $P_{Mix} = 83.4 kW/rod$ we obtain the following results:

- For solid assembly model: $\Delta P_{Solid} = 17.89\ psi\ (0.123\ MPa)$
- For mixed assembly model: $\Delta P_{Mix} = 18.00\ psi\ (0.124\ MPa)$

The larger pressure drop for the mixed assembly than for the solid assembly is consistent with the fact that the annular assembly has a smaller equivalent diameter than the solid assembly and thus sligthly larger ΔP. Nevertheless, the difference in pressure drops is very small (less than 1%) and this is due to the fact that in the design of the annular assembly, an assembly geometry yielding comparable pressure

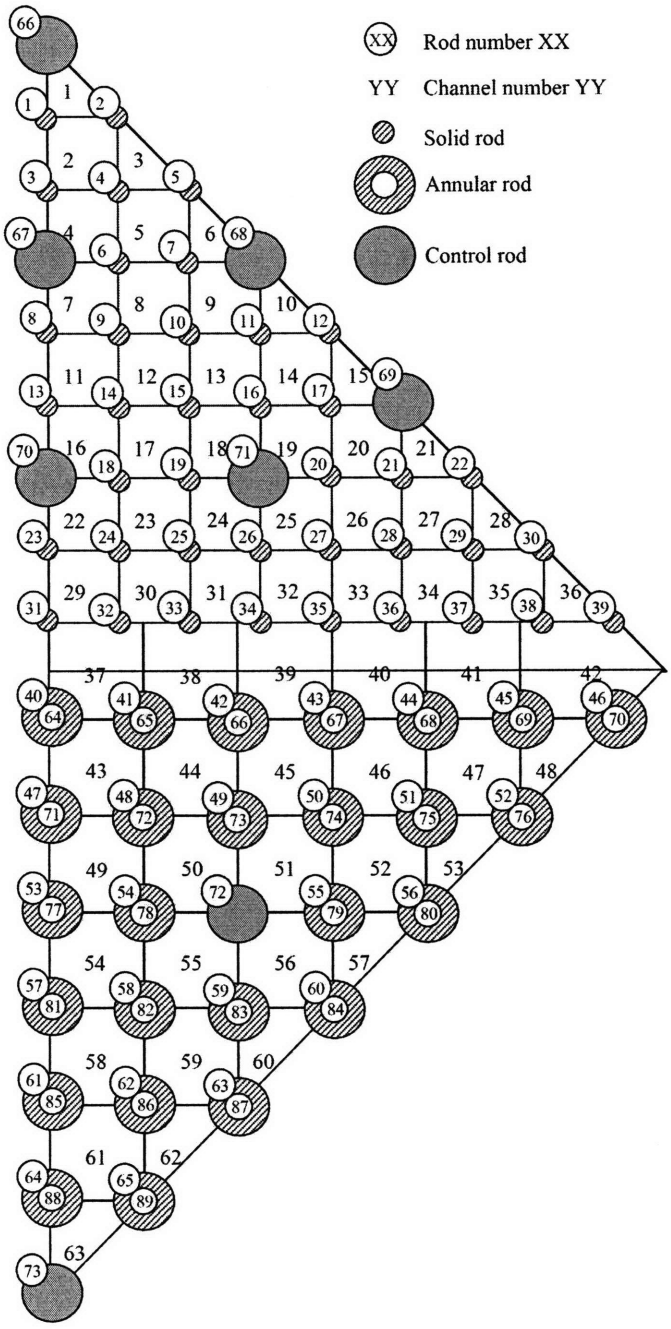

Figure 3-6: Channels and rods numbering for Mixed assembly model.

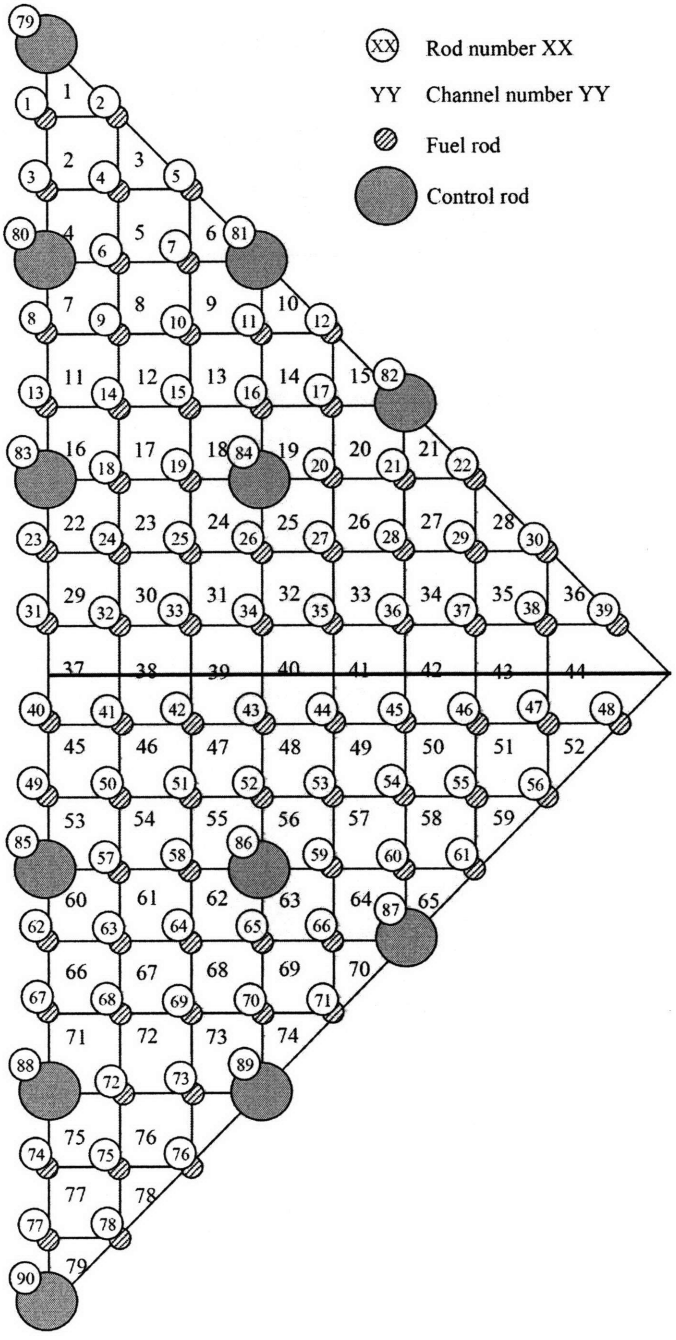

Figure 3-7: Channels and rods numbering for Mixed assembly model.

drops (with slightly larger ΔP in annular fuel assemblies) with the solid assembly was developed [9].

MDNBR at "hot" power

As explained above, the code was then run with the fixed ΔP found at 100%. It is intersting to note that the MDNBR was reached in both the Solid assembly model and the Mixed assembly model in the same channel, located in the solid part, and which corresponds to the solid hot channel.

- For solid assembly model: $MDNBR_{Solid} = 1.309$
- For mixed assembly model outer channels: $MDNBR_{Mix\ Out} = 1.320$
- For mixed assembly model inner channels: $MDNBR_{Mix\ In} = 1.828$

These results show that the annular fuel part not only has a large DNBR, but it also has a positive effect on the MDNBR which occurs in solid rods.

The explanation of this phenomenon is to be found in what mostly drives the DNB. The peaking factors of the rods surrounding a channel are very important, but we were cautious enough in our normalization to assign the same power per rod in the Mixed assembly model as in the Solid assembly model. The mass flux is also important: the higher the mass flow, the higher DNBR is.

It turns out that the mass flow rate in the Mixed model is different than in the Solid model. To illustrate this, we have plotted in Figures 3-8 and 3-9 the axial evolution of the mass flow rate for the mixed assembly model, and for the solid assembly model.

Note: the hot channel is channel 14 for both models.

Figure 3-9 shows the classic picture expected in case of solid fuel: the mass flow rate in the hot channel has overall decreased from the inlet to the outlet. On the other hand Figure 3-8 is much more intriguing at first sight: we can see that in the hot channel (and in the solid channels in general) the channel tends to first gain some mass flux, before eventually gradually loosing some. Overall, the hot channel has almost the same mass velocity at the inlet and at the oulet.

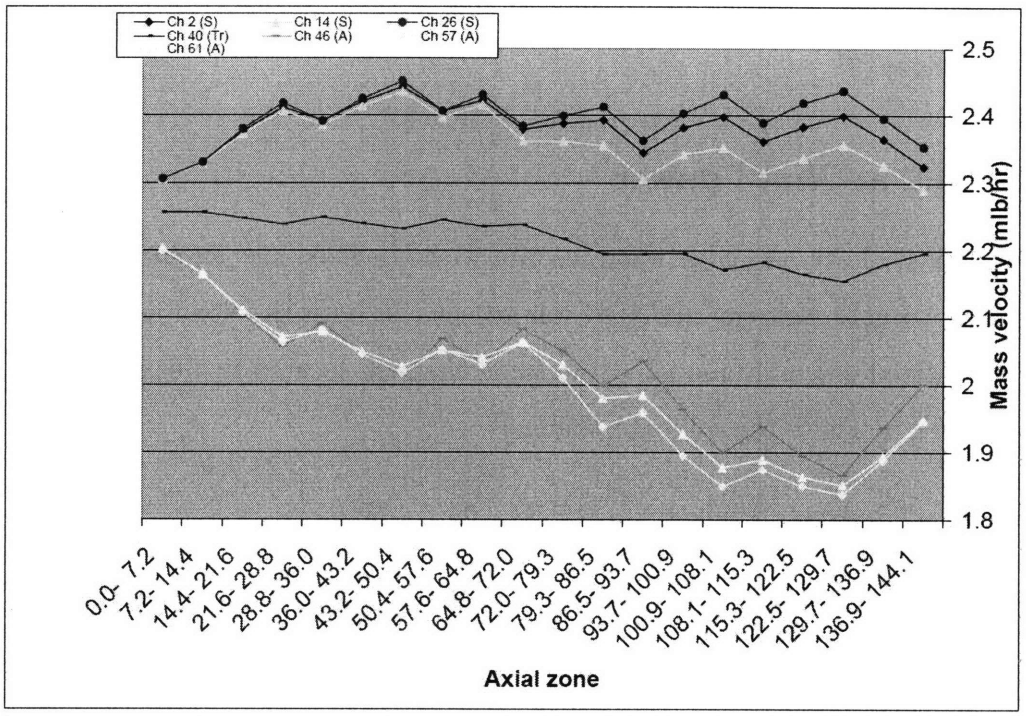

Figure 3-8: Mass velocity in different channels (S: Solid channel, A: Annular outter channel, Tr: transition channel) for mixed assembly model

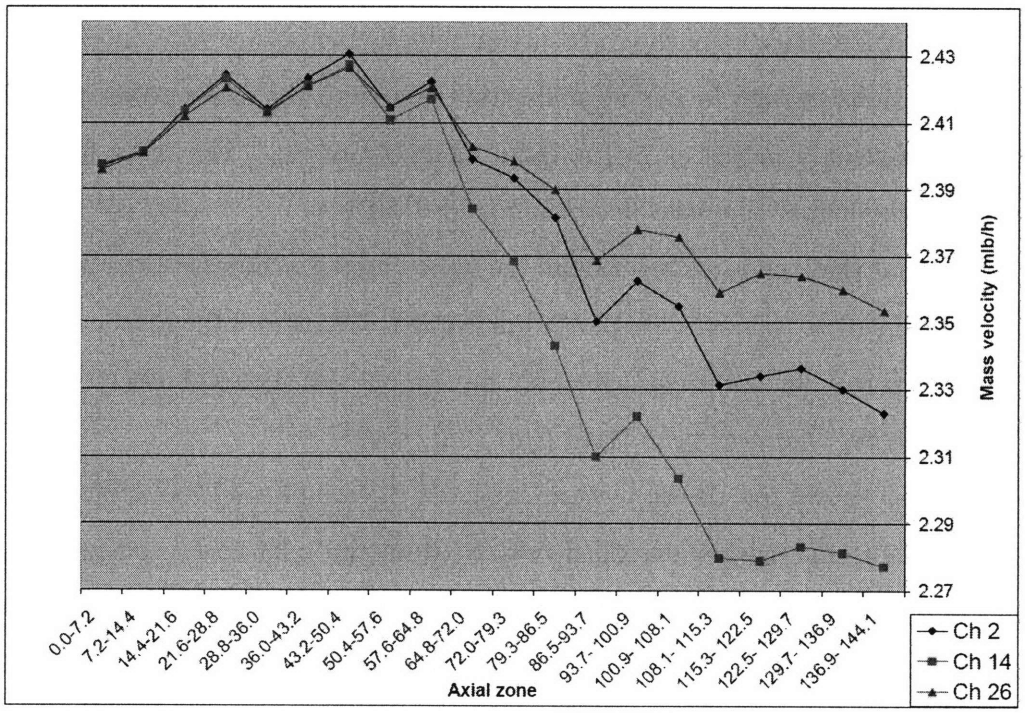

Figure 3-9: Mass velocity in different channels for the solid assembly model

Figure 3-10 compares the two mass velocities in the hot channel.

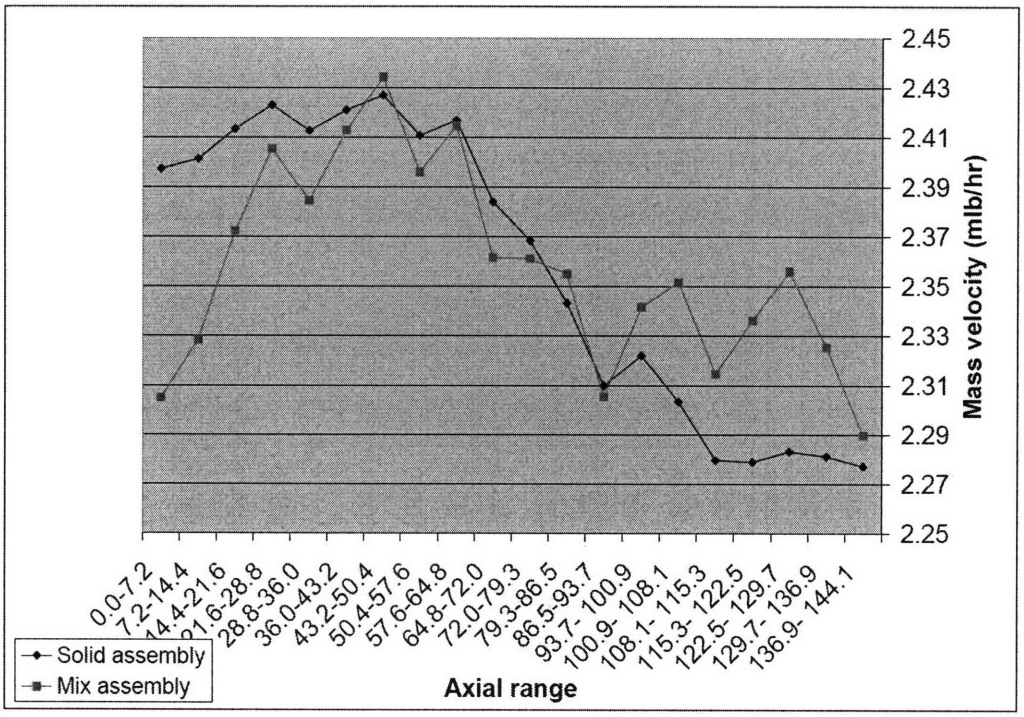

Figure 3-10: Comparison of mass velocities in the hot channel of the Solid model *v.s.* the mixed model

It is also of interest for us to locate more precisely the occurrence of MDNBR. Figure 3-11 shows that MDNBR is reached around axial nodes 108.1-115.3 inches. Looking at this particular zone in Figure 3-10 we can see that the mass velocity in the mixed assembly model is higher than the solid assembly model. This is the main reason why MDNBR is slightly better in the mixed assembly model.

But why does the mass velocity has this value in the mixed assembly model? An answer to this question is suggested by looking at Figure 3-8. We can clearly see three different trends on this graph:

- Solid channels: mass velocity increases and then decreases. Overall there is a gain or stability of mass flow rate.

- Transition channels (at the interface solid/annular): mass flow rate remains mostly constant.

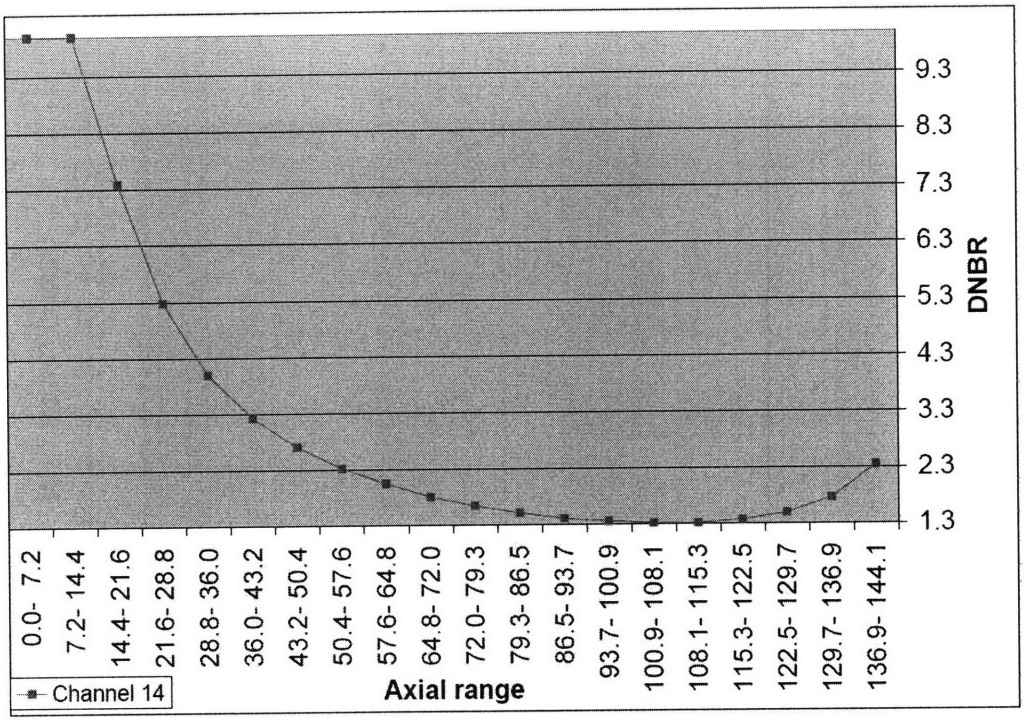

Figure 3-11: DNBR in the hot channel for the mixed assembly model

- Annular channels: mass velocity decreases and then increases. Overall there is loss of mass flow rate.

What is lost in some channels must be gained in others: annular channels loose some mass velocity to the benefit of the solid channels.

In order to understand this behavior, we have to ask ourselves what is driving the mass flux? Part of the answer is the equilibrium quality. Figure 3-12 shows the axial evolution of the equilibrium quality in different channels for the mixed assembly model. The main conclusion of this graphic is that the annular channels have a higher equilibrium quality than the solid channels. Therefore, the fluid boils earlier in the annular channels increasing earlier the hydraulic resistance and forcing the mass flow to decrease.

Another very intersting conclusion of this model is that the inside channels (which were the channels where DNB occured for a full annular core) have an MDNBR well above 1.300. This is important because previous work (Ref. [9]) showed that the limiting channels in annular assemblies at 150% power are the inner channels. At

100% power, annular fuel channels have a large MDNBR margin and can therefore easily loose some flow in the favor of solid fuel channels where the MDNBR occurs.

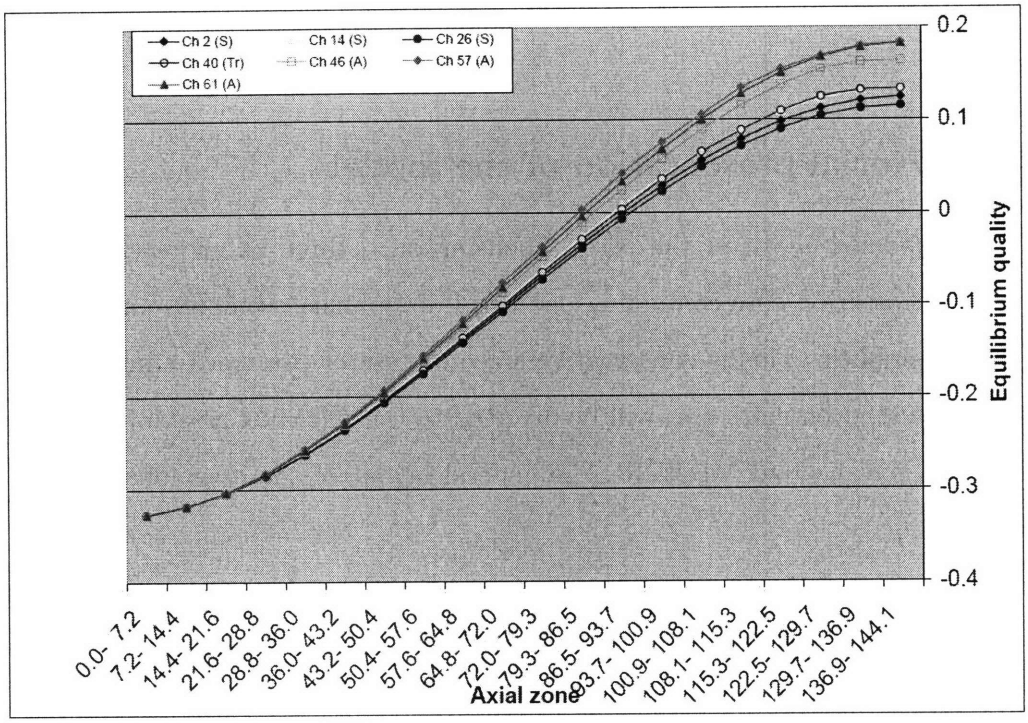

Figure 3-12: Equilibrium quality in different channels (S: Standard, A: Annular, Tr: transition) for the mixed assembly model

3.3 Mixed core model

Having investigated the simple case of a mix assembly, we will simulate the whole core.

3.3.1 Overall presentation of the model

We have modeled 1/8th of the core. Focusing on a three batch reactor, we have modeled a transition core containing one third of annular assemblies and two thirds of solid assemblies. This is conservative since in case of two third annular and one third solid fuel, even more flow will be diverted to the solid fuel assemblies which are limiting with respect to MDNBR. The general layout of the assemblies is given in Figure 3-13.

We also developed a very similar solid core model to be able to compare our results to a referene case. The general layout of this model is given in Figure 3-14.

3.3.2 Power Peaking and Model Numbering for Full Core Model

Parameters

The power distribution used in Ref. [9] was used for both the mixed core and the solid core. The distribution is reproduced in Figure 3-15. It is important to note that the hot channel corresponds to a solid assembly. This is a conservative way of modeling the core: we have just seen that the annular rods, kept at 100%, have a larger MDNBR. Therefore, placing the annular assemblies in the hot regions would increase the overall MDNBR. In addition, Figure 3-15 is a conservative power peaking used typically for licensing. Moreover, the hottest channels are all confined in the center of the core to minimize the benefits of mixing from "cold" adjacent assemblies.

The major values of the model are given in Table 3.7.

As done in the mixed assembly case, particular attention is paid to define properly the normalization factors. As explained earlier the fact that annular assemblies are

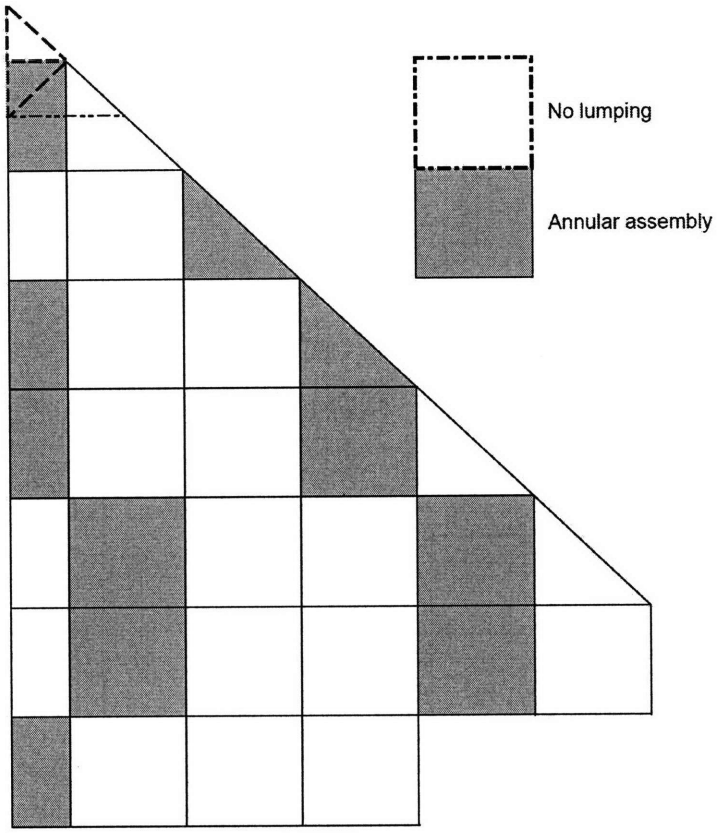

Figure 3-13: General layout of the mixed core model

Table 3.7: Parameters in the Mix-core model

Model size	1/8th of core
Number of solid assemblies	$16 + \frac{1}{8}$
Number of annular assemblies	8
Operating pressure	2248.1 psi (15.5 MPa)
Inlet Temp.*	558.9 F (294.7 C)
Mass flux**	4877.3 lb/s (2212.3 kg/s)
Average power per rod	77.0 kW/rod
Additional overpower	18%

** 2 C higher than operating Temp.*

*** 5% lower than total flow to account for bypass*

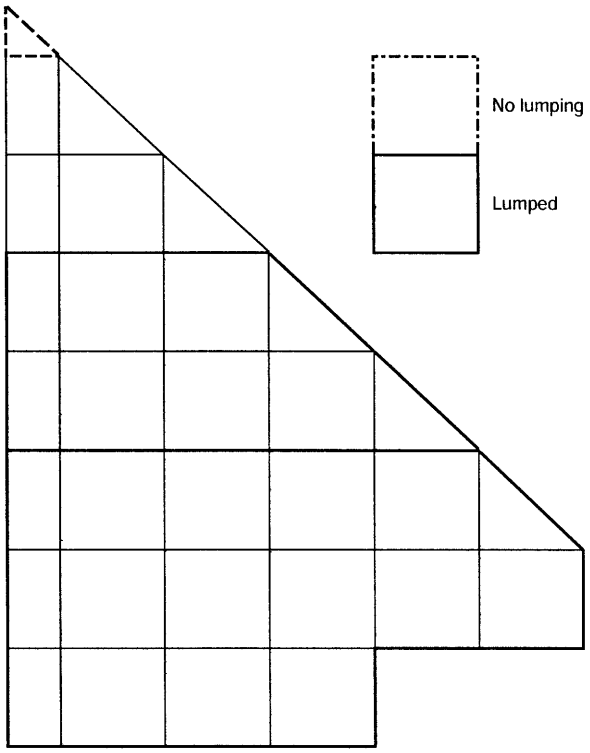

Figure 3-14: General layout of the solid core model

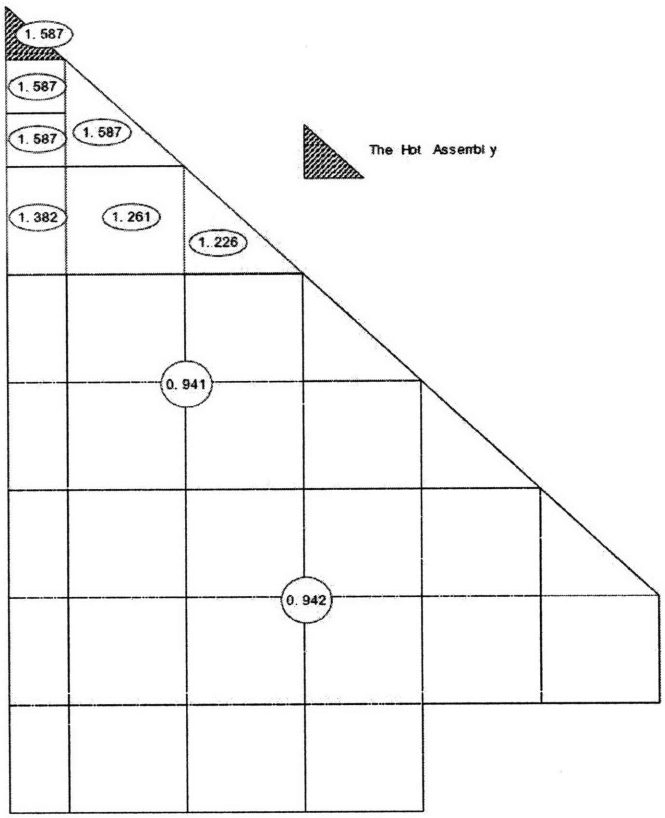

Figure 3-15: Power distribution used in the full core models

13x13, and solid 17x17 changes the number of rods per assembly. Therefore, the peaking factors of individual rods must reflect this difference. We can define n_A and n_S, respectively as the geometry factors for annular and solid rods.

$$n_A = \frac{8N_A + (16 + 1/8)N_S}{(8 + 16 + 1/8)N_A} \approx 1.43 \tag{3.5}$$

$$n_S = \frac{8N_A + (16 + 1/8)N_S}{(8 + 16 + 1/8)N_S} \approx 0.87 \tag{3.6}$$

The average core power is a weigthed average of the core-average power of an annular rod at 100% power and the core-average power of a solid rod at 100%.

$$P_{Mix\ core} = \frac{8N_A P_A + (16 + 1/8)N_S P_S}{8N_A + (16 + 1/8)N_S} \approx 77.0 kW/rod \tag{3.7}$$

We give also in Figure 3-16 and 3-17 the channels and rods numbering of the Mixed Core model.

The input file for VIPRE-01 is given in Appendix B.

Methodology

The methodology that was used here is based on a single run only. The code will compute at each node the pressure drop so that this pressure is uniform across the core but the pressure drop is not pre-determined.

3.3.3 Results

Pressure drop

The calculated pressure drops for both the mixed core and the solid core reference are as follows:

- For solid core model: $\Delta P_{Solid\ core} = 18.27 psi$
- For annular core model: $\Delta P_{Mix\ core} = 18.30 psi$

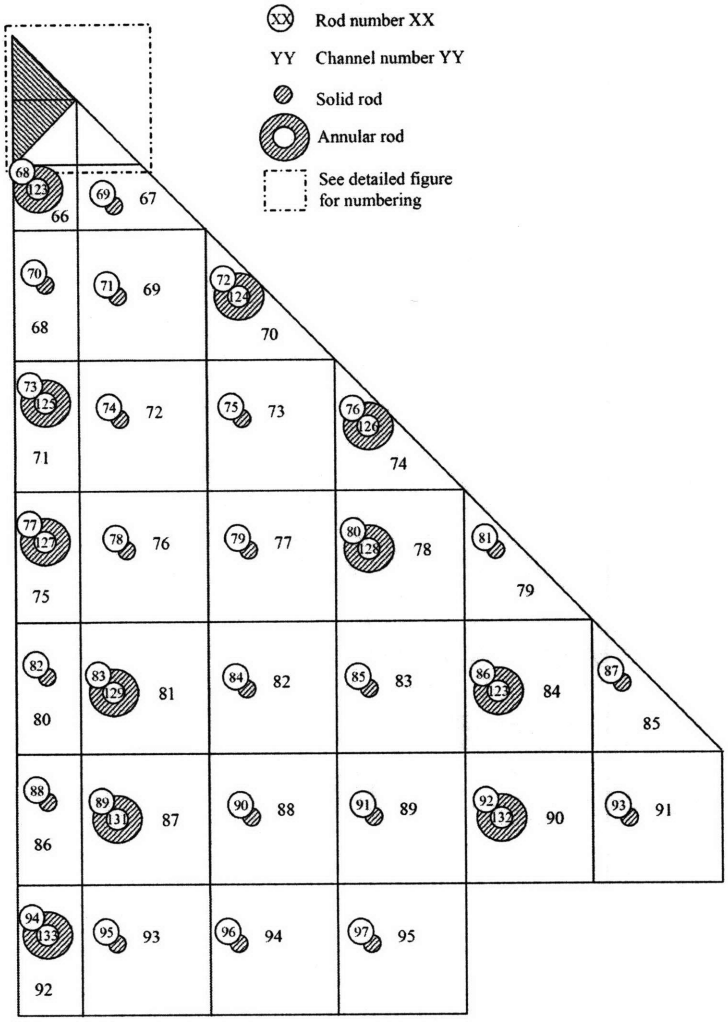

Figure 3-16: Overall Channels and Rods numbering for the Mixed Core model.

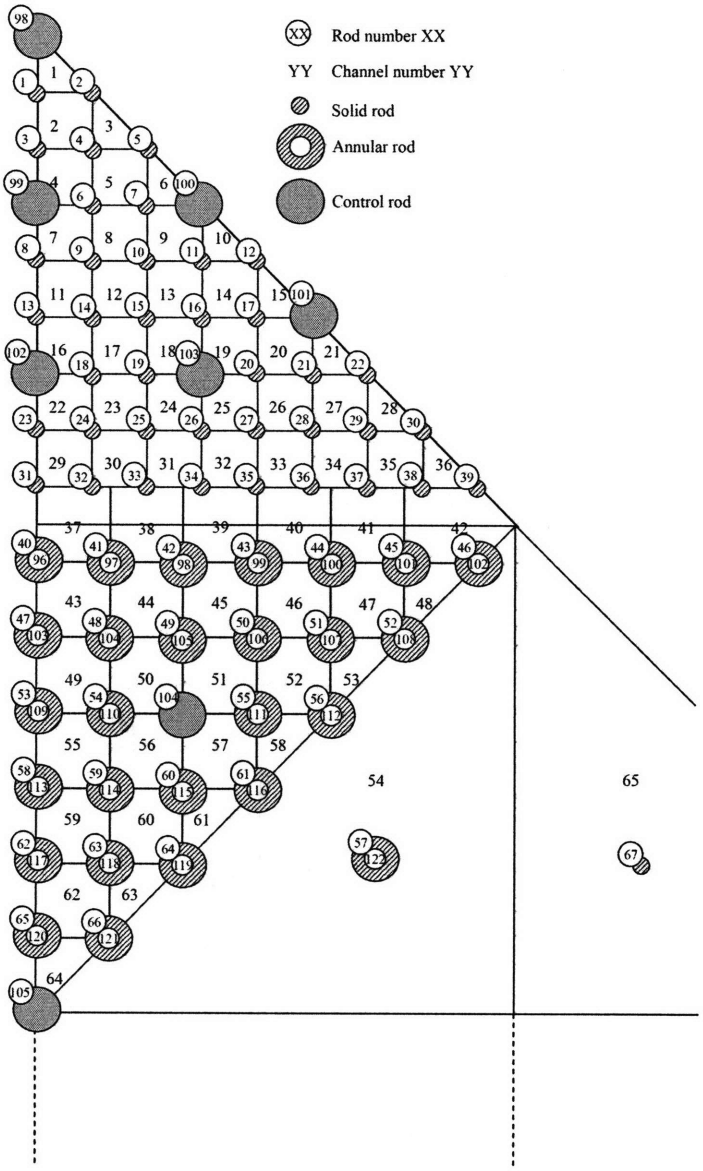

Figure 3-17: Hot Region Channels and Rods numbering for the Mixed Core model.

The results show that the pressure drops are very similar. This result can be explained by the fact that the annular assemblies were primarily designed such as their pressure drop was close to the reference solid core pressure drop. We also have approximetly one third of annular assemblies only, and mostly in cold regions.

A very important conclusion is that the pressure drop of the mixed core is almost the same as the reference case (different by less than 0.2%). This makes this mixed core **technically feasible from the pressure drop point of view, i.e. there is no need to change the reactor coolant pumps during the transition period of Case 2.**

MDNBR

The calculated values of the MDNBR were as follows:

- MDNBR for solid core model: $MDNBR_{Solid\ core} = 1.575$
- MDNBR inner channels for annular core model: $MDNBR_{Mix\ core\ in.} = 1.732$
- MDNBR outer channels for annular core model: $MDNBR_{Mix\ core\ out.} = 1.576$

For the outer channels, it is important to note that the MDNBR occurs on the same rod and in the same channel for both the mixed core and the solid core.

The major results here are, first and foremost that **the MDNBR for the mix core is well above 1.300** ; Secondly the effect of annular assemblies next to hot solid assemblies in the whole core is negligible ; and third the whole core DNB results are better for the outer channels and solid channels but worse for the inner channels compared with the mixed assembly model. The reason for this is that in a whole-core model, hot assemblies communicate with cold assemblies and due to much larger power peaking than in the mixed assembly model more flow is diverted from the cold assemblies to the hot assemblies at the inlet meaning that the inlet flow rate is much higher in the hot assembly of the whole-core than in the hot assembly of the assembly model. Given the fact that MDNBR occurs in the upper part of the assembly, the additional flow will benefit MDNBR. This analysis only applies to solid channels or

outer annular channels. Inner channels are connected with the rest of the core only at the upper and lower plenum. Therefore, they do not benefit from this phenomenon. On the contrary, their mass flow rate is lower in the case of mixed assembly core resulting in lower MDNBR.

The fact that $MDNBR_{Solid} \approx MDNBR_{Mix}$ seems at first sight in controversy with the results of the assembly model, which suggested that coolant flow was driven from annular channels to solid channels, thus benefiting the MDNBR. In the case of a whole core the situation is not as trivial: flow from annular assemblies have the choice between going in a hot solid part, or a cold solid part. Some flow will therefore obviously be deviated from the cold solid parts of the core, and the positive effect we used to have will be diluted.

Another important factor is that in a whole core model a large part of the core has negative equilibrium quality. This means that hot channels will lose mass flux along the axial direction. This feature can be illustrated by ploting the mass velocity in the hot channel for the whole core model and for the assembly model. This is done in Figure 3-18.

It is seen that the mass velocity for the full core is significantly higher at the inlet, but reaches the same level at the oulet compared with the mixed assembly which remains mostly constant. This result is very consistent with the fact that now the hot channels are connected to cold channels, and some flow is diverted from hot channels to cold channels. This feature also explains the increase in pressure drop from the assembly model to the core model. Indeed, in order to compensate for the loss in the hot channel, a larger pressure drop has to be reached so that enough flow is pushed through at the assembly inlet.

This general trend of hot regions loosing mass velocity whereas cold regions gaining mass velocity is illustrated in Figure 3-19.

3.3.4 Conclusions

The conclusions of the thermal-hydraulic assessment of the transition core are very encouraging. We have found that both the pressure drop and the MDNBR of a

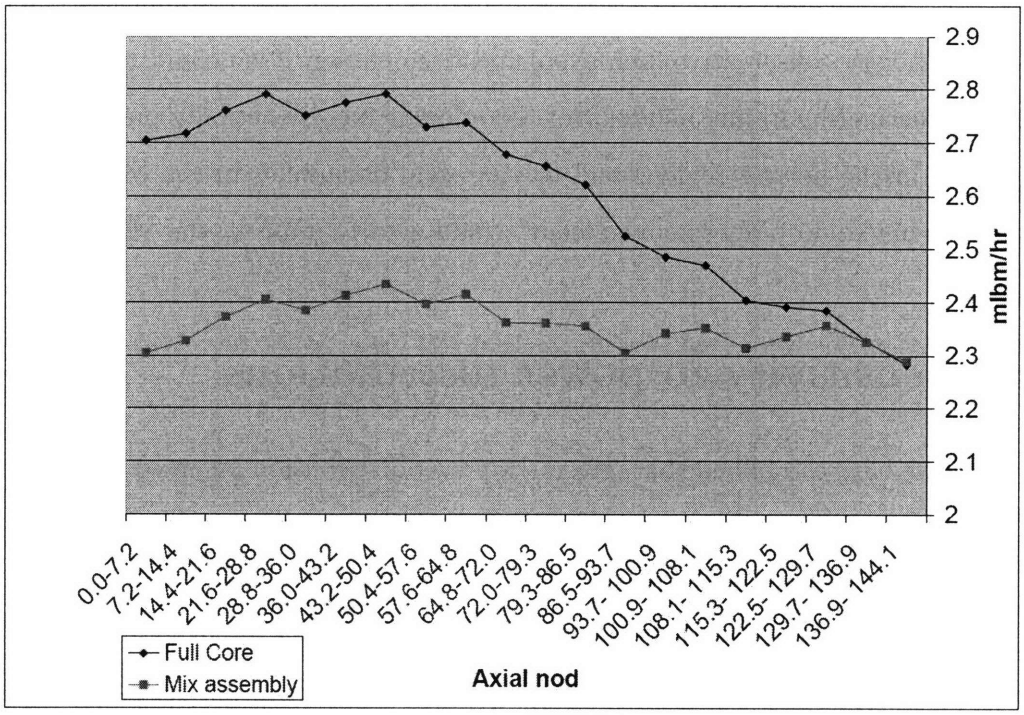

Figure 3-18: Mass velocity in the hot channel in the full core model and in the mixed assembly model

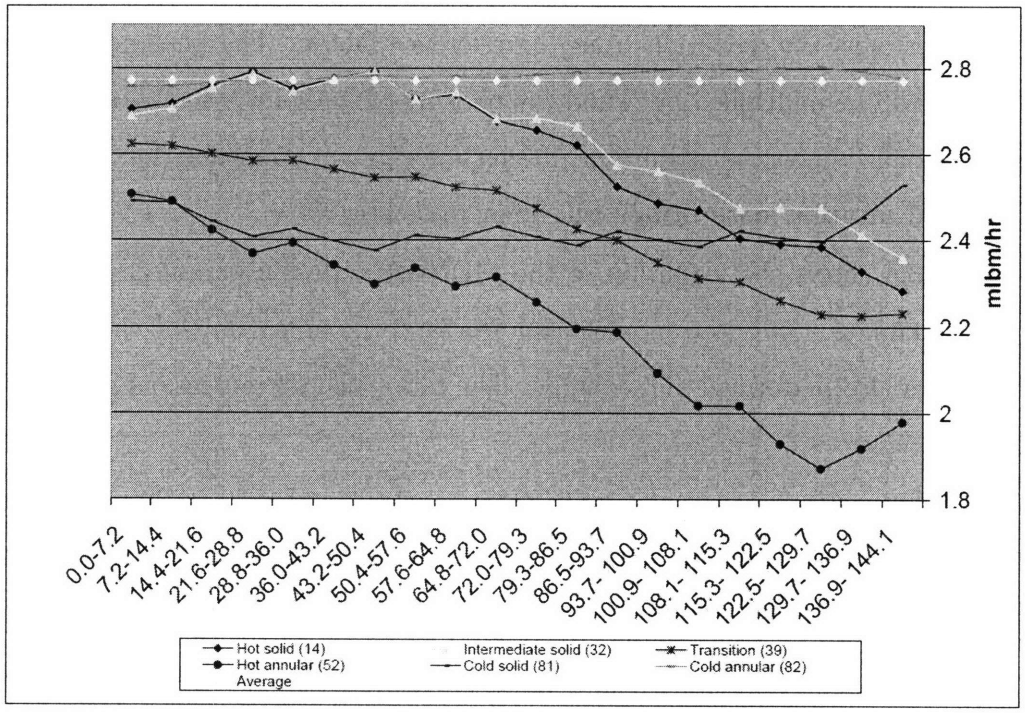

Figure 3-19: Mass velocity of different regions in the full core model

mixed core are not impacted by using a mixed core. The reader should also bear in mind that a very conservative fuel layout has been chosen. One could think of using the good thermal-hydraulic behavior of the annular fuel by actually placing annular assemblies in the hottest regions and leaving solid assemblies in the cold regions of the core. This kind of "fuel management" could greatly improve the MDNBR.

3.4 Sensitivity to power distributions

Now that we have establihed that, given the power distribution assumed, the thermal-hydraulic performance of the core is well within the margins, we will evaluate the effect of perturbating the power distribution.

In order to achieve an increase of 50% in power after the core has been up-rated, higher than solid fuel enrichment will be needed. Therefore, more power might be produced in the annular part than we expect (put differently, peaking may be higher in the annular assemblies).

A deviation from the distribution given in Figure 3-15 was studied. Let us define a parameter α as the deviation from the reference factor. The peaking of annular assemblies will be multiplied by α and the peaking of the solid assemblies reduced to keep a normalized power distribution. For instance, $\alpha = 1.05$ means that the peaking power in **all annular assemblies** will be increased by 5%.

Figure 3.4 shows the evolution of the MDNBR with the parameter α for both the solid channels, the outer annular channels, and the inner annular channels. The analysis was also performed at 5% higher flow rate (such an increase is feasible with existing pumps).

Let us keep in mind that the MDNBR is reached in the outer channels of solid fuel rather than in the annular fuel, and therefore an increase in the share of power in the annular part will result in an increase in the DNBR of the solid channels (upward sloping curve). Conversely, increasing the share of power produced in annular assemblies will decrease the DNBR in the inner channels (downward sloping curve).

The inner channels are much more sensitive to a change in peaking factors. These

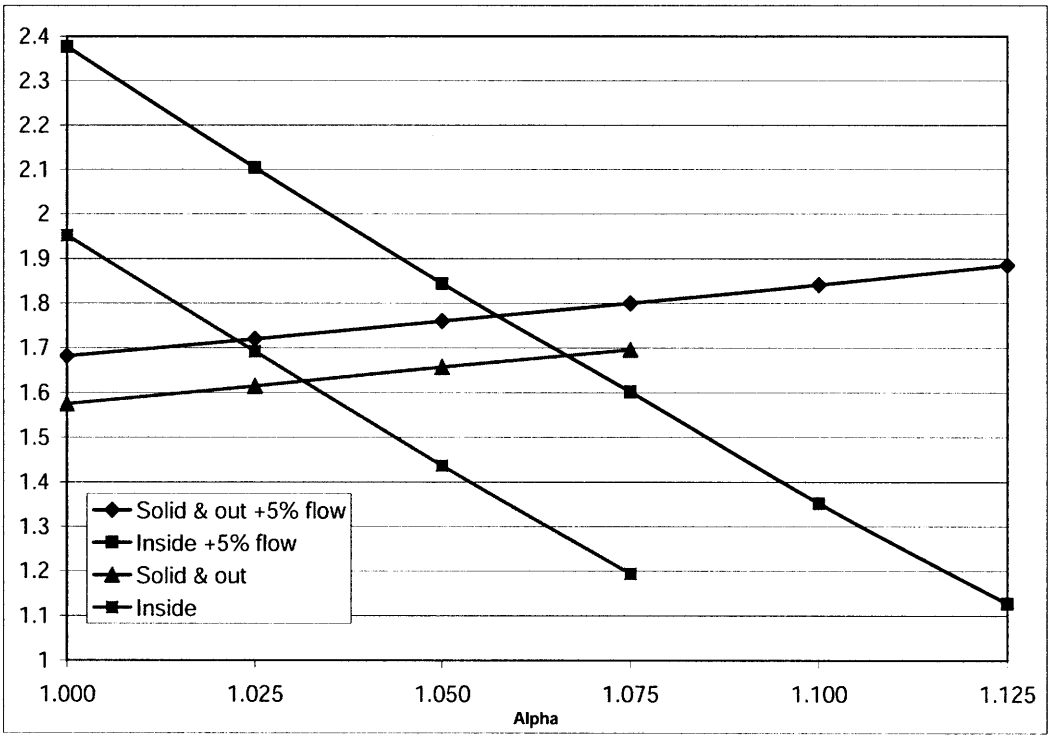

Figure 3-20: Evolution of MDNBR as a function of the power peaking factor alpha for inner channels and outer channels

channels have connections with the rest of the channels only at the upper and lower plenum, so they can't benefit of any mixing feedback the way other channels can.

Therefore, an increase in the power fraction in annular assemblies will first increase MDNBR (positive effect on solid channels) and at some point start reducing MDNBR because of the negative effect on the inner channels.

In conclusion, at 100% flow rate, it is possible to increase the power fraction in annular assemblies by about 3%. If the flow rate is increased by 5%, this figure goes to 8%.

3.5 Conclusions

Three main results were reached. The first one is that, because the initial design of annular fuel was performed such that the pressure drop of annular assemblies is close to the one of solid fuel, the overall pressure drop of a mixed core is very similar to the pressure drop of a standard solid core.

The second conclusion is that, even when assuming very conservative fuel management (*i.e.* using solid fuel in hot regions), MDNBR in the mixed core is very close to the reference case, and annular fuel helps to some extent to have a larger MDNBR.

The third and final conclusion is that the peaking can be increased by about 8% in the annular assemblies while still maintaining the same MDNBR, given the neutronic designer probably enough room to design the core.

The crucial question of the thermal-hydraulic feasibility of this innovative mixed core has been adressed. We will look more carefully at the neutronic aspect of the design in the next chapter.

Chapter 4

Reactor Physics Assessment

In order to complete the feasibility evaluation of a transition core from solid fuel to annular fuel, the neutronic behavior of the core during the transition needs to be assessed. The analysis was performed using the commercial neutronic solver package CASMO-4, TABLES3 and SIMULATE3 developped by Studsvik inc. (see Ref. [8], [10] and [2])

After describing the code and the adjustments that are required to use the package with the annular fuel we will detail the method that was used and the parameters that were assumed. The core was simulated with various poisoning patterns.

4.1 The CASMO-TABLES-SIMULATE package

4.1.1 Description of the codes

The Studsvik Core Management System (CMS) includes CASMO-4, TABLES-3 and SIMULATE-3. The CMS is a licensing-level computer suite that is used by more than 200 nuclear reactors out of the 441 existing commercial reactors. The codes package is capable of simulating steady-state LWR core operations. We will detail briefly the particularity of each code.

CASMO-4 is a lattice physics code. It is a multi-group two-dimensional transport theory solver, entirely written in Fortran 77. CASMO-4 can perform burn-up cal-

culations of LWR assemblies or pin cells of "standard" geometry (*i.e.* either square lattice or hexagonal lattice) composed of solid fuel. A major concerned raised and addressed in Ref. [9] is that CASMO does not have the capability to model directly an annular fuel rod. We will discuss in greater details the issue that this limitation raises, and the solution developped to fix it. CASMO-4 gives as an output the cross-sections of a given assembly for different temperatures, boric acid concentration, burnup, moderator temperature, history variables .etc.

TABLES-3 plays the role of the interface between SIMULATE-3 and CASMO-4. Taking the outputs given by several CASMO-4 runs, TABLES-3 tabulates them into a binary-format library that can then be read by SIMULATE-3.

SIMULATE-3 is an advanced three-dimensional, two-group, nodal code for LWR steady-state analysis. It perfoms a coupled thermal-hydraulic/neutronics calculation and iterate until obtaining the core power distribution. SIMULATE-3 represents the core by dividing it into several regions (called nodes). The parameters inside each node are the homogenized parameters obtain *via* the lattice physics code CASMO-4. Then the code solves the three-dimensional transport equation by first integrating over the two transverse directions and then solving the one-dimensional equation. Note that SIMULATE-3 does not, strictly speaking, need to know the specific geometry of the fuel. Therefore, using annular fuel assemblies should not change the results of SIMULATE-3 if the CASMO-4 calculations already accounts for this type of geometry.

The advantages of using the CMS is that this code is being used extensively in the industry, the results will have credibility. In addition the computational time required to simulate an entire core during several cycles is small compared to probabilistic codes like MCNP.

4.1.2 CASMO-4 adjustments for annular fuel

In order to have a full understanding of the adjustments that were required for the CASMO-4 inputs we will recall the work reported in Ref. [9].

Xu *et al.* performed a benchmark calculation between CASMO-4 and MCNP-4C and showed that CASMO-4 will generally over-predict the eigen value of the transport

equation. The reason for this over-estimation lies in the fact that CASMO-4 is not capable of modeling a hollow shape with internal water, whereas MCNP-4C can. Indeed due to the water presence inside the annular fuel, the shelf-shielding effect is reduced and U-238 resonance captures are effective on both the outter and the inner surface of the fuel. Because a hollow geometry cannot be specified in CASMO-4, the resonance integral of U-238 is computed only on the outter surface and is therfore underestimated.

MIT being not granted the right of access to the source code of CASMO-4, this feature could not be fixed in the source code. Instead, Xu *et al.* fixed the problem by virtually increasing the concentration of U-238. By benchmarking the results of CASMO-4 runs against an MCODE-1.0 simulation, it was demonstrated that CASMO-4 would match MCODE-1.0 with small deviation if **the U-238 content of poison-free fuel is virtually increased by 20%**, and **the U-238 content of poisoned fuel is virtually increased by 30%**.

4.2 General method and parameters

4.2.1 Modeling requirements

As our reference case, we will use a standard 4-loop Westinghouse PWR with an 18-months cycle length, and a three batch loading pattern of solid 17x17 fuel with 4.5% enrichment. We take the total power to be 3411 MWth.

What is needed for assessment of the transition from a 3 solid-batches core to a 3 annular-batches core through 2 intermediary steps, is to ascertain that appropriate reactivity exist for the entire cycle, within acceptable peaking factors.

SIMUALATE-3 makes it possible to simualate the core for several cycles. Thus in each of our input, we will first run SIMULATE-3 for nine cycles recharging each time reference solid fuel in order to reach at the end of cycle 9 the equilibirum core that is expected to be found in an operating reactor ready to be uprated to annular fuel. Then, at cycle 10, cycle 11 and cycle 12 annular-batches are introduced so that at the

begining of cycle 12, the core is fully composed of annular fuel. At this point both the core power, and the total flow rate are increased by 50%. We run 2 additional cycles to validate the results in the up-rated core. Table 4.1 summarizes the loading process.

Table 4.1: Summary of loading process for neutronic analysis

Cycle num.	Fuel-type loaded	Power and Flow rate level
1 to 9	Solid	100%
10	Annular	100%
11	Annular	100%
12 to 14	Annular	150%

4.2.2 Objectives and constraints

The main core design goals in this work are: *(i)* to sustain an 18-months cycle length even during transition and after, *(ii)* to maintain peak critical boron concentration below 1750 ppm, and *(iii)* to maintain power peaking during cycles such that the hot channel factor $F_{\Delta h} \leq 1.65$ and the hot spot factor $F_q \leq 2.5$.

Important note: At this point, we need to make an important note. The peaking factors that we considered as being our design targets are based on rod peaking. Remembering the little mathematical gymnastic that was required in the thermal-hydraulic to accomodate the peakings while accounting for the difference in the number of rods of annular assemblies *versus* solid assemblies we directly conclude that the criterion of the hot channel factor, or hot spot factor are irrelevant for the transition cycles (cycle 10 and 11). Indeed, the peaking factors in the annular parts will be very high compared to the values for in the solid rods. To some extent a "cold" annular rod could have a higher peaking than a "hot" solid rod simplpy because they are $13 * 13 - 9 = 160$ rods in an annular assembly, and $17 * 17 - 25 = 264$ rods in a solid assembly and the larger annular rod generates more power. Instead, a node averaged peaking (as explained later) will make more sense and will not be affected by this

difference.

4.2.3 Three-step method

In order to meet the targets assigned, a general three steps method can be used.

- First, determine the enrichment required to sustain the cycle length desired
- Secondly, determine the total amount of poison that needs to be added
- Finally, adapt the poisoning patern and the loading partern to reduce peaking

Note that determining the enrichment that is required is not too difficult but the next two steps are much more delicate and need a lot of trial-and-error processes. But we remind the reader that the main purpose of this work is not to perfectly determine the exact design of a transition core, but rather to give a general picture and prove that a satisfactory core design can be achieved.

4.2.4 Enrichment

Determining the approriate enrichment is probably the most straightforward question to work on. We are focusing on a three batch core, meaning that the first annular batch loaded at the begining of cycle 10 will be burned at 100% power for two cycles, and at 150% for one cycle. Similarly, the second annular batch loaded at the begining of cycle 11 will be burnt for one cycle at 100%, and for two cycles at 150%. The solid fuel that is loaded in core to run at 100% power has a 4.50 w.t.% enrichment. The annular fuel loaded for operation at 150% needs to have an enrichment of 8.5 w.t.%. In order to accomodate the 50% overpower during three cycles, the annular fuel needs an extra 4.00 w.t.% ; therefore, in order to keep an 18-month cycle length all along the transition, the first batch of annular fuel (loaded at cycle 10) will need one third of 4% more enrichment, and the second batch (loaded at cycle 11) will need two thirds of 4% more enrichment.

Once the required mean enrichment is determined the batch consisting of 72 assemblies, is split into 24 assemblies with a low enrichment, and 48 assemblies with high enrichment.

Table 4.2 summarizes the enrichment choice that was selected for the rest of the study.

Table 4.2: Detail of the enrichment chosen for the transition cycles

	Cycle 09	Cycle 10	Cycle 11	Cycle 12
Low enr.	4.40%	5.60%	6.90%	8.10%
High enr.	4.80%	6.20%	7.60%	9.00%

4.2.5 Poisoning pattern and loading pattern

For this study, the only poison that was considered is gadolinium oxide (Gd_2O_3). Another very popular poison is a thin layer of boron coating applied on the fuel surface: the so-called Integrated Fuel Burnable Absorber (IFBA) developed by Westinghouse. But the use of IFBA was not considered because the manufacturing of externally and internally coated annular fuel rods with the IFBA process seemed complex, and not readily available.

In order to create CASMO-4 input data for different types of assemblies, we will need to compute the weight content in U, Gd, O of our fuel. The details involved in this calculation are given in Appendix C.

Two different parameters can be changed when speaking of the poisoning pattern: the poison content (weight percent of Gd_2O_3 content) but also the number of poisoned rods. In Ref. [9], different arangements of poisoned rods were established and showed good results. So, in order to decrease the number of free variables that we can play with, we intentionally limited ourselves to using the poisoning patterns established in [9]. We reproduce these patterns in Figure 4-1.

In addition, it is important to get a good representation of the effect of poisoning on the neutron flux and on the eigenvalues. In other word we seek to answer the

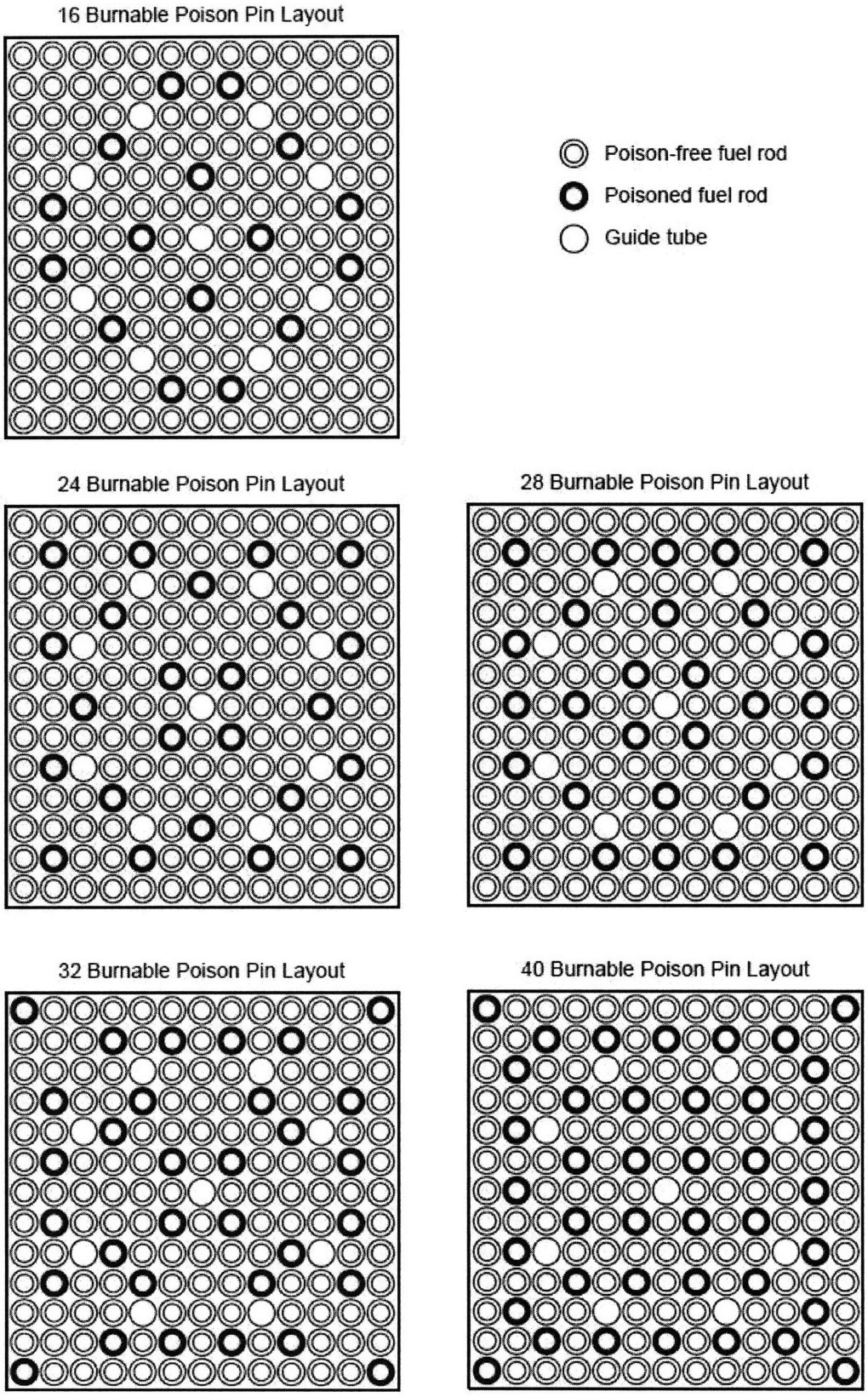

Figure 4-1: Assembly fuel pin layouts for the annular fuel (from [9])

questions: what will the effect of increasing the number of poisoned rods be on k_∞? What will be the effect of increasing the poison weight content?

To answer these two questions, we simulated using CASMO-4 for four annular assemblies with different poisoning content and patern, with enrichment of 6.20 w.t. %: XF620 is the poison free assembly, XF62012G10 has 12 poisoned rods with 10% w.t. poison content, XF62016G10 has 16 poisoned rods with 10% w.t. poison content, and XF62012G80 has 12 poisoned rods with 8% w.t. poison content. Figure 4-2 shows the evolution of k_∞ as a function of the burnup for the four different assemblies. What Figure 4-2 shows is that adding more poison rods with the same poison content will increase the poisoning effect (*i.e.* k_∞ decreases) but will not significantly affect the length of time during which the poison is active. On the other hand, increasing the poison content while maintaining the number of poisoned rods constant will keep the poisoning effect unchanged, but it will increase the length of time during which the poison is active.

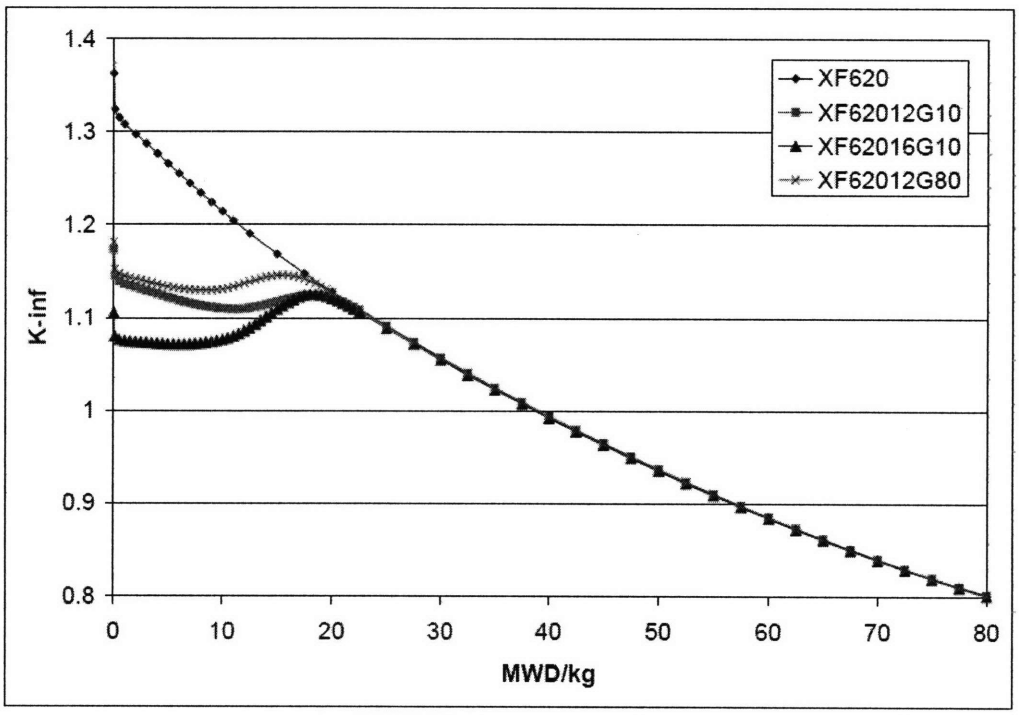

Figure 4-2: Comparative effect of increased number of poisoned rods and increased poison content

Table 4.3 summarizes the discussion above:

Table 4.3: Effect of the number of poisoned rods and the amount of poison on the level of poisoning and the total duration of poisoning.

Effect on:	Initial poisoning	Duration
More Gd in mass	$\rightarrow$	$\uparrow$
More Gd rods	$\uparrow$	$\rightarrow$

4.2.6 Data processing and analysis

As explained earlier, several runs of CASMO-4 were done in order to obtain a library of cross-sections for annular assemblies with different enrichment and different poisoning patterns and poison content.

The data obtained from the simulations do not have to be processed. Instead TABLES-3 will generate a large database with all the CASMO-4 outputs.

What we are after is the hot channel factor $F_{\Delta h}$ and the hot spot factor F_q. SIMULATE computes a value for $F_{\Delta h}$, but given the note made in 4.2.1, it is clear that this value does not have a real meaning for the transition cycles (cycle 10 and 11). Instead it is better to use the pin peaking factor, which is a major factor in determining $F_{\Delta h}$ since a channel is surrounded by different rods.

Therefore, we have to process and interpret the output from SIMULATE-3. In order to be able to compute the core maximum pin peaking factor, we will use the outputs from the code which give us the maximum pin peaking in every assembly. Keeping in mind the important note that we made earlier in Section 4.2.1, the pin peaking given by SIMULATE can not be used as is. Instead, we need to developp some sort of pin peaking renormalization that compensate for the fact that annular assemblies have less rods (and thus larger power per rod) than solid assemblies.

For cycle 10 (1 annular batch, 2 solid batches) In order to be able to compare the peaking factors with one another, we should renormalize the pin peaking values. Let us call n_A the number of annular rods in an annular assembly, and n_S the number of solid rods in a solid assembly. The question we have to answer is: what would be the peaking of the solid/annular rod we consider would this solid/annular rod be

within an homogeneous core (*i.e.* solid/annular core)? For an annular rod we would have to multiply its peaking factor by the total number of rods in an annular core, and divide by the total number of rods in our core. Equation 4.1 gives explicitely this coefficient that we call f_A^{10}.

$$f_A^{10} = \frac{(8+16+1/8)n_A}{8n_A + (16+1/8)n_S} \approx 0.699 \tag{4.1}$$

Applying the same reasoning to a solid rod we obtain the factor f_S^{10} given in Equation 4.2.

$$f_S^{10} = \frac{(8+16+1/8)n_S}{8n_A + (16+1/8)n_S} \approx 1.149 \tag{4.2}$$

For cycle 11 (2 annular batches, 1 solid batch) Following the same approach, we get the renormalization factor f_A^{11} in Equation 4.3 and f_S^{11} in Equation 4.4.

$$f_A^{11} = \frac{(8+16+1/8)n_A}{8n_S + (16+1/8)n_A} \approx 0.820 \tag{4.3}$$

$$f_S^{11} = \frac{(8+16+1/8)n_S}{8n_S + (16+1/8)n_A} \approx 1.351 \tag{4.4}$$

MatLab data processing In order to obtain correct peaking factors (correct in the sense that they can be compared to the licensing criterion given in Section 4.2.1) the output from SIMULATE needs to be processed.

Using MatLab, a routine that opens the output file has been created. We browse it to locate the first depletion step of cycle 10. Then, at each depletion step the map of the assembly-wise pin peaking is extracted and this map is renormalized using the coefficients f_A^{10}, f_S^{10}, f_A^{11} or f_S^{11}. The maximum renormalized pin peaking is sorted along with the depletion and the routine processes to the next depletion step.

Eventually we obtain two vectors for each cycle. One contains the depletion steps, the other contains the maximum renormalized pin peaking.

The main source code is given in Appendix D.

4.3 Simulation results

First a poison free core was simulated. Given the results of the poison free core simulation, a trial and error process was applied to obtain a core that respects the criterion given in Section 4.2.1 and that we summarize below:

- Sustain 18 months cycles
- Keep Boric acid concentration below 1750 ppm
- Keep $F_{\Delta h}$ below 1.65
- Keep F_q below 2.5

Keep in mind that these criteria are stated for an homogeneous core, and that we will need to "renormalize" the peaking factors to use the criterion.

4.3.1 Poison free results

Because the enrichment is so high, the poison free fuel requires abundant use of boron. SIMULATE has an embedded error check that abort the simulation if the boron concentration becomes higher than 3000 ppm. This upper limit is reached at the begining of cycle 11. In order to deactivate this option we used the flag 'ERR.CHK' that disables this feature.

Figure 4-3 shows the evolution of the maximum pin peaking in the core with the burn-up. The absolute values of the peaking factors are not really representative since they correspond to an hypothetic poison free core. But, what is important to note is that cycle 11 (which displays the largest range of enrichment) has the largest peaking factors. This means that this cycle will need more poisoning than the other cycles, if we are to decrease its peaking.

Another important figure is the distribution of the peaking values at the Begining Of Life (BOL) of the batch for cycle 10 and cycle 11. Because the fuel is unpoisoned, the peaking will be higher at the BOL and gradually decrease. Figure 4-4 and Figure

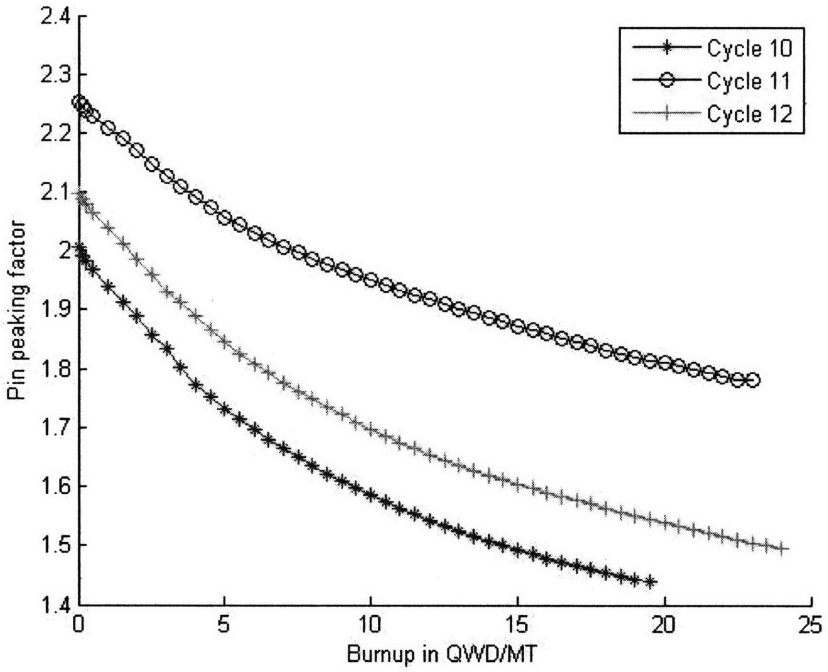

Figure 4-3: Maximum pin peaking for an unpoisoned core for cycle 10, 11 and 12

4-5 show the pin peaking for the BOL of Cycle 10 and Cycle 11 respectively. The Red, Blue and Grey colors represent, fresh, once-burned and twice-burned assemblies.

4.3.2 Poisoned results

Equiped with this preliminary look at an unpoisoned core, we tried to curb the peaking in the hottest spots using burnable poison. The two parameters that can be affected are the number of poisoned rods per assembly and the amount of poison in the poisoned rods. In order to keep things simple we constrained ourselves to use, for cycle 10 the assembly arrangement established for XF fuel (full annular core at 100% power) in Ref. [9], and for cycle 11 the assembly arrangement established for XU fuel (full annular core at 100%) in Ref. [9].

After a series of trial and error SIMULATE-3 runs, we were able to reach a core configuration in which all criteria that we were aiming at were satisfied within reasonable margins.

	H-	G-	F-	E-	D-	C-	B-	A-
8	0.892	1.659	1.376	2.012	1.392	1.733	1.062	0.418
9	1.659	1.102	1.814	1.371	1.922	1.323	1.464	0.474
10	1.376	1.814	1.260	1.716	1.278	1.097	1.389	0.464
11	2.012	1.371	1.716	1.095	0.954	0.955	1.188	0.386
12	1.392	1.922	1.278	0.955	1.025	1.259	0.609	
13	1.733	1.323	1.097	0.955	1.259	1.176	0.475	
14	1.062	1.464	1.389	1.188	0.609	0.475		
15	0.480	0.531	0.525	0.433				

Figure 4-4: Core Map of assembly maximum pin peaking for BOL of cycle 10 (bold are annular assemblies) for unpoisoned core

	H-	G-	F-	E-	D-	C-	B-	A-
8	0.776	1.596	1.351	2.039	1.383	1.748	1.707	0.418
9	1.596	0.986	1.806	2.242	1.934	1.305	1.444	0.474
10	1.351	1.805	1.244	1.730	1.271	1.066	1.375	0.464
11	2.039	2.242	1.730	1.089	1.508	0.923	1.170	0.386
12	1.383	1.934	1.271	1.509	0.991	1.242	0.325	
13	1.748	1.305	1.066	0.923	1.242	1.161	0.418	
14	1.707	1.444	1.375	1.170	0.325	0.418		
15	0.418	0.474	0.464	0.386				

Figure 4-5: Core Map of assembly maximum pin peaking for BOL of cycle 11 (bold are annular assemblies) for unpoisoned core

Boron Concentration Figure 4-6 gives the evolution of the total boron concentration in the core as a function of the burn-up. Note that this concentration remains well below the 1750 ppm limit that was set.

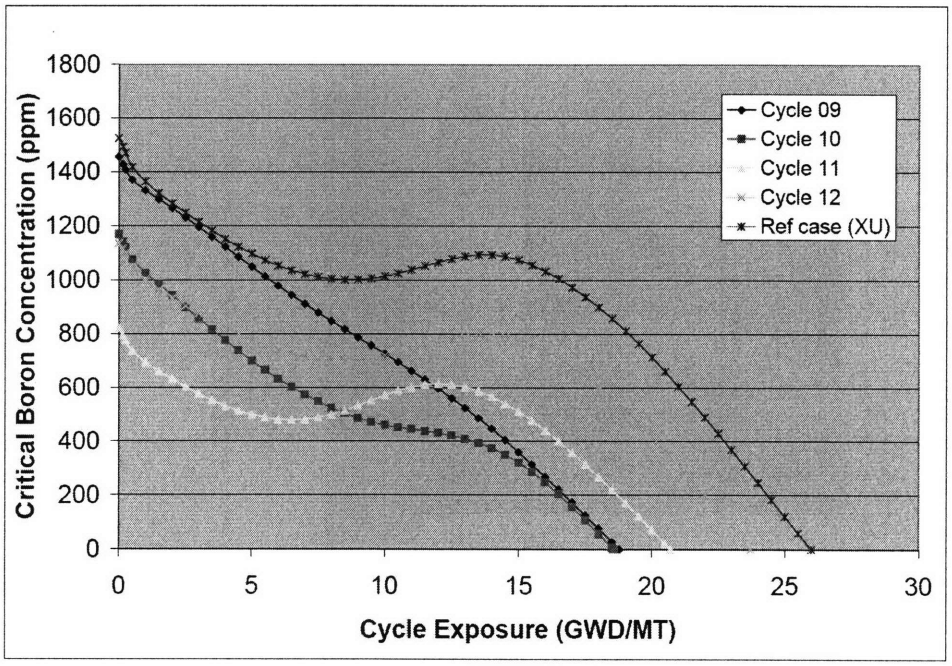

Figure 4-6: Boron concentration in the core

Cycle Length Assuming a capacity factor of 90% we want our core to operate for $18 * 0.90 \approx 16$ *months and* 6 *days*. The effective full power days achieved at every cycle are the following:

- Cycle 9: 15 months and 29 days
- Cycle 10: 16 months and 17 days
- Cycle 11: 19 months
- Cycle 12: 14 months and 24 days
- Cycle 13: 15 months and 24 days
- Cycle 14: 15 months and 27 days

- Average cycle length: 16 months and 10 days

The average cycle length, is very close to the target value. All in all, it is clear that because cycle 10 and mostly cycle 11 have larger than necessary enrichments, their cycle length will increase. But this enrichment increase will be needed to operate the first up-rated core at 150% power. A conclusion that can be drawn is that, leaving aside the transition cycles (10 through 12), we can reach again an equilibrium in a very small number of cycles (two at most).

Peaking factors Using a MatLab algorithm to process SIMULATE's output, we can obtain the renormalized maximum pin peaking factors. Figure 4-7 gives these peaking values for the transition cycles as well as for the reference case from Ref. [9]. Figure 4-8 gives the core-wise maximum pin peakings for cycle 12, 13 and 14 and also for the reference case.

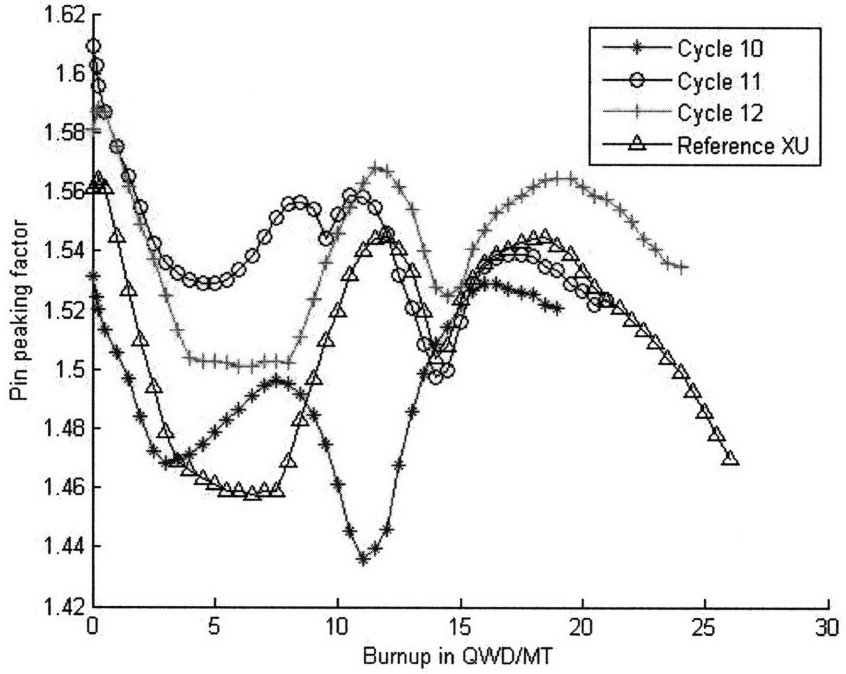

Figure 4-7: Core-wise pin peaking factors for transition cycles (10, 11 and 12) and reference case from Ref. [9].

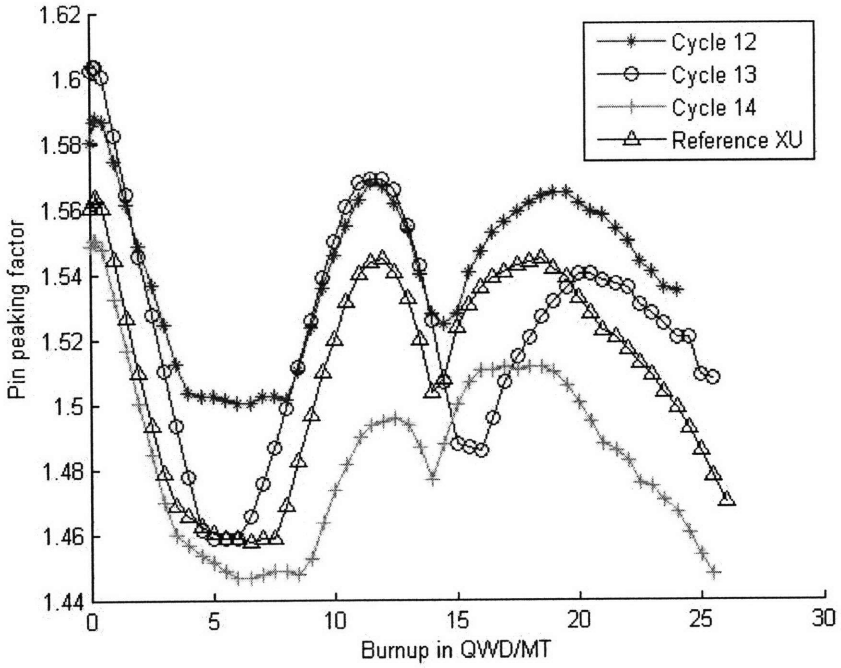

Figure 4-8: Core-wise pin peaking factors for uprated cycles (12, 13 and 14) and reference case from Ref. [9].

For all cycles, the peaking is below 1.65. The maximum peaking encountered arise for a very short period of time during the BOL of cycle 11 reaching an acceptable value of 1.61.

Core maps for cycle 10, 11 and 12 Given that the peaking values are the most important at the BOL for all cycles, we will give the core maps at the BOL for cycles 10, 11 and 12 in Figures 4-9 through 4-11. Each cell represents an assembly. The color of the cell refers to the number of cycles any given assembly has been burned for (Red=Fresh, Blue=Once-burned, Grey=Twice-burned). The first line is the fuel identification (for instance *2L1670* means a twice burned fuel, with low enrichment, that has 16 poison rods with 7.0 % w.t. of Gd). The second line is the assembly power peaking. The third line is the assembly burnup. The last line is the renormalized assembly-wide pin peaking.

	H-	G-	F-	E-	D-	C-	B-
8	2L1670 0.845 46.816 0.852	**0L1212** **1.205** **0.000** 1.394	1L1670 1.160 23.593 1.213	**0H1612** **1.256** **0.000** 1.469	2H2080 0.940 42.938 0.976	**0L1610** **1.164** **0.000** 1.320	1L1670 0.886 25.170 1.022
9	**0L1212** **1.205** **0.000** 1.394	2H1250 0.979 41.107 1.026	**0L1610** **1.223** **0.000** 1.417	2H1250 1.082 33.655 1.126	**0H2010** **1.240** **0.000** 1.485	1H2080 1.206 23.017 1.292	**0H1680** **1.049** **0.000** 1.429
10	1L1670 1.160 23.593 1.213	**0L1610** **1.223** **0.000** 1.418	1L1670 1.168 25.202 1.230	**0L1612** **1.287** **0.000** 1.536	1L1610 1.234 24.608 1.307	1H1670 1.309 21.614 1.403	**0H1680** **1.089** **0.000** 1.481
11	**0H1612** **1.256** **0.000** 1.469	2H1250 1.082 33.655 1.126	**0L1612** **1.287** **0.000** 1.536	1L1670 1.245 25.203 1.301	1H2080 1.312 25.006 1.359	1H1670 1.289 21.575 1.374	**0H1250** **1.081** **0.000** 1.476
12	2H2080 0.940 42.938 0.976	**0H2010** **1.240** **0.000** 1.484	1L1670 1.234 24.613 1.307	1H2080 1.312 25.006 1.359	1H1250 1.344 19.229 1.403	**0H2010** **1.162** **0.000** 1.497	1H1250 0.709 20.200 1.039
13	**0L1610** **1.164** **0.000** 1.320	1H2080 1.205 23.016 1.292	1H1670 1.309 21.614 1.402	1H1670 1.289 21.575 1.372	**0H2010** **1.162** **0.000** 1.497	**0H1250** **0.934** **0.000** 1.342	2H2080 0.313 45.144 0.613
14	1L1670 0.886 25.170 1.022	**0H1680** **1.049** **0.000** 1.429	**0H1680** **1.089** **0.000** 1.481	**0H1250** **1.081** **0.000** 1.476	1H1250 0.709 20.199 1.038	2H2080 0.313 45.145 0.613	
15	1H2080 0.465 24.976 0.676	2H1670 0.390 43.098 0.593	2H1670 0.375 42.582 0.579	2H2080 0.295 45.454 0.544	Fuel ID Assembly power Assembly burnup Normalized Peak pin power		

Figure 4-9: Core Map of assembly maximum pin peaking for BOL of cycle 10 (bold are annular assemblies) for poisoned core

	H-	G-	F-	E-	D-	C-	B-
8	2L1670 0.623 45.358 0.618	**0L2010** **0.886** **0.000** **1.004**	1L1612 0.898 22.688 0.947	**0L2480** **0.970** **0.000** **1.127**	2H1670 0.900 44.165 0.941	**0H2480** **1.335** **0.000** **1.478**	1L1212 1.133 21.946 1.263
9	**0L2010** **0.886** **0.000** **1.004**	2H2080 0.668 46.508 0.677	**0L2480** **0.900** **0.000** **1.039**	2H1670 0.794 43.580 0.838	**0H2480** **1.206** **0.000** **1.489**	1L1610 1.287 23.148 1.365	**0H2480** **1.245** **0.000** **1.501**
10	1L1612 0.898 22.688 0.947	**0L2480** **0.904** **0.000** **1.050**	2H2080 0.838 35.055 0.930	**0L2880** **1.048** **0.000** **1.397**	2H2080 1.016 45.328 1.092	1H1680 1.451 20.559 1.508	**0H2480** **1.262** **0.000** **1.549**
11	**0L2480** **0.970** **0.000** **1.127**	2H1670 0.797 43.579 0.839	**0L2880** **1.051** **0.000** **1.397**	1H1250 1.409 18.062 1.495	1L1610 1.388 22.507 1.449	1H1250 1.441 19.799 1.520	**0H2060** **1.205** **0.000** **1.603**
12	2H1250 0.900 44.165 0.941	**0H2480** **1.207** **0.000** **1.489**	2H2080 1.015 45.327 1.089	1L1612 1.380 22.608 1.446	1H1610 1.354 23.241 1.482	**0H3260** **1.105** **0.000** **1.470**	1H1612 0.712 23.272 1.004
13	**0H2480** **1.335** **0.000** **1.478**	1L1610 1.287 23.152 1.009	1H1680 1.450 20.559 1.115	1H1250 1.439 19.798 1.123	**0H3260** **1.106** **0.000** **1.468**	**0H2880** **0.707** **0.000** **1.085**	2H2080 0.269 46.504 0.459
14	1L1212 1.133 21.946 1.263	**0H2480** **1.244** **0.000** **1.500**	**0H2480** **1.261** **0.000** **1.548**	**0H2060** **1.205** **0.000** **1.602**	1H1610 0.717 23.242 1.001	2H1250 0.285 41.821 0.474	
15	2H1670 0.542 44.163 0.732	1H1680 0.740 20.393 1.013	1H1610 0.707 21.329 0.968	2H1250 0.442 34.138 0.707	Fuel ID Assembly power Assembly burnup Normalized Peak pin power		

Figure 4-10: Core Map of assembly maximum pin peaking for BOL of cycle 11 (bold are annular assemblies) for poisoned core

	H-	G-	F-	E-	D-	C-	B-
8	2L1212 0.680 42.950 0.716	0L2410 0.946 0.000 1.143	1L2480 1.009 25.301 1.108	0L2880 1.044 0.000 1.232	2H1680 0.913 44.502 0.983	0H2880 1.318 0.000 1.532	1L2010 1.109 23.393 1.309
9	0L2410 0.946 0.000 1.143	2H2010 0.793 37.667 0.873	0L2880 0.986 0.000 1.190	2H1680 0.923 34.304 1.006	0H2880 1.240 0.000 1.566	1L2480 1.290 24.541 1.418	0H2880 1.181 0.000 1.520
10	1L2480 1.009 25.301 1.108	0L2880 0.986 0.000 1.190	2H1612 0.860 37.721 0.990	0L3280 1.125 0.000 1.440	2H1250 1.104 34.943 1.216	1H2480 1.360 26.252 1.476	0H2880 1.164 0.000 1.511
11	0L2880 1.044 0.000 1.232	2H1680 0.922 34.300 1.005	0L3280 1.123 0.000 1.439	1H2880 1.391 17.705 1.581	1L2880 1.374 24.764 1.497	1H2060 1.350 24.356 1.486	0H2460 1.085 0.000 1.506
12	2H1680 0.913 44.502 0.983	0H2880 1.239 0.000 1.565	2H2010 1.103 34.937 1.216	1L2880 1.373 24.846 1.496	1H2480 1.312 28.617 1.501	0H4060 1.087 0.000 1.450	1H2480 0.704 26.838 1.014
13	0H2880 1.318 0.000 1.532	1L2480 1.288 24.624 1.417	1H2480 1.360 26.241 1.477	1H2060 1.352 24.327 1.487	0H4060 1.090 0.000 1.452	0H1660 0.973 0.000 1.320	2H2010 0.321 46.060 0.570
14	1L2010 1.109 23.393 1.309	0H2880 1.181 0.000 1.520	0H2880 1.165 0.000 1.511	0H2460 1.087 0.000 1.508	1H2480 0.709 26.859 1.018	2H1250 0.338 41.634 0.592	
15	2H1680 0.499 44.494 0.723	1H2480 0.664 26.152 0.947	1H3260 0.636 24.860 0.926	2H1250 0.353 43.474 0.604	Fuel ID Assembly power Assembly burnup Normalized Peak pin power		

Figure 4-11: Core Map of assembly maximum pin peaking for BOL of cycle 12 for poisoned core

4.4 Conclusions

The neutronic investigation of the transition core has shown that a core composed of annular fuel assemblies and solid fuel assemblies meets the licensing criteria and allows, on average, an 18-month cycle.

It should be noted that the purpose of the present work is not to design an ecomically optimized transition core, but rather to prove that a transition core is feasible. Would a transition from solid assemblies to annular assemblies be industrially considered, an economically optimized design shall be sought after.

Chapter 5

Summary, Conclusions And Recommendations For Future Investigations

5.1 Summary of conclusions

A transition from solid fuel to annular fuel in a PWR has been shown to be both economically attractive and technically feasible. The major results reached in this study are as follows.

Economic Valuation Using the Internal Rate of Return method, we showed that by first replacing the solid fuel by annular fuel before up-rating the plant, the investment will yield very high IRR. More specifically, if the up-rating of the plant coincides with a scheduled Steam-Generator replacement, the project yields an IRR of 27.4%. If this is not the case (*i.e.* the Steam Generator was not planned to be changed), a comfortably high IRR of 22.5% is reached.

Thermal-Hydraulic assessment The preferred approach is to gradually replace the solid fuel assemblies by annular fuel assemblies. The major question raised by such a configuration is whether or not the core is thermal-hydraulicly feasible. In

other words, is the MDNBR sufficiently high. Having a solid 17x17 assembly next to an annular 13x13 assembly has never been studied before, so before modeling the entire core, we studied a simple 2 assemblies model where a hot eighth of a solid assembly was placed next to a hot eighth of an annular assembly. We showed that because the annular assembly has slightly larger pressure drop, some flow is diverted from the annular part to the solid part, and even though the difference in MDNBR between a solid assembly only or a mixed situation are small, this effect benefits the MDNBR of the mixed assemblies.

Equiped with this understanding, we modeled a whole core and found that both the pressure drop for a mixed core and the MDNBR are slightly higher than the reference core of solid fuel assemblies.

The main conclusion is that the envisaged transition is thermal-hydraulically feasible and even slightly improves the margins to limiting criteria.

Neutronic assessment The final stage of our assessment was to demonstrate that a transition fuel management can actually be designed to meet the following criteria: *(i)* to sustain an 18-months cycle length during transition and after, *(ii)* to maintain peak critical boron concentration below 1750 ppm, and *(iii)* to maintain power peaking during cycles such that the hot channel factor $F_{\Delta h} \leq 1.65$ and the hot spot factor $F_q \leq 2.5$.

After several iterations, a core satisfying all criteria was reached with sufficient margins. It was also shown that the new annular core would also be well within the criteria after the 50% over power uprate.

5.2 Recommandations for future investigations

The first and most important piece of work needed is to modify CASMO-4 source code so that the code can handle annular fuel without having to virtually increase the U-238 content. Basically, the code needs to take into account the effect of higher neutron flux reaching the rod inner surface.

Should the industry consider the transition from solid to annular fuel, another recommandation would be to optimize the transition core design. As explained in Chapter 4, the purpose of the neutronic study was more to demonstrate the feasibility of a mixed core rather than reach an optimized design. On the other hand, an optimized design will yield a smaller cycle cost and will therefore enhance the economic attractiveness of the project. It will therefore be also possible to refine the economic assessment by taking into account the exact enrichment needs and the expected cycle lengths.

This study entirely focused on normal operation conditions. Another important track not yet explored is to perform a safety analysis of a mixed core of solid and annular fuel assemblies.

Appendix A

Economic Analysis: Calculation Details

A.1 Detailed modeling

The model is developed using EXCEL spreadsheets. Table A.1 gives the figures of interest for the model.

Depending on the case (Base Case, Case 1 or Case 2) the *Total Capital Post* will be: for Base Case the former capital cost minus the lost power supply during 3 months minus the Replacement Cost of Steam Generator ; for Case 1 and Case 2 the former capital cost minus the lost power supply during 3 months minus the Replacement Cost of Steam Generator minus the Cost of lost fuel.

Tables A.2, A.3 and A.4 present the details of the model for each case. In every case, it was assumed that the costs and prices are constant over one period and are equal to their value at the begining of the period. For instance, if the period spans from month 6 to month 12, we will assume that the cost of the fuel is the price at the begining of the period *e.g.* $Inital\ price\ \times (1 + Inflation\ Rate)^{0.5}$. Also note that because we use annual inflation rate, the inflation over 6 months will be $(1 + Inflation\ Rate)^{0.5}$, or $1 + \frac{Inflation\ Rate}{2}$ if the inflation is small compared to 1.

Even if the project profitability was assesed using the IRR method, two other alternative methods are detailed in the calculation: Benefit Cost Ratio and Net Present

Table A.1: Parameters for economic model

Description	Value
Total initial power	1200 MW(e)
Increase in power	600 MW(e)
Discount rate	11% /yr
Inflation rate for electricity price	1% /yr
Inflation rate for Fuel and O&M Costs	2% /yr
Capacity factor	95%
Former total capital cost	$1,090,200,000
Cost of Marginal Power Increase	$1,817 /kW(e)
Lost Power Supply during classic 3 months maintenance	$124,830,000
Replacement Cost of standard Steam Generators	$150,000,000
Total Capital Cost (w. steam generator cost, w/o 3 months lost power supply)	$940,200,000
Total Capital Cost (w/o steam generator cost, w/o 3 months lost power supply)	$815,370,000
Cost of solid fuel batch	$74,898,000
Construction time for power upgrade	1 year
Economic life-time (for capital cost recovery)	20 years
Retail Price for Produced Power	$0.050 /kWhr(e)
O&M Costs (BOP only)	$0.005 /kWhr(e)
Annular Fuel Cost	$0.00502 /kWhr(e)
Solid Fuel Cost	$0.005 /kWhr(e)

Value. These methods have the drawback of needing a discount rate. For our up-rate project, where the capital cost plays a crucial role in determing the profitability, the ranking of the options is very sensitive to the choice of the discount rate (which is in itself very difficult to evaluate).

Benefit Cost Ratio: the Benefit Cost Ratio (or BC) is the ratio of the total discounted incomes (benefits) over the total discounted costs for the total life-time of the plant.

Net Present Value: the Net Present Value (NPV) is the sum, over the economic life-time of the project, of the discounted profits (incomes minus costs).

Table A.2: Detailed modeling of Base Case

Time (m.)	Marginal Costs	Marginal Income	Net Profit
6	$\frac{Total\ Capital\ Cost}{2}$	0	Income-Cost
12	$\frac{Total\ Capital\ Cost}{2}$	0	Income-Cost
18	$600\ MW(e) \times (O\&M\ Cost + Fuel\ Cost) \times Capacity\ factor \times 6\ months \times (1 + Inflation\ rate)^{1.5-0.5}$	$600\ MW(e) \times (Electricity\ price) \times Capacity\ factor \times 6\ months \times (1 + Inflation\ rate)^{1.5-0.5}$	...
...	...	...	...

Table A.3: Detailed modeling of Case 1

Time (m.)	Marginal Costs	Marginal Income	Net Profit
6	$\frac{Total\ Capital\ Cost}{2}$	0	Income-Cost
12	$\frac{Total\ Capital\ Cost}{2}$	0	Income-Cost
30	$\frac{1}{3} \times 600\ MW(e) \times (O\&M\ Cost + Fuel\ Cost) \times Capacity\ factor \times 18\ months \times (1 + Inflation\ rate)^{2.5-0.5}$	$\frac{1}{3} \times 600\ MW(e) \times (Electricity\ price) \times Capacity\ factor \times 18\ months \times (1 + Inflation\ rate)^{2.5-0.5}$	...
48	$\frac{2}{3} \times 600\ MW(e) \times (O\&M\ Cost + Fuel\ Cost) \times Capacity\ factor \times 18\ months \times (1 + Inflation\ rate)^{4-0.5}$	$\frac{2}{3} \times 600\ MW(e) \times (Electricity\ price) \times Capacity\ factor \times 18\ months \times (1 + Inflation\ rate)^{4-0.5}$	...
66	$\frac{3}{3} \times 600\ MW(e) \times (O\&M\ Cost + Fuel\ Cost) \times Capacity\ factor \times 18\ months \times (1 + Inflation\ rate)^{5.5-0.5}$	$\frac{3}{3} \times 600\ MW(e) \times (Electricity\ price) \times Capacity\ factor \times 18\ months \times (1 + Inflation\ rate)^{5.5-0.5}$	...
...	...	...	...

A.2 Calculations details

EXCEL models for the different cases were developed. Tables A.5, A.6 and A.7 give the detailed calculations for the Base Case, Case 1 and Case 2, respectively. The period length is 6 months, and at each period the cost and incomes are computed . It is then easy to compute the BC ratio and the cash flow at this period (income minus cost). We also give the NPV at this period and the IRR for 6 months and its corresponding value for 1 year.

Table A.4: Detailed modeling of Case 2

Time (m.)	Marginal Costs	Marginal Income	Net Profit
18	$\frac{1}{3} \times 600\ MW(e) \times (\Delta\ Fuel\ Cost) \times Capacity\ factor \times 18\ months \times (1 + Inflation\ rate)^{1.5-0.5}$	0	Income-Cost
36	$\frac{2}{3} \times 600\ MW(e) \times (\Delta\ Fuel\ Cos) \times Capacity\ factor \times 18\ months \times (1 + Inflation\ rate)^{3-0.5}$	0	...
42	$\frac{Total\ Capital\ Cost}{2}$	0	...
48	$\frac{Total\ Capital\ Cost}{2}$	0	...
66	$\times 600\ MW(e) \times (O\&M\ Cost\ +\ Fuel\ Cost) \times Capacity\ factor \times 18\ months \times (1 + Inflation\ rate)^{5.5-0.5}$	$600\ MW(e) \times (Electricity\ price) \times Capacity\ factor \times 18\ months \times (1 + Inflation\ rate)^{5.5-0.5}$	...
84	...	...	...

Table A.5: Base Case economic valuation

Year	*Costs*	*Income*	*BC Ratio*	*Fj*	*NPV*	IRR 6m	IRR 1y
0.5	$488,926,500	$0	0.00%	-$488,926,500			
1	$488,926,500	$0	0.00%	-$488,926,500	-$952,994,997		
1.5	$25,516,251	$126,078,300	12.57%	$100,562,049	-$862,398,556	-82.5%	-96.9%
2	$25,770,150	$126,707,123	24.56%	$100,936,973	-$776,087,623	-54.6%	-79.4%
2.5	$26,026,576	$127,339,083	36.03%	$101,312,507	-$693,860,119	-36.4%	-59.5%
3	$26,285,553	$127,974,195	46.98%	$101,688,642	-$615,523,469	-24.5%	-43.0%
3.5	$26,547,107	$128,612,474	57.46%	$102,065,367	-$540,894,152	-16.4%	-30.2%
4	$26,811,264	$129,253,937	67.50%	$102,442,673	-$469,797,284	-10.8%	-20.4%
4.5	$27,078,049	$129,898,599	77.10%	$102,820,549	-$402,066,203	-6.6%	-12.8%
5	$27,347,489	$130,546,476	86.31%	$103,198,987	-$337,542,092	-3.5%	-6.9%
5.5	$27,619,610	$131,197,585	95.13%	$103,577,974	-$276,073,606	-1.1%	-2.2%
6	$27,894,439	$131,851,941	103.59%	$103,957,502	-$217,516,521	0.7%	1.5%
6.5	$28,172,003	$132,509,560	111.71%	$104,337,558	-$161,733,401	2.2%	4.5%
7	$28,452,328	$133,170,460	119.50%	$104,718,132	-$108,593,282	3.4%	7.0%
7.5	$28,735,443	$133,834,656	126.98%	$105,099,213	-$57,971,362	4.4%	9.0%
8	$29,021,374	$134,502,165	134.16%	$105,480,790	-$9,748,716	5.2%	10.7%
8.5	$29,310,151	$135,173,003	141.07%	$105,862,851	$36,187,980	5.9%	12.1%
9	$29,601,802	$135,847,186	147.70%	$106,245,384	$79,946,714	6.4%	13.3%
9.5	$29,896,354	$136,524,733	154.08%	$106,628,378	$121,630,389	6.9%	14.3%
10	$30,193,838	$137,205,658	160.22%	$107,011,820	$161,337,057	7.3%	15.2%
10.5	$30,494,282	$137,889,980	166.12%	$107,395,698	$199,160,155	7.7%	15.9%
11	$30,797,715	$138,577,715	171.80%	$107,780,000	$235,188,715	8.0%	16.5%
11.5	$31,104,167	$139,268,880	177.26%	$108,164,713	$269,507,574	8.2%	17.1%
12	$31,413,669	$139,963,492	182.52%	$108,549,823	$302,197,569	8.4%	17.6%
12.5	$31,726,250	$140,661,569	187.59%	$108,935,318	$333,335,730	8.6%	18.0%
13	$32,041,942	$141,363,127	192.47%	$109,321,184	$362,995,454	8.8%	18.4%
13.5	$32,360,776	$142,068,184	197.17%	$109,707,409	$391,246,675	8.9%	18.7%
14	$32,682,781	$142,776,758	201.69%	$110,093,977	$418,156,034	9.1%	19.0%
14.5	$33,007,991	$143,488,866	206.05%	$110,480,875	$443,787,025	9.2%	19.2%
15	$33,336,437	$144,204,526	210.26%	$110,868,089	$468,200,150	9.3%	19.4%
15.5	$33,668,151	$144,923,755	214.30%	$111,255,604	$491,453,055	9.4%	19.6%
16	$34,003,166	$145,646,571	218.21%	$111,643,405	$513,600,666	9.5%	19.8%
16.5	$34,341,514	$146,372,992	221.97%	$112,031,478	$534,695,320	9.5%	20.0%
17	$34,683,229	$147,103,037	225.59%	$112,419,808	$554,786,882	9.6%	20.1%
17.5	$35,028,344	$147,836,722	229.09%	$112,808,378	$573,922,862	9.6%	20.2%
18	$35,376,893	$148,574,067	232.46%	$113,197,174	$592,148,530	9.7%	20.3%
18.5	$35,728,911	$149,315,089	235.71%	$113,586,178	$609,507,017	9.7%	20.4%
19	$36,084,431	$150,059,808	238.84%	$113,975,376	$626,039,418	9.8%	20.5%
19.5	$36,443,489	$150,808,240	241.86%	$114,364,751	$641,784,887	9.8%	20.6%
20	$36,806,120	$151,560,406	244.77%	$114,754,286	$656,780,728	9.9%	20.7%

Note: BC=Benefit Cost ; NPV=Net Present Value ; IRR=Internal Rate of Return

Table A.6: Case 1 economic valuation

Year	*Costs*	*Income*	*BC Ratio*	*Fj*	*NPV*	IRR 6m	IRR 1y
0.5	$451,477,500	$0	0.00%	-$451,477,500			
1	$451,477,500	$0	0.00%	-$451,477,500	-$880,000,979		
1.5	$8,505,417	$42,026,100	4.61%	$33,520,683	-$849,802,165	-93.1%	-99.5%
2	$8,590,050	$42,235,708	9.16%	$33,645,658	-$821,031,854	-72.7%	-92.6%
2.5	$8,675,525	$42,446,361	13.64%	$33,770,836	-$793,622,687	-56.1%	-80.7%
3	$17,523,702	$85,316,130	22.41%	$67,792,428	-$741,398,253	-37.8%	-61.3%
3.5	$17,698,071	$85,741,649	30.89%	$68,043,578	-$691,645,375	-27.4%	-47.3%
4	$17,874,176	$86,169,291	39.10%	$68,295,115	-$644,247,463	-20.4%	-36.6%
4.5	$27,078,049	$129,898,599	50.93%	$102,820,549	-$576,516,382	-13.5%	-25.1%
5	$27,347,489	$130,546,476	62.18%	$103,198,987	-$511,992,271	-8.9%	-17.0%
5.5	$27,619,610	$131,197,585	72.90%	$103,577,974	-$450,523,785	-5.6%	-10.9%
6	$27,894,439	$131,851,941	83.12%	$103,957,502	-$391,966,700	-3.1%	-6.1%
6.5	$28,172,003	$132,509,560	92.86%	$104,337,558	-$336,183,581	-1.2%	-2.4%
7	$28,452,328	$133,170,460	102.15%	$104,718,132	-$283,043,461	0.3%	0.7%
7.5	$28,735,443	$133,834,656	111.03%	$105,099,213	-$232,421,541	1.6%	3.2%
8	$29,021,374	$134,502,165	119.51%	$105,480,790	-$184,198,895	2.6%	5.2%
8.5	$29,310,151	$135,173,003	127.61%	$105,862,851	-$138,262,199	3.4%	6.9%
9	$29,601,802	$135,847,186	135.37%	$106,245,384	-$94,503,465	4.1%	8.4%
9.5	$29,896,354	$136,524,733	142.78%	$106,628,378	-$52,819,791	4.7%	9.6%
10	$30,193,838	$137,205,658	149.89%	$107,011,820	-$13,113,122	5.2%	10.7%
10.5	$30,494,282	$137,889,980	156.69%	$107,395,698	$24,709,976	5.6%	11.6%
11	$30,797,715	$138,577,715	163.20%	$107,780,000	$60,738,536	6.0%	12.4%
11.5	$31,104,167	$139,268,880	169.44%	$108,164,713	$95,057,395	6.3%	13.0%
12	$31,413,669	$139,963,492	175.43%	$108,549,823	$127,747,390	6.6%	13.6%
12.5	$31,726,250	$140,661,569	181.17%	$108,935,318	$158,885,551	6.8%	14.2%
13	$32,041,942	$141,363,127	186.68%	$109,321,184	$188,545,274	7.1%	14.6%
13.5	$32,360,776	$142,068,184	191.96%	$109,707,409	$216,796,496	7.2%	15.0%
14	$32,682,781	$142,776,758	197.04%	$110,093,977	$243,705,855	7.4%	15.4%
14.5	$33,007,991	$143,488,866	201.91%	$110,480,875	$269,336,846	7.6%	15.7%
15	$33,336,437	$144,204,526	206.58%	$110,868,089	$293,749,971	7.7%	16.0%
15.5	$33,668,151	$144,923,755	211.08%	$111,255,604	$317,002,875	7.8%	16.2%
16	$34,003,166	$145,646,571	215.39%	$111,643,405	$339,150,487	7.9%	16.4%
16.5	$34,341,514	$146,372,992	219.54%	$112,031,478	$360,245,141	8.0%	16.6%
17	$34,683,229	$147,103,037	223.52%	$112,419,808	$380,336,703	8.1%	16.8%
17.5	$35,028,344	$147,836,722	227.35%	$112,808,378	$399,472,683	8.2%	17.0%
18	$35,376,893	$148,574,067	231.03%	$113,197,174	$417,698,351	8.2%	17.1%
18.5	$35,728,911	$149,315,089	234.57%	$113,586,178	$435,056,838	8.3%	17.2%
19	$36,084,431	$150,059,808	237.97%	$113,975,376	$451,589,239	8.3%	17.4%
19.5	$36,443,489	$150,808,240	241.24%	$114,364,751	$467,334,708	8.4%	17.5%
20	$36,806,120	$151,560,406	244.39%	$114,754,286	$482,330,549	8.4%	17.6%

Note: BC=Benefit Cost ; NPV=Net Present Value ; IRR=Internal Rate of Return

Table A.7: Case 2 economic valuation

Year	*Costs*	*Income*	*BC Ratio*	*Fj*	*NPV*	IRR 6m	IRR 1y
0.5	$16,644	$0	0.00%	-$16,644			
1	$16,810	$0	0.00%	-$16,810	-$32,599		
1.5	$16,977	$0	0.00%	-$16,977	-$47,893		
2	$34,292	$0	0.00%	-$34,292	-$77,216		
2.5	$34,633	$0	0.00%	-$34,633	-$105,325		
3	$34,977	$0	0.00%	-$34,977	-$132,270		
3.5	$451,477,500	$0	0.00%	-$451,477,500	-$330,248,727		
4	$451,477,500	$0	0.00%	-$451,477,500	-$643,581,401		
4.5	$27,078,049	$129,898,599	13.96%	$102,820,549	-$575,850,321	-80.9%	-96.3%
5	$27,347,489	$130,546,476	27.20%	$103,198,987	-$511,326,210	-52.2%	-77.2%
5.5	$27,619,610	$131,197,585	39.75%	$103,577,974	-$449,857,724	-33.9%	-56.3%
6	$27,894,439	$131,851,941	51.68%	$103,957,502	-$391,300,639	-22.1%	-39.3%
6.5	$28,172,003	$132,509,560	63.00%	$104,337,558	-$335,517,519	-14.2%	-26.3%
7	$28,452,328	$133,170,460	73.78%	$104,718,132	-$282,377,400	-8.6%	-16.5%
7.5	$28,735,443	$133,834,656	84.03%	$105,099,213	-$231,755,480	-4.6%	-9.0%
8	$29,021,374	$134,502,165	93.80%	$105,480,790	-$183,532,834	-1.6%	-3.1%
8.5	$29,310,151	$135,173,003	103.11%	$105,862,851	-$137,596,138	0.7%	1.4%
9	$29,601,802	$135,847,186	111.99%	$106,245,384	-$93,837,404	2.5%	5.1%
9.5	$29,896,354	$136,524,733	120.46%	$106,628,378	-$52,153,729	3.9%	8.0%
10	$30,193,838	$137,205,658	128.55%	$107,011,820	-$12,447,061	5.0%	10.3%
10.5	$30,494,282	$137,889,980	136.28%	$107,395,698	$25,376,037	6.0%	12.3%
11	$30,797,715	$138,577,715	143.66%	$107,780,000	$61,404,597	6.7%	13.9%
11.5	$31,104,167	$139,268,880	150.73%	$108,164,713	$95,723,456	7.3%	15.2%
12	$31,413,669	$139,963,492	157.49%	$108,549,823	$128,413,451	7.9%	16.3%
12.5	$31,726,250	$140,661,569	163.96%	$108,935,318	$159,551,612	8.3%	17.3%
13	$32,041,942	$141,363,127	170.15%	$109,321,184	$189,211,336	8.7%	18.1%
13.5	$32,360,776	$142,068,184	176.08%	$109,707,409	$217,462,557	9.0%	18.8%
14	$32,682,781	$142,776,758	181.77%	$110,093,977	$244,371,916	9.3%	19.4%
14.5	$33,007,991	$143,488,866	187.22%	$110,480,875	$270,002,907	9.5%	19.9%
15	$33,336,437	$144,204,526	192.44%	$110,868,089	$294,416,032	9.7%	20.3%
15.5	$33,668,151	$144,923,755	197.46%	$111,255,604	$317,668,937	9.9%	20.7%
16	$34,003,166	$145,646,571	202.26%	$111,643,405	$339,816,548	10.0%	21.0%
16.5	$34,341,514	$146,372,992	206.88%	$112,031,478	$360,911,202	10.1%	21.3%
17	$34,683,229	$147,103,037	211.30%	$112,419,808	$381,002,764	10.3%	21.6%
17.5	$35,028,344	$147,836,722	215.55%	$112,808,378	$400,138,744	10.4%	21.8%
18	$35,376,893	$148,574,067	219.63%	$113,197,174	$418,364,412	10.4%	22.0%
18.5	$35,728,911	$149,315,089	223.55%	$113,586,178	$435,722,899	10.5%	22.1%
19	$36,084,431	$150,059,808	227.31%	$113,975,376	$452,255,300	10.6%	22.3%
19.5	$36,443,489	$150,808,240	230.93%	$114,364,751	$468,000,769	10.6%	22.4%
20	$36,806,120	$151,560,406	234.40%	$114,754,286	$482,996,610	10.7%	22.5%

Note: BC=Benefit Cost ; NPV=Net Present Value ; IRR=Internal Rate of Return

Appendix B

VIPRE-01 Inputs

B.1 Mixed assembly model input

```
*                                                                      *
*  1/4 Mix assembly (1/8 annular & 1/8 solid)                          *
*                                                                      *
************************************************************************
1,0,0                                          *vipre.1
1/4 Mix assembly (1/8 annular & 1/8 solid)                  *vipre.2
************************************************************************
geom,89,89,20,0,0,0 *normal input geometry                  *geom.1
144.0945,0.0,0.5                                  *geom.2
1, 0.0594, 0.6309, 0.4416, 1, 2, 0.1224, 0.4144, , , , , ,
2, 0.1369, 1.1777, 1.1777, 2, 3, 0.1224, 0.4144, 4, 0.1224, 0.4972, , ,
3, 0.0684, 0.5889, 0.5889, 1, 5, 0.1224, 0.4144, , , , , ,
4, 0.1189, 1.2619, 0.8833, 2, 5, 0.1224, 0.4972, 7, 0.0688, 0.4972, , ,
5, 0.1369, 1.1777, 1.1777, 2, 6, 0.1224, 0.4144, 8, 0.1224, 0.4972, , ,
6, 0.0594, 0.6309, 0.4416, 1, 9, 0.0688, 0.4144, , , , , ,
7, 0.1189, 1.2619, 0.8833, 2, 8, 0.1224, 0.4972, 11, 0.1224, 0.4972, , ,
8, 0.1369, 1.1777, 1.1777, 2, 9, 0.1224, 0.4972, 12, 0.1224, 0.4972, , ,
9, 0.1189, 1.2619, 0.8833, 2, 10, 0.0688, 0.4144, 13, 0.1224, 0.4972, , ,
10, 0.0594, 0.6309, 0.4416, 1, 14, 0.1224, 0.4144, , , , , ,
11, 0.1369, 1.1777, 1.1777, 2, 12, 0.1224, 0.4972, 16, 0.1224, 0.4972, , ,
12, 0.1369, 1.1777, 1.1777, 2, 13, 0.1224, 0.4972, 17, 0.1224, 0.4972, , ,
13, 0.1369, 1.1777, 1.1777, 2, 14, 0.1224, 0.4972, 18, 0.1224, 0.4972, , ,
14, 0.1369, 1.1777, 1.1777, 2, 15, 0.1224, 0.4144, 19, 0.1224, 0.4972, , ,
15, 0.0594, 0.6309, 0.4416, 1, 20, 0.0688, 0.4144, , , , , ,
16, 0.1189, 1.2619, 0.8833, 2, 17, 0.1224, 0.4972, 22, 0.0688, 0.4972, , ,
17, 0.1369, 1.1777, 1.1777, 2, 18, 0.1224, 0.4972, 23, 0.1224, 0.4972, , ,
18, 0.1189, 1.2619, 0.8833, 2, 19, 0.0688, 0.4972, 24, 0.0688, 0.4972, , ,
19, 0.1189, 1.2619, 0.8833, 2, 20, 0.1224, 0.4972, 25, 0.0688, 0.4972, , ,
20, 0.1189, 1.2619, 0.8833, 2, 21, 0.0688, 0.4144, 26, 0.1224, 0.4972, , ,
21, 0.0594, 0.6309, 0.4416, 1, 27, 0.1224, 0.4144, , , , , ,
22, 0.1189, 1.2619, 0.8833, 2, 23, 0.1224, 0.4972, 29, 0.1224, 0.4972, , ,
23, 0.1369, 1.1777, 1.1777, 2, 24, 0.1224, 0.4972, 30, 0.1224, 0.4972, , ,
24, 0.1189, 1.2619, 0.8833, 2, 25, 0.0688, 0.4972, 31, 0.1224, 0.4972, , ,
25, 0.1189, 1.2619, 0.8833, 2, 26, 0.1224, 0.4972, 32, 0.1224, 0.4972, , ,
26, 0.1369, 1.1777, 1.1777, 2, 27, 0.1224, 0.4972, 33, 0.1224, 0.4972, , ,
27, 0.1369, 1.1777, 1.1777, 2, 28, 0.1224, 0.4972, 34, 0.1224, 0.4972, , ,
28, 0.0684, 0.5889, 0.5889, 1, 35, 0.1224, 0.4144, , , , , ,
29, 0.1369, 1.1777, 1.1777, 2, 30, 0.1224, 0.4972, 37, 0.1224, 0.3758, , ,
30, 0.1369, 1.1777, 1.1777, 2, 31, 0.1224, 0.4972, 38, 0.1224, 0.3758, , ,
31, 0.1369, 1.1777, 1.1777, 3, 32, 0.1224, 0.4972, 38, 0.1181, 0.3758,?
 39, 0.004 , 0.376
32, 0.1369, 1.1777, 1.1777, 2, 33, 0.1224, 0.4972, 39, 0.1224, 0.3758, , ,
33, 0.1369, 1.1777, 1.1777, 2, 34, 0.1224, 0.4972, 40, 0.1224, 0.3758, , ,
34, 0.1369, 1.1777, 1.1777, 2, 35, 0.1224, 0.4972, 41, 0.1224, 0.3758, , ,
35, 0.1369, 1.1777, 1.1777, 3, 36, 0.1224, 0.4144, 41, 0.0791, 0.3758,?
 42, 0.043, 0.376
36, 0.0684, 0.5889, 0.5889, 1, 42, 0.1224, 0.2929, , , , , ,
37, 0.1573, 1.7178, 1.7178, 2, 38, 0.1755, 0.6500, 43, 0.0450, 0.6183, , ,
38, 0.1798, 1.6551, 1.6551, 2, 39, 0.2841, 0.6500, 44, 0.0450, 0.6183, , ,
39, 0.1620, 1.7944, 1.7944, 2, 40, 0.1008, 0.6500, 45, 0.0450, 0.6183, , ,
40, 0.1552, 1.7007, 1.7007, 2, 41, 0.1352, 0.6500, 46, 0.0450, 0.6183, , ,
41, 0.1747, 1.7114, 1.7114, 2, 42, 0.2841, 0.8667, 47, 0.0450, 0.6183, , ,
42, 0.2124, 2.2184, 2.2184, 2, 48, 0.0450, 0.5100, , , , , ,
43, 0.1350, 1.9007, 1.9007, 2, 44, 0.0450, 0.6500, 49, 0.0450, 0.6500, , ,
44, 0.1350, 1.9007, 1.9007, 2, 45, 0.0450, 0.6500, 50, 0.0450, 0.6500, , ,
45, 0.1350, 1.9007, 1.9007, 2, 46, 0.0450, 0.6500, 51, 0.0450, 0.6500, , ,
46, 0.1350, 1.9007, 1.9007, 2, 47, 0.0450, 0.6500, 52, 0.0450, 0.6500, , ,
47, 0.1350, 1.9007, 1.9007, 2, 48, 0.0450, 0.5417, 53, 0.0450, 0.5417, , ,
48, 0.0675, 0.9503, 0.9503, 1, , , , , , , , ,
49, 0.1350, 1.9007, 1.9007, 2, 50, 0.0450, 0.6500, 54, 0.0450, 0.6500, , ,
50, 0.1350, 1.9007, 1.4255, 2, 51, 0.0450, 0.6500, 55, 0.0450, 0.6500, , ,
51, 0.1350, 1.9007, 1.4255, 2, 52, 0.0450, 0.6500, 56, 0.0450, 0.6500, , ,
52, 0.1350, 1.9007, 1.9007, 2, 53, 0.0450, 0.5417, 57, 0.0450, 0.5417, , ,
53, 0.0675, 0.9503, 0.9503, 1, , , , , , , , ,
54, 0.1350, 1.9007, 1.9007, 2, 55, 0.0450, 0.6500, 58, 0.0450, 0.6500, , ,
55, 0.1350, 1.9007, 1.4255, 2, 56, 0.0450, 0.6500, 59, 0.0450, 0.6500, , ,
56, 0.1350, 1.9007, 1.4255, 2, 57, 0.0450, 0.5417, 60, 0.0450, 0.5417, , ,
57, 0.0675, 0.9503, 0.9503
58, 0.1350, 1.9007, 1.9007, 2, 59, 0.0450, 0.6500, 61, 0.0450, 0.6500, , ,
59, 0.1350, 1.9007, 1.9007, 2, 60, 0.0450, 0.5417, 62, 0.0450, 0.5417, , ,
```

```
60, 0.0675, 0.9503, 0.9503
61, 0.1350, 1.9007, 1.9007, 2, 62, 0.0450, 0.5417, 63, 0.0450, 0.5417, , ,
62, 0.0675, 0.9503, 0.9503
63, 0.0675, 0.9503, 0.7127
64, 0.0454, 0.5339, 0.5339
65, 0.0907, 1.0678, 1.0678
66, 0.0907, 1.0678, 1.0678
67, 0.0907, 1.0678, 1.0678
68, 0.0907, 1.0678, 1.0678
69, 0.0907, 1.0678, 1.0678
70, 0.0454, 0.5339, 0.5339
71, 0.0454, 0.5339, 0.5339
72, 0.0907, 1.0678, 1.0678
73, 0.0907, 1.0678, 1.0678
74, 0.0907, 1.0678, 1.0678
75, 0.0907, 1.0678, 1.0678
76, 0.0454, 0.5339, 0.5339
77, 0.0454, 0.5339, 0.5339
78, 0.0907, 1.0678, 1.0678
79, 0.0907, 1.0678, 1.0678
80, 0.0454, 0.5339, 0.5339
81, 0.0454, 0.5339, 0.5339
82, 0.0907, 1.0678, 1.0678
83, 0.0907, 1.0678, 1.0678
84, 0.0454, 0.5339, 0.5339
85, 0.0454, 0.5339, 0.5339
86, 0.0907, 1.0678, 1.0678
87, 0.0454, 0.5339, 0.5339
88, 0.0454, 0.5339, 0.5339
89, 0.0454, 0.5339, 0.5339                                    *geom.4
*******************************************************************************
prop,0,0,2,1  *internal EPRI functions                          *prop.1
*******************************************************************************
rods,1,99,1,3,4,0,0,0,0,0,0    *3 geometry types, w/ cond rod          *rods.1
0.0,0.0,0,0                                                    *rods.2
-1                                                             *rods.3
1.55  *chopped cosine with peak to average = 1.55                       *rods.5
******rods geometry inputs*********
1, 2, 0.825, 1, 1, 0.250, 2, 0.250
2, 2, 0.803, 1, 1, 0.125, 2, 0.250, 3, 0.125
3, 2, 0.825, 1, 2, 0.250, 4, 0.250
4, 2, 0.799, 1, 2, 0.250, 3, 0.250, 4, 0.250, 5, 0.250
5, 2, 0.804, 1, 3, 0.125, 5, 0.250, 6, 0.125
6, 2, 0.826, 1, 4, 0.250, 5, 0.250, 7, 0.250, 8, 0.250
7, 2, 0.829, 1, 5, 0.250, 6, 0.250, 8, 0.250, 9, 0.250
8, 2, 0.823, 1, 7, 0.250, 11, 0.250
9, 2, 0.805, 1, 7, 0.250, 8, 0.250, 11, 0.250, 12, 0.250
10, 2, 0.805, 1, 8, 0.250, 9, 0.250, 12, 0.250, 13, 0.250
11, 2, 0.837, 1, 9, 0.250, 10, 0.250, 13, 0.250, 14, 0.250
12, 2, 0.825, 1, 10, 0.125, 14, 0.250, 15, 0.125
13, 2, 0.829, 1, 11, 0.250, 16, 0.250
14, 2, 0.805, 1, 11, 0.250, 12, 0.250, 16, 0.250, 17, 0.250
15, 2, 0.808, 1, 12, 0.250, 13, 0.250, 17, 0.250, 18, 0.250
16, 2, 0.837, 1, 13, 0.250, 14, 0.250, 18, 0.250, 19, 0.250
17, 2, 0.841, 1, 14, 0.250, 15, 0.250, 19, 0.250, 20, 0.250
18, 2, 0.822, 1, 16, 0.250, 17, 0.250, 22, 0.250, 23, 0.250
19, 2, 0.825, 1, 17, 0.250, 18, 0.250, 23, 0.250, 24, 0.250
20, 2, 0.832, 1, 19, 0.250, 20, 0.250, 25, 0.250, 26, 0.250
21, 2, 0.813, 1, 20, 0.250, 21, 0.250, 26, 0.250, 27, 0.250
22, 2, 0.781, 1, 21, 0.125, 27, 0.250, 28, 0.125
23, 2, 0.813, 1, 22, 0.250, 29, 0.250
24, 2, 0.793, 1, 22, 0.250, 23, 0.250, 29, 0.250, 30, 0.250
25, 2, 0.797, 1, 23, 0.250, 24, 0.250, 30, 0.250, 31, 0.250
26, 2, 0.813, 1, 24, 0.250, 25, 0.250, 31, 0.250, 32, 0.250
27, 2, 0.789, 1, 25, 0.250, 26, 0.250, 32, 0.250, 33, 0.250
28, 2, 0.778, 1, 26, 0.250, 27, 0.250, 33, 0.250, 34, 0.250
29, 2, 0.763, 1, 27, 0.250, 28, 0.250, 34, 0.250, 35, 0.250
30, 2, 0.752, 1, 28, 0.125, 35, 0.250, 36, 0.125
31, 2, 0.790, 1, 29, 0.250, 37, 0.250
32, 2, 0.787, 1, 29, 0.250, 30, 0.250, 37, 0.402, 38, 0.098
```

33, 2, 0.786, 1, 30, 0.250, 31, 0.250, 38, 0.500
34, 2, 0.788, 1, 31, 0.250, 32, 0.250, 39, 0.500
35, 2, 0.785, 1, 32, 0.250, 33, 0.250, 39, 0.217, 40, 0.283
36, 2, 0.775, 1, 33, 0.250, 34, 0.250, 40, 0.354, 41, 0.146
37, 2, 0.765, 1, 34, 0.250, 35, 0.250, 41, 0.500
38, 2, 0.764, 1, 35, 0.250, 36, 0.250, 42, 0.500
39, 2, 0.776, 1, 36, 0.125, 42, 0.375
40, 1, 1.299, 1, 37, 0.250, 43, 0.250
-40, 1, 1.299, 1, 64, 0.500
41, 1, 1.308, 1, 37, 0.250, 38, 0.250, 43, 0.250, 44, 0.250
-41, 1, 1.308, 1, 65, 1.000
42, 1, 1.315, 1, 38, 0.250, 39, 0.250, 44, 0.250, 45, 0.250
-42, 1, 1.315, 1, 66, 1.000
43, 1, 1.312, 1, 39, 0.250, 40, 0.250, 45, 0.250, 46, 0.250
-43, 1, 1.312, 1, 67, 1.000
44, 1, 1.299, 1, 40, 0.250, 41, 0.250, 46, 0.250, 47, 0.250
-44, 1, 1.299, 1, 68, 1.000
45, 1, 1.290, 1, 41, 0.250, 42, 0.250, 47, 0.250, 48, 0.250
-45, 1, 1.290, 1, 69, 1.000
46, 1, 1.313, 1, 42, 0.375, 48, 0.125
-46, 1, 1.313, 1, 70, 0.500
47, 1, 1.286, 1, 43, 0.250, 49, 0.250
-47, 1, 1.286, 1, 71, 0.500
48, 1, 1.321, 1, 43, 0.250, 44, 0.250, 49, 0.250, 50, 0.250
-48, 1, 1.321, 1, 72, 1.000
49, 1, 1.389, 1, 44, 0.250, 45, 0.250, 50, 0.250, 51, 0.250
-49, 1, 1.389, 1, 73, 1.000
50, 1, 1.321, 1, 45, 0.250, 46, 0.250, 51, 0.250, 52, 0.250
-50, 1, 1.321, 1, 74, 1.000
51, 1, 1.278, 1, 46, 0.250, 47, 0.250, 52, 0.250, 53, 0.250
-51, 1, 1.278, 1, 75, 1.000
52, 1, 1.267, 1, 47, 0.250, 48, 0.125, 53, 0.125
-52, 1, 1.267, 1, 76, 0.500
53, 1, 1.301, 1, 49, 0.250, 54, 0.250
-53, 1, 1.301, 1, 77, 0.500
54, 1, 1.387, 1, 49, 0.250, 50, 0.250, 54, 0.250, 55, 0.250
-54, 1, 1.387, 1, 78, 1.000
55, 1, 1.394, 1, 51, 0.250, 52, 0.250, 56, 0.250, 57, 0.250
-55, 1, 1.394, 1, 79, 1.000
56, 1, 1.299, 1, 52, 0.250, 53, 0.125, 57, 0.125
-56, 1, 1.299, 1, 80, 0.500
57, 1, 1.290, 1, 54, 0.250, 58, 0.250
-57, 1, 1.290, 1, 81, 0.500
58, 1, 1.326, 1, 54, 0.250, 55, 0.250, 58, 0.250, 59, 0.250
-58, 1, 1.326, 1, 82, 1.000
59, 1, 1.408, 1, 55, 0.250, 56, 0.250, 59, 0.250, 60, 0.250
-59, 1, 1.408, 1, 83, 1.000
60, 1, 1.383, 1, 56, 0.250, 57, 0.125, 60, 0.125
-60, 1, 1.383, 1, 84, 0.500
61, 1, 1.290, 1, 58, 0.250, 61, 0.250
-61, 1, 1.290, 1, 85, 0.500
62, 1, 1.301, 1, 58, 0.250, 59, 0.250, 61, 0.250, 62, 0.250
-62, 1, 1.301, 1, 86, 1.000
63, 1, 1.317, 1, 59, 0.250, 60, 0.125, 62, 0.125
-63, 1, 1.317, 1, 87, 0.500
64, 1, 1.385, 1, 61, 0.250, 63, 0.250
-64, 1, 1.385, 1, 88, 0.500
65, 1, 1.322, 1, 61, 0.250, 62, 0.125, 63, 0.125
-65, 1, 1.322, 1, 89, 0.500
66, 3, 0.000, 1, 1, 0.125
67, 3, 0.000, 1, 4, 0.250, 7, 0.250
68, 3, 0.000, 1, 6, 0.125, 9, 0.250, 10, 0.125
69, 3, 0.000, 1, 15, 0.125, 20, 0.250, 21, 0.125
70, 3, 0.000, 1, 16, 0.250, 22, 0.250
71, 3, 0.000, 1, 18, 0.250, 19, 0.250, 24, 0.250, 25, 0.250
72, 3, 0.000, 1, 50, 0.250, 51, 0.250, 55, 0.250, 56, 0.250
73, 3, 0.000, 1, 63, 0.125
0 *rods.9
2,nucl,0.37488,0.325,8,0.0,0.0225 *rods.62
0,0,0,0,0,1000.0,0.95,0.0 *rods.63

```
1,tube,0.605,0.339882,5                                    *rods.68
2,1,0.0224921,0.0,?  *inner cladding                         *rods.69
2,2,0.0024488,0.0,?  *inner gap                             *rods.69
8,3,0.0826772,1.0,?  *fuel ring                             *rods.69
2,4,0.0024409,0.0    *outer gap                             *rods.69
2,1,0.0225000,0.0    *outer cladding                          *rods.69
3, dumy, 0.4820,0.0,0                                      *rods.68
1,17,409.0,clad                                  *rods.70
0.0,0.0671,7.3304509,?
25,0.0671,7.3304509
50,0.0671,7.33045093,?
65,0.0671,7.33045093
80.33,0.0671,7.33045093,?
260.33,0.07212,8.11585329
692.33,0.07904,9.80167423,?
1502.33,0.08955,13.2923001
1507.73,0.11988,13.3211893,?
1543.73,0.14089,13.5166505
1579.73,0.14686,13.717249,?
1615.73,0.1717,13.9231981
1651.73,0.1949,14.1347101,?
1687.73,0.18388,14.3519980
1723.73,0.1478,14.5752746,?
1759.73,0.112,14.804753
1786.73,0.085,14.9810589
*2240.33,0.085,18.5665964
2,1,0.025,igap                                  *rods.70
1,1.240834,0.2156263   *Cp=5195J/kg-K *gap=6000              *rods.71
3,22,650.617,FUO2                                  *rods.70
86,0.05677357,4.73275874,?
176,0.06078589,4.29917259
266,0.06366347,3.93877428,?
356,0.06581210,3.63454049
446,0.06747631,3.37435643,?
536,0.06880819,3.1493668
626,0.06990545,2.95294976,?
716,0.07083283,2.78005572
806,0.07163441,2.62676801,?
896,0.07234099,2.49000319
986,0.07297458,2.36730189,?
1076,0.07355124,2.25667975
1166,0.07408294,2.1565193,?
1256,0.07457886,2.06549023
1346,0.07504628,1.98248979,?
1436,0.07549123,1.90659753
1526,0.0759191,1.83704065,?
1616,0.07633503,1.77316713
1706,0.0767443,1.7144247,?
1796,0.07715268,1.66034425
1886,0.07756663,1.61052668,?
1976,0.07799351,1.5646323                          *rods.71
4,1,0.025,ogap                                  *rods.70
1,1.240834,0.2149314   *Cp=5195J/kg-K *gap=6000              *rods.71
******oper input*****************************************************************
oper,1,1,0,1,0,1,0,0,0                                     *oper.1
18.00,1.3,0.0,0.005,0                                       *oper.2
0                                                 *oper.3
2248.1,562.46,50.421,156.2,0.0                                *oper.5
0          *no forcing functions                            *oper.12
*******************************************************************************
corr,2,2,0                                          *corr.1
epri,epri,epri,none                                    *corr.2
0.2                                               *corr.3
ditb,thsp,thsp,w-3l,cond,g5.7    *correlation for boiling curve          *corr.6
w-3s,w-3l              *dnb analysis by w-3l                    *corr.9
0.0            *w-3s input data                          *corr.10
0.042,0.066,0.986  *w-3l input data                            *corr.11
*******************************************************************************
drag,1,1,4                                          *drag.1
0.316,-0.25,0.0,64.0,-1.0,0.0        *axial friction correlation         *drag.2
```

```
0.3749,0.4972    *rod diameter,Pitch                              *drag.7
*7.333,-0.2,0.0,7.333,-0.2,0.0
3.098,-0.2,0.0,0.0,0.0,0.5 * lateral drag correlation for Standard       *drag.8
*0.5,0.496       *pitch=0.496,kij=0.5l/p                          *drag.5
*********************************************************************************
grid,0,3                                                  *grid.1
0.6,0.4,1.0                                               *grid.2
63,9                                                      *grid.4
1, 2, 3, 4, 5, 6, 7, 8, 9, 10, 11, 12, 13, 14, 15, 16
17, 18, 19, 20, 21, 22, 23, 24, 25, 26, 27, 28, 29, 30, 31, 32
33, 34, 35, 36, 37, 38, 39, 40, 41, 42, 43, 44, 45, 46, 47, 48
49, 50, 51, 52, 53, 54, 55, 56, 57, 58, 59, 60, 61, 62, 63              *grid.5
0.0,2,12.0079,1,32.0079,1,52.0079,1,?
72.0079,1,92.0079,1,112.0079,1,132.0079,1,
144.0945,3                    *grid loc.                  *grid.6
26,2
64, 65, 66, 67, 68, 69, 70, 71, 72, 73, 74, 75, 76, 77, 78, 79
80, 81, 82, 83, 84, 85, 86, 87, 88, 89
0.0,2,144.0945,3
0
*********************************************************************************
cont          *computational control - see page 2-214                *cont.1
0.0,0,150,50,3,1,   *iterative solution                          *cont.2
0.0,0.0,0.0,0.0,0.0,0.9,1.5,1.0                                  *cont.3
*0,0,0,1,2,0,1,1,0,0,0,1,0,0                                     *cont.6
5,0,0,0,0,0,1,1,0,0,0,1,0,0                                      *cont.6
1000.0,0.0,0.0,0.0,0.0,0.0,0.0                                   *cont.7
endd
*
*end of data input
0
```

B.2 Mixed core model input

```
*                                                                              *
*  Full core (8 annulars, 16+1/8 solids)                                       *
*                                                                              *
********************************************************************************
1,0,0                                                                          *vipre.1
Full core (8 annulars, 16+1/8 solids)                                          *vipre.2
********************************************************************************
geom,133,133,20,0,0,0 *normal input geometry                                    *geom.1
144.0945,0.0,0.5                                                               *geom.2
1,0.0594,0.6309,0.4416,1,2,0.122362205,0.41437
2,0.1369,1.1777,1.1777,2,3,0.122362205,0.41437,4,0.12236,0.49724
3,0.0684,0.5889,0.5889,1,5,0.122362205,0.41437
4,0.1189,1.2619,0.8833,2,5,0.122362205,0.497244,7,0.0688,0.49724
5,0.1369,1.1777,1.1777,2,6,0.122362205,0.41437,8,0.12236,0.49724
6,0.0594,0.6309,0.4416,1,9,0.068799213,0.41437
7,0.1189,1.2619,0.8833,2,8,0.122362205,0.497244,11,0.12236,0.49724
8,0.1369,1.1777,1.1777,2,9,0.122362205,0.497244,12,0.12236,0.49724
9,0.1189,1.2619,0.8833,2,10,0.068799213,0.41437,13,0.12236,0.49724
10,0.0594,0.6309,0.4416,1,14,0.122362205,0.41437
11,0.1369,1.1777,1.1777,2,12,0.122362205,0.497244,16,0.12236,0.49724
12,0.1369,1.1777,1.1777,2,13,0.122362205,0.497244,17,0.12236,0.49724
13,0.1369,1.1777,1.1777,2,14,0.122362205,0.497244,18,0.12236,0.49724
14,0.1369,1.1777,1.1777,2,15,0.122362205,0.41437,19,0.12236,0.49724
15,0.0594,0.6309,0.4416,1,20,0.068799213,0.41437
16,0.1189,1.2619,0.8833,2,17,0.122362205,0.497244,22,0.0688,0.49724
17,0.1369,1.1777,1.1777,2,18,0.122362205,0.497244,23,0.12236,0.49724
18,0.1189,1.2619,0.8833,2,19,0.068799213,0.497244,24,0.0688,0.49724
19,0.1189,1.2619,0.8833,2,20,0.122362205,0.497244,25,0.0688,0.49724
20,0.1189,1.2619,0.8833,2,21,0.068799213,0.41437,26,0.12236,0.49724
21,0.0594,0.6309,0.4416,1,27,0.122362205,0.41437
22,0.1189,1.2619,0.8833,2,23,0.122362205,0.497244,29,0.12236,0.49724
23,0.1369,1.1777,1.1777,2,24,0.122362205,0.497244,30,0.12236,0.49724
24,0.1189,1.2619,0.8833,2,25,0.068799213,0.497244,31,0.12236,0.49724
25,0.1189,1.2619,0.8833,2,26,0.122362205,0.497244,32,0.12236,0.49724
26,0.1369,1.1777,1.1777,2,27,0.122362205,0.497244,33,0.12236,0.49724
27,0.1369,1.1777,1.1777,2,28,0.122362205,0.497244,34,0.12236,0.49724
28,0.0684,0.5889,0.5889,1,35,0.122362205,0.41437
29,0.1369,1.1777,1.1777,2,30,0.122362205,0.497244,37,0.122,0.376
30,0.1369,1.1777,1.1777,2,31,0.122362205,0.497244,38,0.122,0.376
31,0.1369,1.1777,1.1777,3,32,0.122362205,0.497244,38,0.118,0.376 ,?
39,0.004 ,0.376
32,0.1369,1.1777,1.1777,2,33,0.122362205,0.497244,39,0.122,0.376
33,0.1369,1.1777,1.1777,2,34,0.122362205,0.497244,40,0.122,0.376
34,0.1369,1.1777,1.1777,2,35,0.122362205,0.497244,41,0.122,0.376
35,0.1369,1.1777,1.1777,3,36,0.122362205,0.41437,41,0.079,0.376,?
42,0.043,0.376
36,0.0684,0.5889,0.5889,1,42,0.122,0.293
37,0.1573,1.7178,1.7178,2,38,0.175 ,0.650 ,43,0.045 ,0.618
38,0.1798,1.6551,1.6551,2,39,0.284 ,0.650 ,44,0.045 ,0.618
39,0.1620,1.7944,1.7944,2,40,0.101 ,0.650 ,45,0.045 ,0.618
40,0.1552,1.7007,1.7007,2,41,0.135 ,0.650 ,46,0.045 ,0.618
41,0.1747,1.7114,1.7114,2,42,0.284 ,0.867 ,47,0.045 ,0.618
42,0.2124,2.2184,2.2184,2,48,0.045 ,0.510 ,54,0.042 ,0.470
43,0.1350,1.9007,1.9007,2,44,0.045 ,0.650 ,49,0.045 ,0.650
44,0.1350,1.9007,1.9007,2,45,0.045 ,0.650 ,50,0.045 ,0.650
45,0.1350,1.9007,1.9007,2,46,0.045 ,0.650 ,51,0.045 ,0.650
46,0.1350,1.9007,1.9007,2,47,0.045 ,0.650 ,52,0.045 ,0.650
47,0.1350,1.9007,1.9007,2,48,0.045 ,0.542 ,53,0.045 ,0.542
48,0.0675,0.9503,0.9503,1,54,0.064 ,0.700
49,0.1350,1.9007,1.9007,2,50,0.045 ,0.650 ,55,0.045 ,0.650
50,0.1350,1.9007,1.4255,2,51,0.045 ,0.650 ,56,0.045 ,0.650
51,0.1350,1.9007,1.4255,2,52,0.045 ,0.650 ,57,0.045 ,0.650
52,0.1350,1.9007,1.9007,2,53,0.045 ,0.542 ,58,0.045 ,0.542
```

```
53,0.0675,0.9503,0.9503,1,54,0.064 ,1.159
54,2.8832,40.1515,38.0132,6,58,0.064 ,1.619 ,61,0.064 ,2.079 ,?
63,0.064 ,2.538
64,0.064 ,2.998,65,0.672785,2.821522,66,0.672785,3.526903
55,0.1350,1.9007,1.9007,2,56,0.045 ,0.650 ,59,0.045 ,0.650
56,0.1350,1.9007,1.4255,2,57,0.045 ,0.650 ,60,0.045 ,0.650
57,0.1350,1.9007,1.4255,2,58,0.045 ,0.542 ,61,0.045 ,0.542
58,0.0675,0.9503,0.9503,
59,0.1350,1.9007,1.9007,2,60,0.045 ,0.650 ,62,0.045 ,0.650
60,0.1350,1.9007,1.9007,2,61,0.045 ,0.542 ,63,0.045 ,0.542
61,0.0675,0.9503,0.9503,
62,0.1350,1.9007,1.9007,2,63,0.045 ,0.542 ,64,0.045 ,0.542
63,0.0675,0.9503,0.9503,
64,0.0675,0.9503,0.7127,
65,4.7434,43.5971,38.8650,1,67,0.6728,3.5269
66,5.7664,80.3030,76.0265,2,67,0.6728,5.6430,68,0.6728,6.3484
67,14.2303,130.7912,116.5949,1,69,2.091574803,6.3484
68,18.9738,174.3883,155.4599,2,69,2.0916,6.3484,71,0.6728,8.4646
69,37.9475,348.7765,310.9197,2,70,1.345570866,7.0538,?
72,2.09157,8.4646
70,11.5328,160.6059,152.0530,1,73,1.345570866,7.053806
71,11.5328,160.6059,152.0530,2,72,1.3456,6.3484,75,0.2998,8.4646
72,37.9475,348.7765,310.9197,2,73,2.0916,8.4646,76,2.0916,8.4646
73,37.9475,348.7765,310.9197,2,74,1.345570866,7.053806,?
77,2.09157,8.46457
74,11.5328,160.6059,152.0530,1,78,0.599566929,7.053806
75,11.5328,160.6059,152.0530,2,76,1.3456,6.3484,80,0.6728,8.4646
76,37.9475,348.7765,310.9197,2,77,2.091574803,8.4646,?
81,1.34557,8.4646
77,37.9475,348.7765,310.9197,2,78,1.345570866,8.464567,?
82,2.09157,8.46457
78,23.0656,321.2119,304.1059,2,79,1.345570866,7.053806,?
83,1.34557,8.46457
79,18.9738,174.3883,155.4599,1,84,1.345570866,7.053806
80,18.9738,174.3883,155.4599,2,81,1.3456,6.3484,?
86,1.0458,8.4646
81,23.0656,321.2119,304.1059,2,82,1.3456,8.464567,?
87,0.5996,8.46457
82,37.9475,348.7765,310.9197,2,83,2.091574803,8.464567,?
88,2.09157,8.46457
83,37.9475,348.7765,310.9197,2,84,1.3456,8.464567,?
89,2.09157,8.46457
84,23.0656,321.2119,304.1059,2,85,1.345570866,7.053806,?
90,0.59957,8.46457
85,18.9738,174.3883,155.4599,1,91,2.091574803,7.053806
86,18.9738,174.3883,155.4599,2,87,1.3456,6.3484,?
92,0.6728,8.4646
87,23.0656,321.2119,304.1059,2,88,1.345570866,8.4646,?
93,1.34557,8.4646
88,37.9475,348.7765,310.9197,2,89,2.091574803,8.464567,?
94,2.09157,8.46457
89,37.9475,348.7765,310.9197,2,90,1.345570866,8.464567,?
95,2.0916,8.46457
90,23.0656,321.2119,304.1059,1,91,1.3456,8.464567
91,37.9475,348.7765,310.9197,
92,11.5328,160.6059,152.0530,1,93,1.345570866,6.348425
93,37.9475,348.7765,310.9197,1,94,2.0916,8.4646
94,37.9475,348.7765,310.9197,1,95,2.091574803,8.4646
95,37.9475,348.7765,310.9197,
96,0.0454,0.5339,0.5339,
97,0.0907,1.0678,1.0678,
98,0.0907,1.0678,1.0678,
99,0.0907,1.0678,1.0678,
```

```
100,0.0907,1.0678,1.0678,
101,0.0907,1.0678,1.0678,
102,0.0907,1.0678,1.0678,
103,0.0454,0.5339,0.5339,
104,0.0907,1.0678,1.0678,
105,0.0907,1.0678,1.0678,
106,0.0907,1.0678,1.0678,
107,0.0907,1.0678,1.0678,
108,0.0907,1.0678,1.0678,
109,0.0454,0.5339,0.5339,
110,0.0907,1.0678,1.0678,
111,0.0907,1.0678,1.0678,
112,0.0907,1.0678,1.0678,
113,0.0454,0.5339,0.5339,
114,0.0907,1.0678,1.0678,
115,0.0907,1.0678,1.0678,
116,0.0907,1.0678,1.0678,
117,0.0454,0.5339,0.5339,
118,0.0907,1.0678,1.0678,
119,0.0907,1.0678,1.0678,
120,0.0454,0.5339,0.5339,
121,0.0907,1.0678,1.0678,
122,1.5424,18.1521,18.1521,
123,3.6292,42.7108,42.7108,
124,7.2583,85.4216,85.4216,
125,7.2583,85.4216,85.4216,
126,7.2583,85.4216,85.4216,
127,7.2583,85.4216,85.4216,
128,14.5166,170.8431,170.8431,
129,14.5166,170.8431,170.8431,
130,14.5166,170.8431,170.8431,
131,14.5166,170.8431,170.8431,
132,14.5166,170.8431,170.8431,
133,7.2583,85.4216,85.4216,                                          *geom.4
*****************************************************************************
prop,0,0,2,1  *internal EPRI functions                               *prop.1
*****************************************************************************
rods,1,143,1,3,4,0,0,0,0,0,0     *3 geometry types, w/ cond rod
*rods.1
0.0,0.0,0,0                                                          *rods.2
-1                                                                   *rods.3
1.55   *chopped cosine with peak to average = 1.55                   *rods.5
******rods geometry inputs*********
1, 2, 1.417, 1, 1, 0.250, 2, 0.250,
2, 2, 1.380, 1, 1, 0.125, 2, 0.250, 3, 0.125,
3, 2, 1.418, 1, 2, 0.250, 4, 0.250,
4, 2, 1.373, 1, 2, 0.250, 3, 0.250, 4, 0.250, 5, 0.250
5, 2, 1.381, 1, 3, 0.125, 5, 0.250, 6, 0.125,
6, 2, 1.420, 1, 4, 0.250, 5, 0.250, 7, 0.250, 8, 0.250
7, 2, 1.425, 1, 5, 0.250, 6, 0.250, 8, 0.250, 9, 0.250
8, 2, 1.414, 1, 7, 0.250, 11, 0.250,
9, 2, 1.384, 1, 7, 0.250, 8, 0.250, 11, 0.250, 12, 0.250
10, 2, 1.384, 1, 8, 0.250, 9, 0.250, 12, 0.250, 13, 0.250
11, 2, 1.438, 1, 9, 0.250, 10, 0.250, 13, 0.250, 14, 0.250
12, 2, 1.417, 1, 10, 0.125, 14, 0.250, 15, 0.125,
13, 2, 1.425, 1, 11, 0.250, 16, 0.250,
14, 2, 1.382, 1, 11, 0.250, 12, 0.250, 16, 0.250, 17, 0.250
15, 2, 1.388, 1, 12, 0.250, 13, 0.250, 17, 0.250, 18, 0.250
16, 2, 1.438, 1, 13, 0.250, 14, 0.250, 18, 0.250, 19, 0.250
17, 2, 1.445, 1, 14, 0.250, 15, 0.250, 19, 0.250, 20, 0.250
18, 2, 1.413, 1, 16, 0.250, 17, 0.250, 22, 0.250, 23, 0.250
19, 2, 1.417, 1, 17, 0.250, 18, 0.250, 23, 0.250, 24, 0.250
20, 2, 1.429, 1, 19, 0.250, 20, 0.250, 25, 0.250, 26, 0.250
```

```
21, 2, 1.398, 1, 20, 0.250, 21, 0.250, 26, 0.250, 27, 0.250
22, 2, 1.342, 1, 21, 0.125, 27, 0.250, 28, 0.125,
23, 2, 1.398, 1, 22, 0.250, 29, 0.250,
24, 2, 1.363, 1, 22, 0.250, 23, 0.250, 29, 0.250, 30, 0.250
25, 2, 1.369, 1, 23, 0.250, 24, 0.250, 30, 0.250, 31, 0.250
26, 2, 1.396, 1, 24, 0.250, 25, 0.250, 31, 0.250, 32, 0.250
27, 2, 1.356, 1, 25, 0.250, 26, 0.250, 32, 0.250, 33, 0.250
28, 2, 1.337, 1, 26, 0.250, 27, 0.250, 33, 0.250, 34, 0.250
29, 2, 1.311, 1, 27, 0.250, 28, 0.250, 34, 0.250, 35, 0.250
30, 2, 1.293, 1, 28, 0.125, 35, 0.250, 36, 0.125,
31, 2, 1.358, 1, 29, 0.250, 37, 0.250,
32, 2, 1.352, 1, 29, 0.250, 30, 0.250, 37, 0.402, 38, 0.098
33, 2, 1.351, 1, 30, 0.250, 31, 0.250, 38, 0.500,
34, 2, 1.353, 1, 31, 0.250, 32, 0.250, 39, 0.500,
35, 2, 1.348, 1, 32, 0.250, 33, 0.250, 39, 0.217, 40, 0.283
36, 2, 1.331, 1, 33, 0.250, 34, 0.250, 40, 0.354, 41, 0.146
37, 2, 1.315, 1, 34, 0.250, 35, 0.250, 41, 0.500,
38, 2, 1.313, 1, 35, 0.250, 36, 0.250, 42, 0.500,
39, 2, 1.333, 1, 36, 0.125, 42, 0.375,
40, 1, 2.232, 1, 37, 0.250, 43, 0.250
-40, 1, 2.232, 1, 96, 0.500
41, 1, 2.247, 1, 37, 0.250, 38, 0.250, 43, 0.250, 44, 0.250
-41, 1, 2.247, 1, 97, 1.000
42, 1, 2.260, 1, 38, 0.250, 39, 0.250, 44, 0.250, 45, 0.250
-42, 1, 2.260, 1, 98, 1.000
43, 1, 2.254, 1, 39, 0.250, 40, 0.250, 45, 0.250, 46, 0.250
-43, 1, 2.254, 1, 99, 1.000
44, 1, 2.232, 1, 40, 0.250, 41, 0.250, 46, 0.250, 47, 0.250
-44, 1, 2.232, 1, 100, 1.000
45, 1, 2.217, 1, 41, 0.250, 42, 0.250, 47, 0.250, 48, 0.250
-45, 1, 2.217, 1, 101, 1.000
46, 1, 2.255, 1, 42, 0.375, 48, 0.125, 54, 0.500,
-46, 1, 2.255, 1, 102, 1.000
47, 1, 2.209, 1, 43, 0.250, 49, 0.250,
-47, 1, 2.209, 1, 103, 0.500
48, 1, 2.270, 1, 43, 0.250, 44, 0.250, 49, 0.250, 50, 0.250
-48, 1, 2.270, 1, 104, 1.000
49, 1, 2.386, 1, 44, 0.250, 45, 0.250, 50, 0.250, 51, 0.250
-49, 1, 2.386, 1, 105, 1.000
50, 1, 2.270, 1, 45, 0.250, 46, 0.250, 51, 0.250, 52, 0.250
-50, 1, 2.270, 1, 106, 1.000
51, 1, 2.197, 1, 46, 0.250, 47, 0.250, 52, 0.250, 53, 0.250
-51, 1, 2.197, 1, 107, 1.000
52, 1, 2.176, 1, 47, 0.250, 48, 0.125, 53, 0.125, 54, 0.500
-52, 1, 2.176, 1, 108, 1.000
53, 1, 2.235, 1, 49, 0.250, 55, 0.250,
-53, 1, 2.235, 1, 109, 0.500
54, 1, 2.383, 1, 49, 0.250, 50, 0.250, 55, 0.250, 56, 0.250
-54, 1, 2.383, 1, 110, 1.000
55, 1, 2.395, 1, 51, 0.250, 52, 0.250, 57, 0.250, 58, 0.250
-55, 1, 2.395, 1, 111, 1.000
56, 1, 2.231, 1, 52, 0.250, 53, 0.125, 58, 0.125, 54, 0.500
-56, 1, 2.231, 1, 112, 1.000
57, 1, 1.587, 1, 54, 17.000, 54
-57, 1, 1.587, 1, 122, 17.000
58, 1, 2.217, 1, 55, 0.250, 59, 0.250,
-58, 1, 2.217, 1, 113, 0.500
59, 1, 2.278, 1, 55, 0.250, 56, 0.250, 59, 0.250, 60, 0.250
-59, 1, 2.278, 1, 114, 1.000
60, 1, 2.419, 1, 56, 0.250, 57, 0.250, 60, 0.250, 61, 0.250
-60, 1, 2.419, 1, 115, 1.000
61, 1, 2.376, 1, 57, 0.250, 58, 0.125, 61, 0.125, 54, 0.500
-61, 1, 2.376, 1, 116, 1.000
```

```
62, 1, 2.217, 1, 59, 0.250, 62, 0.250,
-62, 1, 2.217, 1, 117, 0.500
63, 1, 2.235, 1, 59, 0.250, 60, 0.250, 62, 0.250, 63, 0.250
-63, 1, 2.235, 1, 118, 1.000
64, 1, 2.263, 1, 60, 0.250, 61, 0.125, 63, 0.125, 54, 0.500
-64, 1, 2.263, 1, 119, 1.000
65, 1, 2.379, 1, 62, 0.250, 64, 0.250,
-65, 1, 2.379, 1, 120, 0.500
66, 1, 2.271, 1, 62, 0.250, 63, 0.125, 64, 0.125, 54, 0.500
-66, 1, 2.271, 1, 121, 1.000
67, 2, 1.380, 1, 65, 33.000
68, 1, 2.276, 1, 66, 40.000
-68, 1, 2.276, 1, 123, 40.000
69, 2, 1.380, 1, 67, 99.000
70, 2, 1.201, 1, 68, 132.000
71, 2, 1.096, 1, 69, 264.000
72, 1, 1.759, 1, 70, 80.000
-72, 1, 1.759, 1, 124, 80.000
73, 1, 1.350, 1, 71, 80.000
-73, 1, 1.350, 1, 125, 80.000
74, 2, 0.818, 1, 72, 264.000
75, 2, 0.818, 1, 73, 264.000
76, 1, 1.350, 1, 74, 80.000
-76, 1, 1.350, 1, 126, 80.000
77, 1, 1.350, 1, 75, 80.000
-77, 1, 1.350, 1, 127, 80.000
78, 2, 0.818, 1, 76, 264.000
79, 2, 0.818, 1, 77, 264.000
80, 1, 1.350, 1, 78, 160.000
-80, 1, 1.350, 1, 128, 160.000
81, 2, 0.818, 1, 79, 132.000
82, 2, 0.819, 1, 80, 132.000
83, 1, 1.351, 1, 81, 160.000
-83, 1, 1.351, 1, 129, 160.000
84, 2, 0.819, 1, 82, 264.000
85, 2, 0.819, 1, 83, 264.000
86, 1, 1.351, 1, 84, 160.000
-86, 1, 1.351, 1, 130, 160.000
87, 2, 0.819, 1, 85, 132.000
88, 2, 0.819, 1, 86, 132.000
89, 1, 1.351, 1, 87, 160.000
-89, 1, 1.351, 1, 131, 160.000
90, 2, 0.819, 1, 88, 264.000
91, 2, 0.819, 1, 89, 264.000
92, 1, 1.351, 1, 90, 160.000
-92, 1, 1.351, 1, 132, 160.000
93, 2, 0.819, 1, 91, 264.000
94, 1, 1.351, 1, 92, 80.000
-94, 1, 1.351, 1, 133, 80.000
95, 2, 0.819, 1, 93, 264.000
96, 2, 0.819, 1, 94, 264.000
97, 2, 0.819, 1, 95, 264.000
98, 3, 0.000, 1, 1, 0.125
99, 3, 0.000, 1, 4, 0.250, 7, 0.250,
100, 3, 0.000, 1, 6, 0.125, 9, 0.250, 10, 0.125,
101, 3, 0.000, 1, 15, 0.125, 20, 0.250, 21, 0.125,
102, 3, 0.000, 1, 16, 0.250, 22, 0.250,
103, 3, 0.000, 1, 18, 0.250, 19, 0.250, 24, 0.250, 25, 0.250
104, 3, 0.000, 1, 50, 0.250, 51, 0.250, 56, 0.250, 57, 0.250
105, 3, 0.000, 1, 64, 0.125
0                                                                    *rods.9
2,nucl,0.37488,0.325,8,0.0,0.0225
*rods.62
```

```
0,0,0,0,0,1000.0,0.95,0.0
*rods.63
1,tube,0.605,0.339882,5
*rods.68
2,1,0.0224921,0.0,?   *inner cladding
*rods.69
2,2,0.0024488,0.0,?   *inner gap
*rods.69
8,3,0.0826772,1.0,?    *fuel ring
*rods.69
2,4,0.0024409,0.0      *outer gap
*rods.69
2,1,0.0225000,0.0       *outer cladding
*rods.69
3, dumy, 0.4820,0.0,0
*rods.68
1,17,409.0,clad                                                    *rods.70
0.0,0.0671,7.3304509,?
25,0.0671,7.3304509
50,0.0671,7.33045093,?
65,0.0671,7.33045093
80.33,0.0671,7.33045093,?
260.33,0.07212,8.11585329
692.33,0.07904,9.80167423,?
1502.33,0.08955,13.2923001
1507.73,0.11988,13.3211893,?
1543.73,0.14089,13.5166505
1579.73,0.14686,13.717249,?
1615.73,0.1717,13.9231981
1651.73,0.1949,14.1347101,?
1687.73,0.18388,14.3519980
1723.73,0.1478,14.5752746,?
1759.73,0.112,14.804753
1786.73,0.085,14.9810589
*2240.33,0.085,18.5665964
2,1,0.025,igap                                                     *rods.70
1,1.240834,0.2156263    *Cp=5195J/kg-K *gap=6000                   *rods.71
3,22,650.617,FU02                                                  *rods.70
86,0.05677357,4.73275874,?
176,0.06078589,4.29917259
266,0.06366347,3.93877428,?
356,0.06581210,3.63454049
446,0.06747631,3.37435643,?
536,0.06880819,3.1493668
626,0.06990545,2.95294976,?
716,0.07083283,2.78005572
806,0.07163441,2.62676801,?
896,0.07234099,2.49000319
986,0.07297458,2.36730189,?
1076,0.07355124,2.25667975
1166,0.07408294,2.1565193,?
1256,0.07457886,2.06549023
1346,0.07504628,1.98248979,?
1436,0.07549123,1.90659753
1526,0.0759191,1.83704065,?
1616,0.07633503,1.77316713
1706,0.0767443,1.7144247,?
1796,0.07715268,1.66034425
1886,0.07756663,1.61052668,?
1976,0.07799351,1.5646323                                          *rods.71
4,1,0.025,ogap                                                     *rods.70
1,1.240834,0.2149314    *Cp=5195J/kg-K *gap=6000                   *rods.71
******oper input*****************************************************************
```

```
oper,1,1,0,1,0,1,0,0,0                                                    *oper.1
-1.0,1.3,0.0,0.005,0                                                      *oper.2
0                                                                         *oper.3
2248.1,562.46,4877.3,90.87,0.0                                           *oper.5
0              *no forcing functions                                      *oper.12
*****************************************************************************
corr,2,2,0                                                                *corr.1
epri,epri,epri,none                                                       *corr.2
0.2                                                                       *corr.3
ditb,thsp,thsp,w-3l,cond,g5.7     *correlation for boiling curve          *corr.6
w-3s,w-3l                  *dnb analysis by w-3l                          *corr.9
0.0                 *w-3s input data
*corr.10
0.042,0.066,0.986   *w-3l input data
*corr.11
*****************************************************************************
drag,1,1,4                                                                *drag.1
0.316,-0.25,0.0,64.0,-1.0,0.0          *axial friction correlation        *drag.2
0.3749,0.4972     *rod diameter,Pitch                                     *drag.7
*7.333,-0.2,0.0,7.333,-0.2,0.0
3.098,-0.2,0.0,0.0,0.0,0.5 * lateral drag correlation for Standard       *drag.8
*0.5,0.496        *pitch=0.496,kij=0.5l/p                                 *drag.5
*****************************************************************************
grid,0,3                                                                  *grid.1
0.6,0.4,1.0                                                               *grid.2
95,9                                                                      *grid.4
1, 2, 3, 4, 5, 6, 7, 8, 9, 10, 11, 12, 13, 14, 15, 16
17, 18, 19, 20, 21, 22, 23, 24, 25, 26, 27, 28, 29, 30, 31, 32
33, 34, 35, 36, 37, 38, 39, 40, 41, 42, 43, 44, 45, 46, 47, 48
49, 50, 51, 52, 53, 54, 55, 56, 57, 58, 59, 60, 61, 62, 63, 64
65, 66, 67, 68, 69, 70, 71, 72, 73, 74, 75, 76, 77, 78, 79, 80
81, 82, 83, 84, 85, 86, 87, 88, 89, 90, 91, 92, 93, 94, 95                *grid.5
0.0,2,12.0079,1,32.0079,1,52.0079,1,?
72.0079,1,92.0079,1,112.0079,1,132.0079,1,
144.0945,3                              *grid loc.                        *grid.6
38,2
96, 97, 98, 99, 100, 101, 102, 103, 104, 105, 106, 107, 108, 109, 110, 111
112, 113, 114, 115, 116, 117, 118, 119, 120, 121, 122, 123, 124, 125, 126, 127
128, 129, 130, 131, 132, 133
0.0,2,144.0945,3
0
*****************************************************************************
*
cont            *computational control - see page 2-214                   *cont.1
0.0,0,150,50,3,1,   *iterative solution
*cont.2
0.0,0.0,0.0,0.0,0.0,0.9,1.5,1.0                                           *cont.3
*0,0,0,1,2,0,1,1,0,0,0,1,0,0                                              *cont.6
5,0,0,0,0,0,1,1,0,0,0,1,0,0                                               *cont.6
1000.0,0.0,0.0,0.0,0.0,0.0                                                *cont.7
endd
*end of data input
0
```

Appendix C

Gd Content Calculation

In order to define a fuel pin composition with enrichment X and Gd_2O_3 content of G (X and G are weight fraction) for use in CASMO-4, we need to compute the content in the different isotopes of U, Gd and O.

We are after the atomic concentration (*i.e.* number of atoms per cm^3).

Mixture density First of all we have to compute the actual density of the fuel. The initial concentration of UO_2 will be altered by two phenomena following the introduction of Gd_2O_3. One is the fact that poison will take the place of UO_2 and modify the overall density. The second one comes from the fact that Gd_2O_3 can form phases with UO_2, and therefore its density (in solution) can vary from 7.4 g/cm^3 to 8.3 g/cm^3. The only effect that we will consider is the first one. The variation of Gd_2O_3 density will be disregarded since we will deal with enrichment in a relatively close range, and we will choose $\rho_{Gd_2O_3} = 7.64\ g/cm^3$.

Let us apply the conservation of volume (which holds since we disregarded the eventual formation of phases) to a gram of mixture with Gd_2O_3 weight content of G. Its total volume is $\frac{1g}{\rho_{mixture}}$. The volume of Gd_2O_3 is $\frac{1g*G}{\rho_{Gd_2O_3}}$ and the volume of UO_2 is $\frac{1g*(1-G)}{\rho_{UO_2}}$. Writing the conservation of volume we obtain Equation C.1. Rearranging Equation C.1 gives Equation C.2.

$$\frac{1}{\rho_{mixture}} = \frac{G}{\rho_{Gd_2O_3}} + \frac{1-G}{\rho_{UO_2}} \tag{C.1}$$

$$\rho_{mixture} = \frac{1}{\frac{G}{\rho_{Gd_2O_3}} + \frac{1-G}{\rho_{UO_2}}} \tag{C.2}$$

We take for $\rho_{UO_2} = 10.4 g/cm^3$ and $\rho_{Gd_2O_3} = 7.64 g/cm^3$. The density of UO_2 is taken to be 95% of theoretical density.

Atomic concentration of U and Gd isotopes and of O The calculation of the different atomic concentrations complies with the CASMO-4 procedure (see Ref. [8]). It is assumed that the weight fraction of U in UO_2 is 0.8815 and the weigth fraction of Gd in Gd_2O_3 is 0.8676.

Following are the equations that give, as a function of G and X the atomic concentrations of U-234, U-235, U-238, Gd-152, Gd-154, Gd-155, Gd-156, Gd-157, Gd-158, Gd-160 and O-16. For the sake of simplicity, the atomic concentration of an element Y-n, will simply be written as Yn (for instance, U235 refers to the atomic concentration of U-235).

Equation C.3 gives the molecular weight (in g/mol) of UO_2 with X % in weight of U-235.

$$M_{UO_2} = X * 235.0439 + (1 - X) * 238.0508 + 2 * 15.9994 \tag{C.3}$$

Equation C.4 gives the molecular weigth (in g/mol) of U with X % in weight of U-235.

$$M_U = X * 235.0439 + (1 - X) * 238.0508 \tag{C.4}$$

The Avogadro constant $N_A \approx 6.022E + 23\ mol^{-1}$ is the number of individual atom or molecule in a given mole of matter. Following we can write that the atomic concentration UO_2 is given by Equation C.5.

$$UO_2 = \frac{\rho_{UO_2} * N_A}{M_{UO_2}} \tag{C.5}$$

$$U235 = \frac{X * (1 - G) * \rho_{mixture}}{M_{UO_2}} * \frac{M_U}{M_{U-325}} * N_A \tag{C.6}$$

Equation C.6 is the atomic concentration of U-235 in the fuel. The first term $(\frac{X*(1-G)*\rho_{mixture}}{M_{UO_2}})$ is the number of moles of U-235 in the fuel per unit volume. The second term $(\frac{M_U}{M_{U-325}})$ corrects the difference in mass between average U and U-235. By enventually multiplying by N_A, we get the number of atoms of U-235 per unit volume, which is what we are after.

$$U234 = U235 * 0.008 * \frac{M_{U-235}}{M_{U-234}} \tag{C.7}$$

Equation C.7 gives the atomic concentration of U-234. It is stated in Ref. [8] that, in mass, 0.8% of U-235 is U-234. This means that in terms of atomic concentration, they are $0.008 * \frac{M_{U-235}}{M_{U-234}}$ atoms of U-234 for one atom of U-235.

$$U238 = (UO_2 - U235 - U234) * (1 - G) * \frac{\rho_{mixture}}{\rho_{UO_2}} * 1.3 \tag{C.8}$$

Equation C.8 gives the atomic concentration of U-238. Note that the total concentration of U-238 is artificially increased by 30% in order to compensante for the fact that CASMO-4 cannot directly simulate hollow rods.

$$Gd = 2 * G * \rho mixture * \frac{N_A}{M_{Gd_2O_3}} \tag{C.9}$$

Equation C.9 only gives the atomic concentration of all Gd isotopes. In order to obtain the atomic concentration of all isotopes, we will use the natural occurence of Gd isotopes found in Ref. [7]. The distribution is summurized in Table C.1.

Table C.1: Natural atomic occurence of Gd isotopes (from Ref. [7])

Gd total	Gd152	Gd154	Gd155	Gd156	Gd157	Gd158	Gd160
100%	0.21%	2.15%	14.73%	20.47%	15.67%	24.87%	21.90%

Eventually, it is easy to compute the atomic concentration of oxygen: indeed O

comes from either UO_2 or Gd_2O_3. O is given in Equation C.10.

$$O = 2 * UO_2 + 3 * Gd \tag{C.10}$$

Appendix D

MatLab Code For Data Processing

Main code

```
function Retrieve(infile)

fid=fopen(infile,'r');

go=true;

Expo10=[];
Expo11=[];

Peak10=[];
Peak11=[];

is10=false;
is11=false;

Mfull=zeros(8,9);
M=zeros(8,8);
```

```
tline=fgetl(fid);

while (go)

   if (is10)
        if strncmp(tline,' CYCLE EXPOSURE AT END OF THIS STEP =',length(' 
CYCLE EXPOSURE AT END OF THIS STEP ='))
            Expo10=[Expo10;fscanf(fid,'%e',5)];
        elseif ( strcmp(tline, ' PIN.EDT 2PIN - PEAK PIN POWER: ASSEMBLY 
2D') )
            %extract the data
            tline=fgetl(fid);
            tline=fgetl(fid);
            tline=fgetl(fid);

            Mfull(1,:)=fscanf(fid,'%e',9)';
            tline=fgetl(fid);

            Mfull(2,:)=fscanf(fid,'%e',9)';
            tline=fgetl(fid);

            Mfull(3,:)=fscanf(fid,'%e',9)';
            tline=fgetl(fid);

            Mfull(4,1:8)=fscanf(fid,'%e',9)';
            tline=fgetl(fid);

            Mfull(5,1:8)=fscanf(fid,'%e',8)';
            tline=fgetl(fid);
```

```
            Mfull(6,1:8)=fscanf(fid,'%e',8)';
            tline=fgetl(fid);

            Mfull(7,1:7)=fscanf(fid,'%e',7)';
            tline=fgetl(fid);

            Mfull(8,1:5)=fscanf(fid,'%e',5)';
            tline=fgetl(fid);

            M=Mfull;
            M(:,1)=[];

            Peak10=[Peak10;Peaking10(M)];

        end

    elseif (is11)
        if strncmp(tline,' CYCLE EXPOSURE AT END OF THIS STEP =',length(' CYCLE EXPOSURE AT END OF THIS STEP ='))
            Expo11=[Expo11;fscanf(fid,'%e',5)];
        elseif ( strcmp(tline, ' PIN.EDT 2PIN - PEAK PIN POWER: ASSEMBLY 2D') )
            %extract the data
            tline=fgetl(fid);
            tline=fgetl(fid);
            tline=fgetl(fid);

            Mfull(1,:)=fscanf(fid,'%e',9)';
            tline=fgetl(fid);
```

```
            Mfull(2,:)=fscanf(fid,'%e',9)';
            tline=fgetl(fid);

            Mfull(3,:)=fscanf(fid,'%e',9)';
            tline=fgetl(fid);

            Mfull(4,1:8)=fscanf(fid,'%e',9)';
            tline=fgetl(fid);

            Mfull(5,1:8)=fscanf(fid,'%e',8)';
            tline=fgetl(fid);

            Mfull(6,1:8)=fscanf(fid,'%e',8)';
            tline=fgetl(fid);

            Mfull(7,1:7)=fscanf(fid,'%e',7)';
            tline=fgetl(fid);

            Mfull(8,1:5)=fscanf(fid,'%e',5)';
            tline=fgetl(fid);

            M=Mfull;
            M(:,1)=[];

            Peak11=[Peak11;Peaking11(M)];
        end

end

if ( strncmp(tline, ' CASE 1 STEP 0 CYCLE 10XF', length(' CASE 1 STEP 0
```

```
CYCLE 10XF')) )
            is10=true;
            is11=false;
            tline=fgetl(fid);
    elseif ( strncmp(tline, ' CASE 1 STEP 0 CYCLE 11XF', length(' CASE 1 STEP
0 CYCLE 11XF')) )
            is10=false;
            is11=true;
            tline=fgetl(fid);
    elseif ( strcmp(tline,' P W R S U M M A R Y O F S T E A D Y - S T A T E S I
M U L A T E - 3 V E R S I O N M . I . T . ') )
            go=FALSE;
    else
            tline=fgetl(fid);

    end


end

plot(Expo10,Peak10);
plot(Expo11,Peak11);
```

Peaking10 subroutine

```
function Peak10=Peaking10(M)

Peaking10=M;
Annular10=[0,1,0,1,0,1,0,0;
```

```
    1,0,1,0,1,0,1,0;
    0,1,0,1,0,0,1,0;
    1,0,1,0,0,0,1,0;
    0,1,0,0,0,1,0,0;
    1,0,0,0,1,1,0,0;
    0,1,1,1,0,0,0,0;
    0,0,0,0,0,0,0,0];

a10=((16+1/8)*(17*17-25)+8*(13*13-9))/((16+8+1/8)*(13*13-9));
s10=((16+1/8)*(17*17-25)+8*(13*13-9))/((16+8+1/8)*(17*17-25));

n=8;
m=8;

for i=1:n;
    for j=1:m;
        if (Annular10(i,j)==1)
            Peaking10(i,j)=M(i,j)/a10;
        else
            Peaking10(i,j)=M(i,j)/s10;
        end
    end
end

Peak10=max(max(Peaking10)');
```

Peaking11 subroutine

```
function Peak11=Peaking11(M)

Peaking11=M;
Annular11=[0,1,1,1,0,1,1,0;
    1,0,1,0,1,1,1,1;
    1,1,0,1,0,1,1,1;
    1,0,1,1,1,1,1,0;
    0,1,0,1,1,1,1,0;
    1,1,1,1,1,1,0,0;
    1,1,1,1,1,0,0,0;
    0,1,1,0,0,0,0,0];

a11=((8)*(17*17-25)+(16+1/8)*(13*13-9))/((16+8+1/8)*(13*13-9));
s11=((8)*(17*17-25)+(16+1/8)*(13*13-9))/((16+8+1/8)*(17*17-25));

n=8;
m=8;

for i=1:n;
    for j=1:m;
            if (Annular11(i,j)==1)
                Peaking11(i,j)=M(i,j)/a11;
            else
                Peaking11(i,j)=M(i,j)/s11;
            end
    end
end
```

```
Peak11=max(max(Peaking11)');
```

Bibliography

[1] *Hydrodynamic resistance hand-out.* p608-610.

[2] J. Rhodes III A. DiGiovine. *SIMULATE-3, Advanced Three-Dimensional Two-Group Reactor Analysis Code.*

[3] Richard de Neufville. *Applied Systems Analysis: Engineering Planning and Technology Management.* McGraw-Hill, 1990.

[4] J. Beccherle E. Lahoda, J.P. Mazzoccoli. High power density annular fuel: Economic benefits. *accepted for publication in Nuclear Technology*, 2007.

[5] E Pilat Edward. Private communication. 01 2007.

[6] MacMahon et. al. 1997.

[7] http://atom.kaeri.re.kr.

[8] B.H. Forssen D. Knott M. Edenius, K. Ekberg. *CASMO-4, A Fuel Assembly Burnup Program.*

[9] P. Hejzlar M.S. Kazimi. High performance fuel design for next generation pwrs. Final report MIT-NFC-PR-082, CANES, January 2006.

[10] D. Ver Planck. *TABLES-3, Library Preparation Code for SIMULATE-3.*

[11] T. Wang R. de Neufville, S. Scholtes. Real options by spreadsheet : Parking garage case example. *ASCE Journal of Infrastructure Systems*, 12(2):107–111, 2006.

[12] J. M. Cuta *et al. VIPRE-01 A Thermal-Hydraulic Code for reactor Cores*, volume 1-3 of *NP-2511-CCM.* EPRI, July 1985.

[13] L. S. Tong D. F. Fitzsimmons W. Thorne Weisman J., A. H. Wenzel and J. Batch. Experimental determination of the departure from nucleate boiling in large rod bundles at high pressures. *Chemical Engineering Progress*, Vol. 64(Symposium Series):pp. 82–114, 1968.